THERMAL IMAGING TO MONITOR SOIL AND CANOPY TEMPERATURE UNDER MULCHING AND NATURAL SOIL COVER CONDITIONS

Guglielmo Piazzoli

Dissertation to obtain a Master's degree in
Oenology and Viticulture engineering

PRESIDENT
Carlos Manuel Antunes Lopes (PhD), Associate Professor with Habilitation at Instituto Superior de Agronomia, Universidade de Lisboa.

MEMBERS
Joaquim Miguel Rangel da Cunha Costa (PhD), Assistant Professor at Instituto Superior de Agronomia, Universidade de Lisboa;
Francisca Constança Frutuoso de Aguiar (PhD), Assistant Professor at Instituto Superior de Agronomia, Universidade de Lisboa;
Francisco Mateus Marnoto de Oliveira Campos (PhD), Assistant Professor at Instituto Superior de Engenharia de Lisboa, Instituto Politécnico de Lisboa.

Lisboa

2022

AKNOWLEDGMENTS

We thank the support of the INTERPHENO project and FCT - Fundação para a Ciência e Tecnologia, Portugal

ABSTRACT

The Mediterranean viticulture is increasingly exposed to more severe and frequent heat waves and droughts. Therefore, short to medium-term adaptation strategies are needed to minimize risks and losses. The use of organic mulching can be a potential a short-term adaptation strategy as well as a tool to control soil water loss and decrease soil and canopy temperature. Meanwhile, imaging technologies are becoming more affordable and can be used to support crop and soil monitoring. However, low-cost thermal imaging and low-cost image analysis need still optimization to be applied in modern viticulture. In this study, we evaluated the impact of organic mulching, by analysing its effects on the temperature of the ground surface and of vine's canopy using low-cost thermography.

A preliminary study was carried out at the Instituto Superior de Agronomia to optimise the use of two low to medium-cost thermal cameras (Flir One Pro LT and Flir A35) and further image analysis and processing, to assess their potential use for field monitoring and in order to implement simple protocols to support ground-based thermal imaging analysis.

Three treatments were monitored: 1) Control – natural soil vegetation 2) Eucalyptus leaves and branches mulching 3) Rice straw mulching. Visible RGB and thermal images were done from the soil (sunlit and shadow) and from the sunlit side of the canopies along the season, on 9 June, (Flowering) 1 July (Veraison) and 12 August (pre-harvest) at 9-10.30h and 15-16.30h. Thermal data was complemented by leaf gas exchange and chlorophyll fluorescence at veraison and at pre-harvest. The Flir tools software (FLIR Systems) was used for image acquisition, while the Fiji (ImageJ distribution) adapted with a ThermimageJ plug was used for further image analysis.

The output of the Flir A35 revealed to be much superior to the one of Flir One. The A35 was able to detect canopy temperature differences such that thermal indices were constructed. The output of A35 output showed that mulching resulted in lower surface temperature than the control and smaller diurnal variation of the ground surface. The upper part of the canopy remained cooler than the lower part, independently of the mulch treatment. Using the Fiji software, it was possible to standardise the analysis process, but the protocols still require additional work to increase accuracy and precision.

Key words: Leaf and soil temperature, vertical temperature profile, low-cost imaging, protocol, thermal image analyses

RESUMO

A viticultura mediterrânica enfrenta situações cada vez mais frequentes de ondas de calor e de seca extrema pelo que são necessárias estratégias de adaptação de curto a médio prazo para minimizar os riscos e as perdas. O uso de coberturas mortas orgânicas para limitar a perda de água e diminuir a temperatura do solo e da sebe são possíveis estratégias de adaptação. Entretanto, as tecnologias de imagem estão a tornar-se mais acessíveis e podem ser utilizadas para apoiar a monitorização das culturas e do solo. Nesse sentido avaliamos o impacto do mulching orgânico, uma estratégia de adaptação a curto prazo, analisando os seus efeitos na superfície do solo e na temperatura da sebe. O uso de sistemas de imagem térmica de baixo custo e de softwares de análise de imagem de baixo custo necessitam ainda de otimização para serem aplicadas na viticultura moderna. Assim foi realizado um ensaio preliminar no Instituto Superior de Agronomia para testar três tratamentos do solo: 1) Testemunha - solo com vegetação natural 2) Mulch com folhas de Eucalipto folhas e ramos e 3) Mulch com palha de arroz. Testou-se também o uso de duas câmaras térmicas de baixo a médio custo (Flir One Pro LT e Flir A35). Foram feitas imagens térmicas e no visível RGB do solo (lado exposto ao sol e sombra) e da sebe (lado exposto) ao longo do ensaio: - 9 Junho, (Floração) 1 Julho (Veraison) e 12 Agosto (pré-colheita). As medições foram feitas de manhã (9-10,30h) e á tarde (15-16,30h). Os dados térmicos foram complementados com a medição das trocas gasosas e fluorescência de clorofila ao pintor e na pré-colheita.

Os resultados obtidos pela Flir A35 foram superiores aos da Flir One Pro LT. A FlirA435 mostrou diferenças de temperatura no solo e na sebe e permitiu calcular índices térmicos (CWSI). Os resultados obtidos com a Flir A35 mostraram que mulching resultou numa temperatura superficial mais baixa que a da testemunha e que a parte superior da sebe estava mais fresca que a inferior (zona dos cachos), independentemente dos tratamentos. Utilizando o software de Fiji, foi possível padronizar o processo de análise de imagem, mas é ainda necessário otimizar o protocolo de campo para se obter dados térmicos mais precisos e de uma forma mais eficiente

Palavras-chave: Temperatura da folha e do solo, perfil vertical de temperatura, imagem de baixo custo, protocolo, análise de imagem térmica.

RESUMO ALARGADO

O setor vitivinícola, sobretudo no Sul da Europa, enfrenta situações de stress hídrico e térmico motivados por ondas de calor mais frequentes e condições de secura mais extrema. Torna-se assim necessário implementar estratégias de curto/médio prazo para reduzirmos o impacto que das alterações climáticas no setor. Por exemplo, o uso de coberturas orgânicas mortas ("mulchs") pode limitar a perda de água por evaporação do solo e reduzir a temperatura das folhas (e cachos), reduzindo o stress hídrico e térmico e permitindo uma maior eficiência fotossintética e do uso de água e, melhor composição dos bagos. Por sua vez, o uso de câmaras térmicas tem vindo a ter uma aplicação cada vez mais vasta nos sectores das ciências das plantas e na agronomia e pode ajudar a monitorizar as temperaturas das culturas e do solo em condições de campo, e detetar condições de stress em videira e otimizar o uso de água de rega. Além disso o uso de soluções de baixo custo ao nível de sistemas de imagem térmica e de software de análise de imagem necessitam ainda de ser otimizados para aplicação prática na viticultura moderna.

Nesse sentido avaliamos o impacte da aplicação de coberturas mortas orgânicas (mulchs), como estratégia de adaptação de curto prazo, analisando os seus efeitos na temperatura da superfície do solo e da sebe com recurso à imagem térmica. Para isso foi testado um equipamento de termografia de baixo custo e análise de imagem que necessita de ser otimizado para aplicação prática na viticultura moderna. Assim foi realizado um ensaio preliminar no Instituto Superior de Agronomia, U. Lisboa, com o objetivo de testar os efeitos das coberturas orgânicas e de otimizar a aquisição e análise de imagens térmicas na monitorização da vinha em condições de campo.

Foram testados três tratamentos para se avaliar o impacte de coberturas orgânicas na temperatura da superfície do solo e da sebe: 1) Testemunha, - cobertura natural do solo 2) cobertura morta (mulch) com folhas e galhos de eucalipto 3) cobertura morta (mulch) com palha de arroz. Foram também testadas duas câmaras térmicas de baixo custo e "open software" de análise de imagem que necessitam de ser otimizados para aplicação prática na viticultura moderna. Foram captadas imagens térmicas e de RGB do solo (zona exposta ao sol e zona de sombra) e das videiras (apenas lado iluminado) durante três momentos: 9 junho (floração),1 de julho (pintura) e 12 de agosto (pré-colheita) e em duas fases do dia (9 - 10h30 e 3- 16h30). Duas câmaras térmicas foram usadas para aquisição de imagem: 1) câmara Flir One PROLT de baixo custo e baixa resolução (60 x 80 pixéis) e 2) câmera Flir A35 de custo moderado e resolução média (320 × 256 pixels). Os dados térmicos foram complementados com a medição das trocas gasosas foliares e por medições da fluorescência da clorofila ao pintor e pré-colheita. O impacto dos tratamentos no estado hídrico da videira, foi também

avaliado pelo cálculo do índice de stress hídrico da cultura (CWSI) estimado a partir dos dados térmicos obtidos pelas câmaras térmicas.

A FLIR A35, funcionando em conexão com um PC, exigiu o uso do software gratuito de aquisição de imagens FLIR tools, enquanto o Flir ONE PROLT, conectado a um *smartphone*, exigia o aplicativo dedicado. Posteriormente, as imagens adquiridas foram analisadas usando o software gratuito Fiji (distribuição imageJ). As duas câmaras térmicas permitiram obter imagens em formatos digitais diferentes, pelo que foi necessário estabelecer dois protocolos. Verificou-se ser muito mais simples e rápido a análise das imagens com a FLIR A35 pois é possível utilizar-se um plug-in e um pacote de macros chamado ThermimageJ. Este pacote permite a análise de imagens diretamente em formato JPEG radiométrico e também permite definir os valores térmicos desejados. No entanto este software não pôde ser usado com imagens obtidas pela FLIR ONE PROLT pois as imagens eram RGB.

Os resultados da FLIR ONE PROLT mostraram que esta apenas deteta diferenças na temperatura da superfície do solo, entre zonas sombreadas e zonas expostas á luz solar não sendo capaz de detetar pequenas diferenças de temperatura, pelo que o seu uso revelou.se inadequado para o cálculo do índice térmico CWSI. Os resultados obtidos pela câmara térmica FLIR A35 foram significativamente mais robustos que os obtidos pela FLIR One. A Flir A35 foi capaz de distinguir diferenças de temperatura entre tratamentos quer para a superfície do solo quer para as folhas/sebe (monitorizar o perfil vertical de temperatura da sebe).

Os resultados da Flir A35 mostraram que a cobertura morta reduziu a temperatura de superfície comparativamente á testemunha e que a parte superior da sebe tinha valores mais baixos de temperatura que a parte inferior (zona dos cachos), embora tal fosse independente do tratamento. Os valores de CWSI calculados com os dados da Flir A35, mostraram uma tendência sazonal de aumento que se deve provavelmente ao aumento do stress longo da estação, principalmente durante a tarde, sendo a cobertura com palha de arroz a que resultou aparentemente num menor nível de stress. Este estudo preliminar mostrou que, tantas câmaras térmicas de baixa e média resolução e custo, necessitam ainda de optimização ao nível dos protocolos de aquisição e processamento de imagem tendo em vista reduzir o tempo de trabalho e padronizar metodologias para se obterem resultados mais robustas.

Table of contents

AKNOWLEDGMENTS 1

ABSTRACT 2

RESUMO 3

LIST OF TABLES *8*

LIST OF FIGURES *9*

LIST OF ABBREVIATIONS *12*

1. GENERAL INTRODUCTION AND AIMS *14*

2. LITERATURE REVIEW *17*

2.1. Viticulture vs Climate Change 17

2.1.1. Viticulture in Europe 17

2.2. Adaptation strategies to climate change: short-term vs long-term 19

2.2.1. Short-term adaptation strategies 20

2.2.2. Long-term adaptation strategies 21

2.3. Precision viticulture: sensors and platforms 22

2.3.1. The electromagnetic radiation and related sensors 22

2.3.2. Remote sensing technologies 23

2.3.3. Aerial Platforms 25

2.3.4. Terrestrial/ground-based platforms 27

2.4. Thermal imaging: principles and characteristic 27

2.4.1. Thermal Radiation characteristics 29

2.4.2. Thermography and plants 30

2.5. Thermal indexes and canopy temperature 33

2.6. Applications of thermography to plant science and viticulture 33

2.7. Low-cost sensors in thermography: advantages vs disadvantages 34

2.8. Image analyses and open-source software 35

2.8.2. The IRimage open-source tools 36

2.9. Conclusions and future prospects 37

3. MATERIAL AND METHODS *39*

3.1. Location, climate, and soil conditions 39

3.2. Plant material 40

3.3. Soil and canopy management and soil water 40

3.4. Experimental set-up and treatments 40

3.5. Visible RGB and Thermal imaging 43

3.5.1. Thermal sensors 43

3.5.2. Imaging set-up 44
3.6. Measurements 46
3.7. Imaging analyses protocol development 47
3.7.1. Protocol steps to analyse Flir A35 Images using the Fiji software 47
3.7.2. Protocol steps to analyse Flir One Images with FIJI (ImageJ Distribution) 51
3.8. Leaf gas exchange and chlorophyll fluorescence measurements 53
3.9. Statistical analysis 54
4. RESULTS 55
4.1. Climate conditions and soil water 55
4.2. Soil surface temperature 56
4.3. Canopy and vertical temperature profile 59
4.4. Thermal index CWSI 62
4.5. Stomatal conductance to water vapour and PSII efficiency 64
5. DISCUSSION 67
5.1. Imaging set up and image analysis 67
5.2. Image analysis and processing 69
5.3. Soil and canopy temperature vs mulching treatments 70
5.4. Canopy temperature and CWSI 71
5.5. Leaf gas exchange and Chl fluorescence 72
5.6. Flir One Pro LT 72
6. CONCLUSION AND FUTURE 74
REFERENCES 76
APPENDIX 97

LIST OF TABLES

Table 1 Sensing technology, platforms, and their uses in viticulture 25
Table 2 Pros and cons of using Satellite and UAV platforms at the level of acquisition and data processing (++ excellent, + good, o medium, - low) (adapted from Manfreda et al., 2018).....27
Table 3 Different optical characteristics for different materials, from high reflecting material like aluminium to a black body (adapted from Kaplan, 2007). 28
Table 4 Characteristics of the different low-cost thermal sensor. Prices are taken in commercial information available on the companies or commercial sites (Adapted from Villa et al. 2020) 35
Table 5 Indicative list of open-source and paid software analyses 36
Table 6 Resume of the characteristics of the two thermal cameras used in the trial (Flir A35 and Flir One). NETD - Noise Equivalent Temperature Difference. 43
Table 7 Climate conditions and soil moisture measured along the season and during the day (9.00-10.30 and 15-16.30h) 55
Table 8 Twet and Tdry values obtained by Flir A35 camera along the season. Twet – Fully transpiring leaf; Tdry no transpiration.....62

LIST OF FIGURES

Fig. 1 Left panel: highest and lowest yield decrease due to heatwaves for each winemaking region at the peak date. Right panel: geographical representation of the highest and lowest decrease in yields over Europe at the peak date (Fraga et al., 2020). 18
Fig. 2 An electromagnetic wave consisting of electric and magnetic oscillating fields. In this example, the oscillating electric field vectors are indicated in red, while the green lines represent the magnetic field vectors (Potter et al., 2019) 22
Fig. 3 The electromagnetic spectra and the infrared (IR) spectra (Abbas et al., 2012) 23
Fig. 4 *Comparison of the most important aspects of UAS and satellite monitoring (Manfreda et al., 2018)* 26
Fig. 5 Schematic functioning of a typical Infrared radiation thermometer (Kaplan, 2007). 30
Fig. 6 Energy exchange of a young leaf, where LE = latent heat flux, cooling of the leaf by transpiration, LWin = longwave radiation, i.e., the LW radiation absorbed by the leaf, LWout = longwave radiation emitted by the leaf at Tleaf, SW = longwave radiation, i.e., incoming SW radiation absorbed by the leaf, H = heat detected, where the blue and red colors indicate cooling and heating of the leaf by the environment, respectively the last term in the equation is LWout, which stands for Tleaf and contains the Stefan-Boltzmann constant Ϭ (5.67x 10^{-8} W · 10^{-8} W · m^{-2} · K^{-4}) Source: (Still et al., 2019). 31
Fig. 7 *Vineyards are located in the campus of Instituto Superior de Agronomia. The red line indicates the location of the experimental plot used in the trial. Source (Google Earth).* 39
Fig. 8 Diagram of the experimental set up showing the filed plots with the different treatments (control, eucalyptus mulch and rice straw mulch). The two central rows (lines 24 and 25) were used in the trial described in this thesis. We used a total of 10 vines per treatment (5 vines per row per treatment). Losana, (2022) 41
Fig. 9 *The three different treatments; a) control with natural soil cover; b) the eucalyptus mulch* 42
Fig. 10 Flir A35 (on the left) and Flir One Pro LT (on the right) 43
Fig. 11 Overall view of the imaging set up in the vineyards. RGB and thermal images were taken from the sunlit side of the canopy. Each RGB and thermal image contained

a total of 5 vines per row. Images were taken in the morning (9-10.30h) and in the afternoon (15-16.30h). 45
Fig. 12 Example of a set of RGB and respective thermal images for canopy measurement taken with the Flir A35 (320x256 pixels) (B) and the Flir One (80x60 pixels) (C). 46
Fig. 13 *Example of a set of RGB and respective thermal images for ground-surface measurement taking with the Flir A35 (320x256 pixels) (**B**) and the Flir One (80x60 pixels) (**C**)* 46
Fig. 14 All steps required to image analyses for Flir One Pro LT using FIJI software52
Fig. 15 ROIs selected for ground-surface measurement using Fiji software 52
Fig. 16 Licor 600 components (on the top) and field measuring (bottom) 53
Fig. 17 Soil moisture data from 2022 season (JAN-SEP) collected by the soil capacitance probe located at “Meia Encosta” vineyard. Blue bars represent LRAW, red bar URAW. (Source: https://www.aquacheckweb.com/index.html) 55
Fig. 18 Soil moisture data from 2022 season (JUNE-SEP) with the treatments indicated with black lines, collected by the soil capacitance probe located at “Meia Encosta” vineyard Blue bar represent LRAW, red bar URAW. (Source: https://www.aquacheckweb.com/index.html). 56
Fig. 19 Ground-surface temperature values obtained by Flir A35 thermal camera along the season and at two times of the day (morning-afternoon). *Values are means from two ROI areas selected in the thermal images (see M&M).* 57
Fig. 20 *Ground-surface temperature values obtained by the Flir One Pro LT thermal camera during the season and at two times of the day (morning-afternoon). Values are means from two ROI areas selected in the thermal images (see M&M)* 58
Fig. 21 *Canopy temperatures obtained by using a Flir A35 thermal camera during the season and at two times of the day (morning-afternoon). Full filled coloured bars indicate the lower part of the canopy (cluster zone) while the pattern bars indicate the top part of the canopy. Values are means of (n= 10) 12 August rice straw 9h (n=5). Different letters indicate significant differences between treatments considering a p-value (0.05). Upper caps letter refers to cluster zone and small size to the top part of the canopy.* 60
Fig. 22 *Canopy temperatures obtained by using a Flir One ProLT thermal camera during the season and at two times of the day (morning-afternoon). Fuller bars indicate*

the cluster zone of the canopy while drawn bars indicate the higher part. Values are means n=10..... 61
Fig. 23 *Value of the Crop Water Stress Index (CWSI) measured for the three treatments (soil cover – control., Eucalyptus leaves and Rice straw) along the season and based on the data retrieved by the Flir A35 camera*..... 63
Fig. 24 Value of Stomatal conductance obtained by the porometer LI-600 (Licor Biosystems). Values are means ± SE (n=30)..... 64
Fig. 25 PSII efficiency measured under light conditions by using LI-600 (Licor Biosystems). Values are means (n=30)..... 65

LIST OF ABBREVIATIONS

ABA- Abscisic acid

CO_2- Carbon dioxide

CWSI- Crop water stress index

FOV- Field of view

GNSS - Global Navigation and Satellite System

GPS - Global positioning system

HIS - Hyperspectral sensors

IMU- Inertial Measurement Unit

IR- Infrared

LW- Longwave radiation

MSI - Multispectral sensors

MTD- Maximum temperature difference

NDVI- Normalized difference vegetation index

NETD- Noise Equivalent Temperature Difference

NIR- Near-infrared

PAR- Photosynthetically active radiation

PCD- Photon-counting detector

PSII- Photosystem 2

RGB- Color space red, green, blue

ROI- Region of interest

SW- Shortwave radiation

TIR- Thermal infrared

UAS - Unmanned Aerial System

UAV - Unmanned Aerial Vehicles

VIS - Visible region

VPD - Vapor pressure deficit

VSP -Vertical shoot positioning

WUE - Water use efficiency

ρ- Reflectance

f - Frequency

E- Transpiration

E_A- Absorbed energy

E_I -Incident energy

E_R- Reflected energy

E_T- Transmitted energy

gbw- Boundary layer conductance to water vapor

gsw-Stomatal conductance to water vapor

gtw- Total conductance to water vapor

ƛ- Wavelength

α- Absorbance

τ- Transmittance

1. GENERAL INTRODUCTION AND AIMS

Water and heat stress experienced by grapevine is a very important aspect to be accounted in Mediterranean viticulture because it influences growth, yield, and berry composition, with a large impact on eco-physiological, biochemical, and molecular processes in plants (Lisar et al., 2012; Chaves et al., 2010; Costa et al., 2016; Gambetta et al., 2021)

Climate change is imposing increasing stress situations. Severe drought and high temperatures, (> 35 ºC) cause the activation of plant adaptation strategies such as stomatal closure by interrupting transpiration and the consequent decrease of photosynthesis by limiting CO_2 supply (Chaves et al., 2010). In more extreme stress conditions, it can occur photoinhibition of photosystem II in parallel with the arrest or decrease of growth or leaf senescence (Feller and Vaseva, 2014)

More sustainable viticulture involves a more precise and efficient use of resources e.g., water and soil. Many existing strategies can be used to optimize sustainability and water use in agriculture and viticulture, improved monitoring of plants and soil conditions has been possible by the use of remote sensing approaches (e.g., thermography, spectral reflectance). Other approaches to promote sustainable crop and soil management in modern viticulture may also include the use of alternative soil management strategies. This is for example the case of organic mulching as means to protect soil from erosion, promote water infiltration, control weeds while improving crop water status. Mulching has shown considerable advantages, not only because it limits water loss from the soil via evaporation, but it also improves soil quality by increasing organic matter in the soil and consequently influencing water retention (Ngosong et al., 2019; Jiang et al., 2015).

Novel imaging technologies can offer new opportunities to support crop and soil monitoring. Nevertheless, there is still the need to find and optimize a more convenient, rapid, and replicable methodology to identify vineyard variability and the condition of individual vines namely in terms of water status. This is particularly important if we consider low-cost technologies that it still requires still validation for agronomic purposes.

One strategy to monitor water deficit in plants is by measuring their surface temperature by using thermal imaging (Jones et al., 2004; Costa et al., 2013). Plant temperature can be a good indicator of stress in plants and crops because leaf temperature is regulated primarily by transpiration, which cools the leaf surface. Under stress conditions, cell guard regulation is a key factor to regulate leaf photosynthesis and plant water relations because cells sense their surroundings and respond rapidly to abiotic and biotic stress factors (Crawford et al., 2012).

Thermal imaging emerges as a tool to use in remote sensing and non-invasive systems to assess plant and soil temperature and water status in agriculture but also in viticulture

(Jones and Vaughan 2010; Costa et al., 2016) vineyard. It is a very useful method because it can help the vine grower decide when and how much water to apply to help the plants in difficult situations. Moreover, this method can be applied manually or by using platforms for accurate quantification (Costa et al., 2010). Nevertheless, it needs still to be optimized and simplified to have a wider use in the sector.

Thermal imaging is a quite flexible tool. It has been successfully applied in different conditions (lab, field, and greenhouse) and to different plant species (fruit trees, grapevine, cereals, forest) (Costa et al., 2013; Jones, 2004). Moreover, thermography can be applied at different scales (e.g., from individual seedlings/leaves, whole trees, or field crops to regions), providing good opportunities to study plant-environment interactions and specific phenomena such as aberrant stomatal closure, genotypic differences in stress tolerance and the impact of different management strategies on crop water status (Jones, 2004; Costa et al., 2013). However, the accuracy of thermographic measurements is affected by environmental variability (e.g., light intensity, temperature, relative humidity, and wind speed) (Jones 2004; Costa et al., 2013; Mangus et al., 2016)

Measurement of the plant water status is a quite important determination, and it is not always fast or easy to do. Therefore, this study aims to develop and optimize a low-cost and fast methodology for field measurements of water stress in grapevine, making use of low to medium-cost thermal sensors coupled to proximal sensing and ground-based platforms. To this extent, we combined the use of thermography with a proximal sensing and ground-based platforms such as the Vinbot robot (Lopes et al., 2016) as means to detect reliably, the temperature of vine's canopy as well as of the soil surface. It is also purposed as a free and simple way to process and analyse thermal images to simplify the retrieval of meaningful thermal data.

Therefore, the aims of this research study are

1) As part of the INTERPHENO project(https://interpheno.rd.ciencias.ulisboa.pt/pt/home-2/), investigate the performance and usefulness of two thermal cameras with low to moderate cost (FLIR One PRO LT and the FLIR A35) in vineyards as means to detect vine condition (water status) on the basis of canopy and soil surface temperature along the season and under conditions of organic mulching or normal soil cover;

2) Optimize image retrieval and further analysis of the images retrieved by the two cameras and compare the output and robustness of the two cameras (for field measurements of both canopy and soil temperature);

3) Evaluate the impact of different organic mulching options on canopy and soil surface temperature along the season;

2. LITERATURE REVIEW

2.1. Viticulture vs Climate Change

2.1.1. Viticulture in Europe

The European Union is the world leader in the production of both bulk and bottled wine. The area planted with vines in the EU covers more than 50,4% of that of the world (7.4 million ha) and about 62,9% in terms of production volumes (292 million hl). (OIV, 2019).

Most of the European wine-producing regions renowned for wine production are characterized by temperate, oceanic, or humid continental climates (Kottek et al.,2006), but the Mediterranean region is expected to suffer from climate change, with major decreases in yield and berry quality (Giorgi 2006; Atkinson et al., 2013; Costa et al., 2016). Within the EU, the countries that suffer or will suffer the most from climate change are the southern Mediterranean areas (Figure 1) characterized by decreased rainfall, and higher soil and air temperatures. Such type of climatic conditions (water deficit and high temperatures) will limit yield and berry composition (Medrano et al., 2003; Chaves et al, 2010; Lionello et al., 2014).

2.1.2. Impact of climate change on European viticulture

It is predicted that climate change will increasingly cause extreme events of greater frequency, duration, and intensity in the future (Ingvordsen et al., 2018). The impact of climate change on viticulture is having very significant effects and the number of publications on this topic has increased steadily (Bernardo et al., 2018; Costa et al., 2022). In recent decades, OIV (International Organisation of Vine and Wine) and academic research has increasingly focused on the topic of “sustainability in viticulture and winemaking” (OIV, 2021; Gerling, 2015). This is evidenced by the increasing number of publications combining topics such as sustainability, viticulture, winemaking, and climate change over the last decade (2010-2020) (Costa et al., 2022).

Climate change has a great impact on the wine sector and especially in Mediterranean areas, where it will lead to significant changes in the natural adaptation mechanisms of the plant such as physiology, biology as well the berry quantity, quality, and date of harvest (Iglesias et al., 2007). This negative effect is caused by variables that impact individually or a combined effect (e.g., interaction between high temperatures and high radiation, water deficits) (Fraga et al., 2012; Costa et al., 2016).

The IPCC report of 2021 reveals that if measures to reduce greenhouse gas emissions are not implemented by 2040, the temperature could increase by at least 1.5°C. (IPCC, 2021). This could become an important problem as far as the impact of high temperatures on grape physiology is concerned. The impact of high air temperatures on grapevine physiology is huge

(Molitor, et al., 2014; Chaves et al. 2010). When exceeding 35°C it will have negative effects (Ferrini et al., 1995) such as a decrease in photosynthesis and therefore a decline in growth and production (Moutinho-Pereira et al., 2004; Levin et al., 2020).

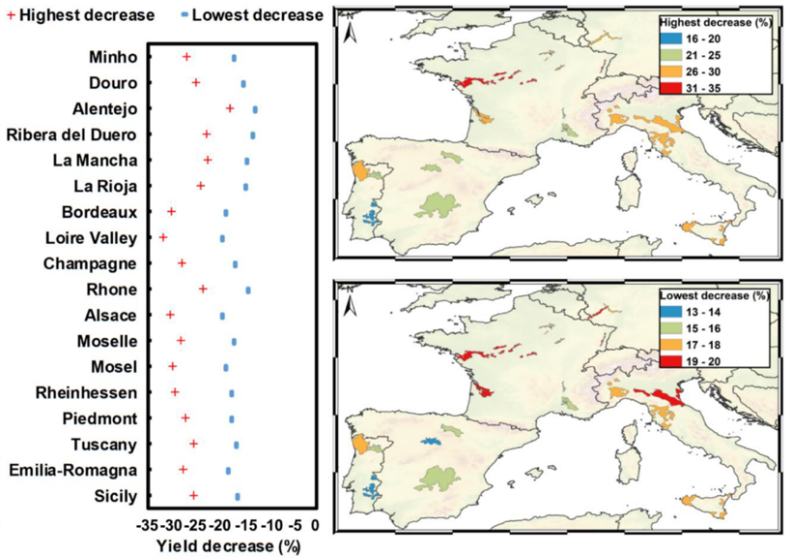

Fig. 1 Left panel: highest and lowest yield decrease due to heatwaves for each winemaking region at the peak date. Right panel: geographical representation of the highest and lowest decrease in yields over Europe at the peak date (Fraga et al., 2020).

Heat waves are defined as extreme events in which, for a minimum period of five days, the daily temperatures exceed the average temperatures by five degrees (Fraga et al., 2020). The impact of heat waves on yield depends on many territorial factors that vary their severity, but two main characteristics change the severity of this phenomenon in the same region: heatwave peak and period. The longer the duration of the heat waves peak, the greater the decrease in yield (Brown, 2020). The role of soil temperature is also important to consider, cause dryer soils will warm faster and contribute to the heatwave.

Drought is one of the main environmental factors reducing crop yields worldwide and the combined effects of drought and high temperatures on physiology, growth, water relations, and yield are much greater than the effects of the individual factors (Grigorova et al., 2011; Carvalho et al., 2015). Water scarcity (drought) and high air and soil temperatures are important environmental factors limiting plant growth in many regions of the world, and although these two stresses often co-occur together little is still known about the effects of their combination on plants (Rizhsky et al., 2004). There is also a link between temperature rise and air relative humidity: as temperature rises, soil moisture, and relative humidity decrease, increasing the VPD which ultimately promotes plants transpiration (Hossain et al., 2012).

The response to water and heat stress can vary with the varieties of grapevine (Costa et al., 2012). In a case study with Riesling and Cabernet Sauvignon, Hernandez-Montes et al. (2019) observed during flowering that water stress reduced leaf gas exchange (transpiration and

photosynthesis) in two combined stress reduced leaf gas exchange only in Riesling. In the pre-flowering period, heat stress reduced leaf water potential, gas exchange and chlorophyll fluorescence in both young and mature leaves. Combined stress significantly reduced most parameters compared to the control plants, but this reduction was greater for Riesling than for Cabernet Sauvignon. The same authors report that during the recovery periods, no significant differences were found between the treatments for any of the parameters, suggesting that both varieties were able to fully recover from the stress they had been exposed to.

Heat stress and drought can also affect the metabolism and thus the chemical composition of grapes, affecting several compounds, mainly water, fermentable sugars, organic acids, nitrogenous compounds, minerals, pectin, phenolic and aromatic compounds.

The metabolic rate of the grapes depends to a large extent on ambient temperature. High temperatures disrupt various metabolic pathways, leading to changes in the biosynthesis of compounds important for the quality of grape must (Blancquaert et al., 2018). In particular, high temperatures are expected to reduce acidity and increase sugar content in the grapefruit, leading to unbalanced wines with higher alcohol content and less freshness and aromatic complexity (Bernardo et al., 2018; Neethling et al., 2012). High temperatures also reduce anthocyanin content, because its expression is strongly influenced by temperature: low temperatures lead to an increase in gene transcript levels, while high temperatures lead to a decrease (Mori et al., 2007)

A decrease in pigmentation is also very common and occurs when temperatures exceed 30°C, while at temperatures above 37°C there is a decrease in wine colour and increased evaporation of aromatic compounds (Bernardo et al., 2018; Neethling et al., 2012). At high temperatures, a decrease in delphinidins, anthocyanins, petunidin and petunidin-based anthocyanins was observed, but no malvidin derivatives biosynthesis was observed in grapes (Bernardo et al., 2018). Under heat stress conditions, especially during the grape ripening phase, the potassium content in the fruit increases, which raises the pH and reduces overall acidity (Bernardo et al., 2018). Malic acid is also metabolized faster than tartaric acid with increasing temperature. The optimum temperature for malic acid accumulation is 20-25°C, while temperatures above 40°C show a significant decrease (Keller, 2010).

2.2. Adaptation strategies to climate change: short-term vs long-term

Adaptation strategies that can be used individually or in combination to counteract the effects of climate change and minimise the impact of heat and water stress on vines. They can be divided into two different categories: short term and long-term adaptation strategies (Santos et al., 2021).

2.2.1. Short-term adaptation strategies

Short-term adaptation strategies include viticultural practices that are used along a growing season or on a year-to-year basis and they can include:

i. Adapted canopy management

Proper and adequate canopy management aimed at mitigating the effects of climate change brings good results by impacting the reproductive cycle and thus delaying the harvest date. This leads to a great benefit by delaying bunch ripening to a period with better climatic temperatures or at least not under conditions of heat stress (Santos et al., 2021). An example of a good strategy of proper canopy management aimed at mitigating the effects of climate change is apical leaf removal. Thanks to this strategy there is a delay in ripening by reducing photosynthesis and by reducing the ratio of leaf area to fruit weight (Santos et al, 2021). For example, after fruit set, the canopy area can be reduced to less than 0.75 m2/kg to increase the time from flowering to harvest by about 5 days (Neethling et al., 2016).

ii. Supplemental irrigation

Irrigation is a widespread and consolidated strategy to overcome the water deficit and to maintain a yield level by economic interests (Neethling et al., 2016; Duchêne et al, 2014; Costa et al. 2016). There are several supplemental and deficit irrigation strategies that can be used in different climatic conditions and depending on a cost/benefit relation. For example, a study conducted in the Mediterranean, used subsurface drip irrigation and kept leaf water potential between -0.4 and -0.6 MPa respectively before and after veraison and led to improvements in WUE and yield without affecting grape quality (Pisciotta et al., 2018)

iii. Soil management and mulching

Proper soil management is a very useful tool to prevent soil water loss and erosion and consequently counteract climate change. Limiting tillage when necessary and using cover crops with low water and nutrient demand reduces water loss and the risk of erosion. One of the most useful techniques, to be considered and further explored, that can contrast climate change is mulching, a technique that maintains moisture in the soil and limits water stress (water scarcity and high temperatures) that climate change is increasingly accentuating (Neethling et al, 2016; Santos et al., 2020a).

Mulching can be implemented by using organic or inorganic materials that can be applied to the soil surface. The use of mulches can help to reduce soil compaction and keep soil moisture while regulating soil temperature and reduce evaporation (Chen et al., 2007; Novak et al., 2000). Mulching not only conserves water but also improves soil quality and increases the amount of organic matter in the soil (Ngosong et al., 2019). Mulching can also be useful for pest and weed control. Previous studies have shown that mulching can help maintain production levels in adverse weather conditions while reducing water consumption (DeVetter et al., 2015). In addition, mulching helps reduce soil erosion and can be adaptable for most

farmers. Therefore, there is a need to better understand the impact of mulching on future yields (Fraga and Santos, 2018). However, in Mediterranean areas, there is a limitation in terms of the availability of organic residues that can be used as mulches. Besides the transport costs are quite high, which forces the use of residues or mulches only in a restricted geographical area.

Ultimately, the role of mulching on soil temperature is also very important. Mulch materials inhibit evaporation and increase soil moisture (Horton et al., 1996). As another consequence, mulches can help reduction of soil temperature (Shinners et al., 1994). Moreover, mulched soils will have a reduced heat load as compared to bare soils which contributes for lower soil surface temperature (Shinners et al., 1994; Onwuka and Mang 2018).

2.2.2. Long-term adaptation strategies

The use of long-term adaptation strategies for winegrowers is still difficult to implement, not because they are particularly complicated but because they embrace so many uncertainties such as the unpredictability of socio-economic development and land use change. Long-term adaptation strategies would require transformational options or structural changes (Santos et al., 2021).

i. Changes in the training system

In the Mediterranean wine-growing areas the choice should be oriented towards farming systems that favour a small leaf area trying to keep the same fruit ratio as means to limit water consumption due to transpiration and increase tolerance to drought. (Costa et al., 2016; Van Leeuwen, et al., 2016; Santos et al., 2020). If it is not possible to transplant or replant, for various reasons such as the desire to preserve the age of the vineyard as a distinguishing characteristic, or the high replanting costs, low-energy training system with semi-minimal hedge pruning combined with a no-thinning treatment can delay bunch rot and fruit ripening (Molitor et al., 2019)

ii. Varietal selection

Because of climate change, berry ripening is now more irregular and it is anticipated by high temperatures and drought. Therefore, over time, more and more late ripening varieties are planted to allow that berry maturation occurs in a period with optimal temperature (Van Leeuwen et al., 2016)

One of the main problems in using cultivars different from those traditionally and culturally used is that implies a great financial risk, especially for those *terroirs* in which the variety issue is a strong matter of differentiation (Santos et al., 2020b).

iii. Site relocation

This is a drastic possibility that involves changing locations from areas where vines suffer too much from the conditions dictated by climate change to coastal, elevated areas with less exposure to the sun (Santos et al., 2020b; Van Leeuwen et al., 2016).

2.3. Precision viticulture: sensors and platforms

Precision viticulture is a strategy to reduce environmental impact by combining advanced information and data analysis technologies to maximize production efficiency (Santesteban, 2019). This permits the use of information to improve quality and increase yields in viticulture while reducing waste production and pollution. Several sensors mounted on different types of platforms can be used to capture images by detecting regions of the electromagnetic spectrum. Subsequently, this process is followed by image analysis that with the use of specific software, allows more accurate decisions to be made.

2.3.1. The electromagnetic radiation and related sensors

The electromagnetic spectrum and spectral resolution

Electromagnetic radiation is a form of energy that starts with low-energy radio waves and ends with high-energy gamma rays. This is not the only form of energy found in nature, there are also others such as mechanical, sound, and nuclear chemistry. Each type of energy can

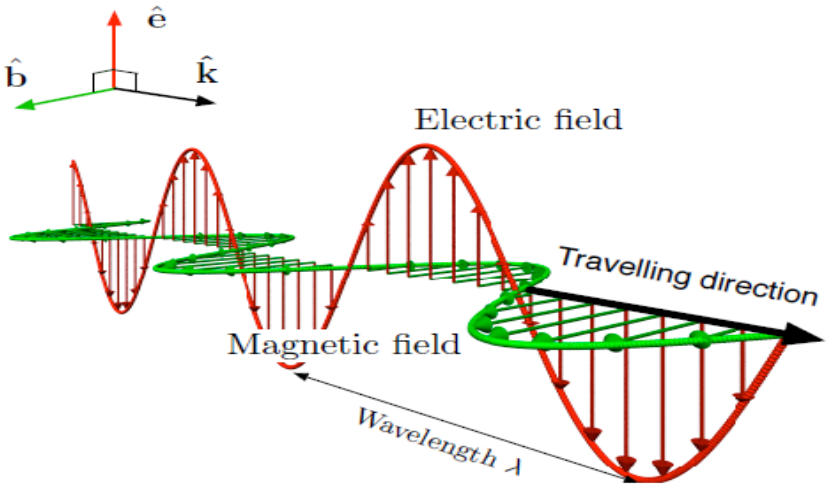

Fig. 2 An electromagnetic wave consisting of electric and magnetic oscillating fields. In this example, the oscillating electric field vectors are indicated in red, while the green lines represent the magnetic field vectors (Potter et al., 2019)

transform into the other but remain constant due to the conservation of energy law (Jones and Vaughan, 2010). Electromagnetic radiation is represented as waves, and to measure these waves, we use wavelength measured in meters and as the distance between adjacent wave crests. The frequency is measured in hertz (cycles per second) as the number of waves passing through a point per second (Jones and Vaughan, 2010) (Figure 2).

All electromagnetic waves are represented in a spectrum that contains them all from high-energy gamma rays to low energy low-energy radio waves and is called the electromagnetic spectrum. Since the velocity (c) of electromagnetic waves is constant, their characteristics are mainly given by their frequency (f) and wavelength (λ) as shown in the following formula:

$$\lambda f = c \; ; \; \lambda = c/f \qquad \text{Eq. 1}$$

Due to their properties, the electromagnetic waves within the spectrum can be divided into different regions as depicted in Figure 3. The human eye can only detect a very small portion called VIS (visible) which corresponds with the photosynthetically active region (PAR) (Jones and Vaughan, 2010). In the case of spectral resolution, we refer to the acquisition of images characterized by several wavelengths that can be recorded simultaneously (Hall et al., 2002). There are different sensors designed to detect different regions of the electromagnetic spectrum and therefore different spectral resolutions.

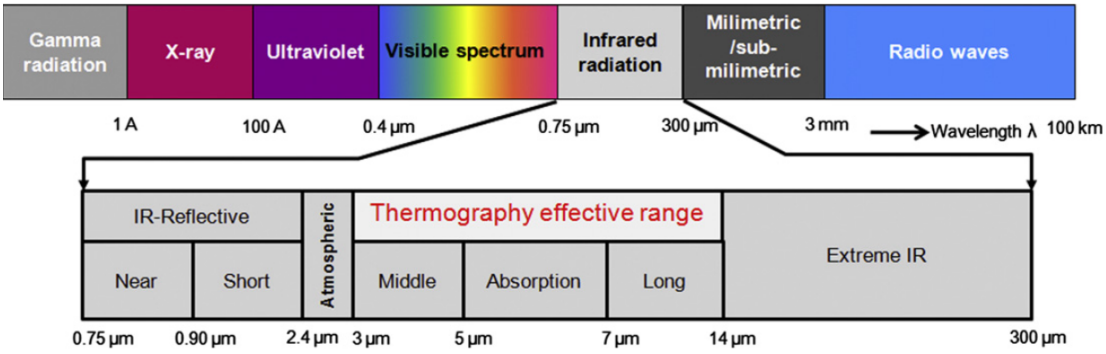

Fig. 3 The electromagnetic spectra and the infrared (IR) spectra (Abbas et al., 2012)

2.3.2. Remote sensing technologies

Remote sensing is based on the detection and measurement of the amount of the reflected or emitted radiation by the crop or the soil at different wavelengths. In addition, the type of wavelength (ultraviolet, visible, IR and microwave) for detection determines the type of sensor to be used (Jones and Vaughan, 2010).

Spectral reflectance can be measured with spectrometers. Particularly important are the wavelengths of the visible (VIS) (400-750 nm) and near infrared (NIR) (750-2500 nm) spectra. In the VIS region, many organic molecules undergo electronic transformations, thus influencing properties such as colour. Therefore, this spectral range is often used to evaluate pigments in vine leaves and fruit. Spectroscopy-based technologies can also be used to assess soil properties (Schirrmann et al., 2013). There are different types of spectral sensors which differ in the number of wavelengths they can record. Multispectral sensors (MSI) measure radiation in several, usually four to six narrow wavelengths. Wavelengths can be

separated using filters or instruments that are sensitive to specific wavelengths. In agricultural production systems, spectral indices are generally related to photosynthetically active biomass, which in turn can be related to vegetation size and/or health. Of these spectral indices, NDVI and PCD (Photon-counting detector) are widely used in viticulture (Hall et al., 2011).

Hyperspectral (HSI) sensors are also a powerful technique for evaluating food and crop condition (Tardaguila et al., 2021; Gutiérrez et al., 2019). The spectral resolution is the main factor that distinguishes HSI from MSI. HSI deals with narrower wavelengths over a continuous spectral range, thereby generating the spectra of all pixels of the object. HSI sensors collect information as a set of 'images', where each image represents a narrow wavelength range of the electromagnetic spectrum (Grahn and Geladi, 2007). Compared to MSI, the principal advantage of HSI is that, because an entire spectrum is recorded at each spatial position, the operator does not require prior knowledge of the object. The main disadvantage of HSI compared to MSI is the cost and complexity, but rapid development of the technology is likely to ease this impediment through the production of faster computers, more sensitive detectors, and larger data storage devices (Fraga & Santos, 2018).

Infrared thermal sensors (also known as thermal imagers) detect and measure the infrared energy emitted by an object (https://www.fluke.com/en-us/learn/blog/thermal-imaging/how-infrared-cameras-work). The camera converts this IR data into an electronic image that shows the surface temperature of the object being observed (Costa et al., 2010). The IR camera has an optical system that focuses IR light onto a special detector chip (sensor array) that contains thousands of gridded detection points. Each pixel of the detector array reacts to the IR radiation directed at it and generates an electronic signal (Kaplan, 2007; https://www.fluke.com/en-us/learn/blog/thermal-imaging/how-infrared-cameras-work). The camera's processor receives the signal from each pixel and uses mathematical calculations to create a colour map of the apparent temperature of the object. Each temperature value is given a different colour. The resulting colour map is sent to memory and sent to the camera display as an image of the object's temperature (thermal image) (https://www.fluke.com/en-us/learn/blog/thermal-imaging/how-infrared-cameras-work).

Table 1 Sensing technology, platforms, and their uses in viticulture

SENSING TECHNOLOGY	PLATFORM	USES IN VITICULTURE	REFERENCES
HYPERSPECTRAL	Aircraft	Chlorosis detection	(Zarco-Tejada et al. 2005)
	Ground vehicle	Disease detection	(Bendel et al., 2020)
	Ground-platforms	Berry composition	(Benelli et al.,2021)
MULTISPECTRAL	Drone / UAV	Disease detection Vegetation monitoring	(Berni et al., 2009)
	Satellite	Vegetation monitoring Vigour	(Campos et al.,2021)
THERMAL	Portable Aircraft Drone / UAV Ground-vehicle	Water status Berry temperature Detecting freezing damage Detecting biotic stress	(Costa et al., 2019; Jones et al.,2002) ;(Sepúlveda-Reyes et al., 2016) ;(Gutiérrez et al.,2018) ;(Pagay et al., 2019); (Stoll & Jones, 2007); (Prashar & Jones, 2014); (Lindenthal et al., 2005; Oerke et al., 2006)

2.3.3. Aerial Platforms

I. Satellite and aircraft

Satellite acquisitions allow large maps to be obtained at the expense of resolution, roughly between 10 m and 60 m. For this type of survey, images can be acquired using the Sentinel-2 satellite, which is unfortunately insufficient for detailed applications, namely when dealing with row crops, where the distinction between soil and canopy is needed. In addition, in the presence of cloud cover, they are not suitable for monitoring phenological phases (Matese, 2015).

II. UAVs

Unmanned Aerial Vehicles (UAVs) such as drones can compete with or complement other remote sensing platforms and technologies such as aircraft satellite. This makes it possible to obtain more precise images, up to a centimetre scale, even if this requires a huge quantity of images.

The UAS (Unmanned Aerial System) consists of several components: the drone, the ground control system, and the operator, that all together manages the flight and controls the area. Position information is provided by the GNSS (Global Navigation and Satellite System) which regularly transmits position measurements sampled in three dimensions. The drone is controlled through the IMU (Inertial Measurement Unit) (Whitehead and Hugenholtz, 2014). Some advantages of using UAVs include: 1) Reduced cost; 2) No pilot on board; 3) Adjusting the focal distance by changing the flight altitude and 4) - Manoeuvrability; 5) Possibility of flying in cloudy conditions; 6) - Possibility of integration with different cameras and sensors and 7) High spatial resolution. These aspects make it possible to decrease costs per survey, acquire very high-resolution images, optimize acquisition times and consequently be more responsive during phenological phases (Stroppiana et al., 2019).

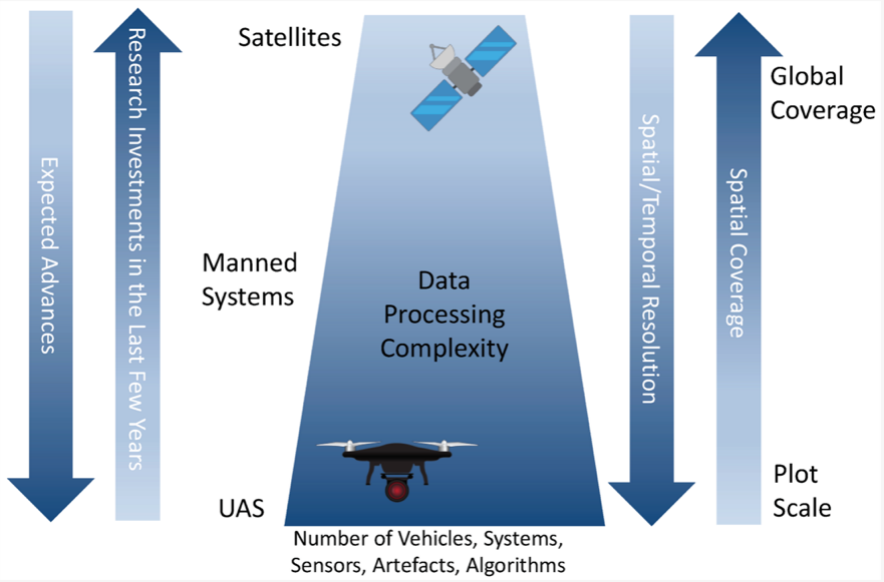

Fig. 4 *Comparison of the most important aspects of UAS and satellite monitoring (Manfreda et al., 2018)*

Among the disadvantages and aspects to be improved it is worth mentioning:

- Reduced flight autonomy
- Meteorological constraints: UAVs are vulnerable in the presence of heavy rain or wind with consequent alteration of detection
- Time of acquisition; it should be borne in mind that acquisitions should be carried out in constant weather conditions and as close to midday as possible.

- Distortion is due to rely low-altitude flights are more prone to this kind of distortion camp (Matese, 2015) (Whitehead et al., 2014; Manfreda et al., 2018).

Table 2 Pros and cons of using Satellite and UAV platforms at the level of acquisition and data processing (++ excellent, + good, o medium, - low) (adapted from Manfreda et al., 2018)

		UAV	Satellite
Acquisition	Areal coverage	**-**	**++**
	Flexibility	**++**	**-**
	Flight autonomy	**-**	**++**
	Dependence on cloud cover	**++**	**-**
Raw data processing	Payload	**-**	**++**
	Resolution	**++**	**o**
	Processing speed	**-**	**+**

2.3.4. Terrestrial/ground-based platforms

Ground-based platforms are widely used for remote sensing. Usually tractors or robots (e.g., Vinbot) are used to install thermal or multispectral sensors. In addition, these platforms are equipped with GPS, which is useful to create high-resolution maps used for precision management (Jones and Grant, 2016). Interest is shifting strongly to proximal sensing, where new technologies make it possible to collect information with a high resolution so that vineyard variability can be defined. The focus is now shifting towards the use of on-the-go terrestrial platforms that allow the acquisition of images by using all-terrain vehicles or tractors thus allowing to have a map that covers a large area. One of the main problems of this method and equipment is that during image acquisition not only vegetation is captured but also all the materials/objects present inside the imaged area. Therefore, these images must be subsequently processed to create Regions Of Interest (ROI) (Gutiérrez et al., 2018). Another limitation is the speed it is still about 5 km/h (SOURCE).

2.4. Thermal imaging: principles and characteristic

Thermal imaging cameras measure plant body temperature, which could potentially be used as an indicator of bunker blockage or water stress. In recent years, the advent of thermal imaging cameras, especially in combination with automated image analysis, has greatly facilitated their use. This imaging method is more accurate than infrared thermometers because it reduces the influence of the ground background by segmenting the thermal image

in areas where ground cover is visible (Maes and Steppe, 2012). However, thermal imaging cameras can measure relative temperatures rather than actual temperatures. To quantify the actual surface temperature, the infrared imager needs to be calibrated under ambient conditions. (Mangus et al., 2016)

Thermography is mainly used to assess the water status of plants. The use of thermographic techniques is based on the fact that when water is lost through the stomata, the temperature of the leaves is lowered. However, when the stomata are closed, transpiration stops, and leaf temperature rises. (Costa et al.,2010)

Specific radiations within the electromagnetic spectrum are used to acquire thermal images. This electromagnetic spectrum consists of different wavelengths corresponding to different frequency ranges. The electromagnetic spectrum is composed of different wavelengths and different frequency ranges. Within the electromagnetic spectrum, we find different regions such as x-rays, visible light, infrared light, and radio waves (Da Silva et al., 2020).

When working with thermal infrared radiation, the TIR (thermal infrared) band, is between 4-15 μm. This region is often split into three different regions such as shortwave thermal <8μm, longwave thermal >8μm and far infrared 15 μm–100μm (Kaplan 2009). This is very important to know because every material reflects in a different TIR spectral band as shown in table 3. Another important characteristic of bodies that influences thermal radiation measurements is their emissivity. Emissivity is a measure of how well a material radiates heat, and it depends on the materials (Fig.3). The more reflective materials such as aluminium have low emissivity values.

Table 3 Different optical characteristics for different materials, from high reflecting material like aluminium to a black body (adapted from Kaplan, 2007).

TYPE OF MATERIAL	**WAVELENGHT (μm)**	**EMISSIVITY**
Aluminium foil	3	0.09
Frozen soil	LONGWAVE	0.93
White paper	SHORTWAVE	0.68
Vines leaf	LONGWAVE	0.96
Black body	/	1

2.4.1. Thermal Radiation characteristics

All matter at a temperature above 0˚K emits radiation, and the higher the temperature, the more energetic is the internal motion of the atoms and molecules, which causes the radiation (Jones and Grant, 2010). According to the Stefan-Boltzmann law we have:

$$W = \varepsilon \boldsymbol{\sigma} (T_{leaf})^4 \qquad \text{Equation 1}$$

W= Radiant flux emitted per unit area (watts/cm^2)

ε= Emissivity (unity for a blackbody target)

$\boldsymbol{\sigma}$= Stefan's constant 5.673 x 10^{-12} watts cm^{-2} K

T= Temperature of the radiator (K)

We can divide the sources into two ideal models called the black body and the white body. In the first case, we have a model in which the material absorbs all the radiation that affects it and emits as much of it as possible at a given temperature. in the second case, it neither emits nor absorbs any energy. The emissivity values vary from 1 for the black body to 0 for the white body (Jones and Vaughan, 2010). The thermal energy radiated by a blackbody radiator per second per unit area is proportional to the fourth power of the absolute temperature (Nave, 2016). In the IR thermal region, the interaction is mainly due to the rotation and vibration of molecules. Therefore, the emissivity of a surface determines the efficiency with which such interaction occurs. This is achieved by electric field vectors in electromagnetic radiation which cause vibrational transitions in the matter. During the interaction between radiation and matter, energy is not lost but is conserved as the sum of the energy dissipated by reflection, transmission, and absorption as indicated by the (eq. 2) and it can be written also as (Eq. 3) (Jones and Vaughan, 2010).

$$E_{I(\lambda)} = E_{R(\lambda)} + E_{A(\lambda)} + E_{T(\lambda)} \qquad \text{Equation2}$$

E_I = *Incident energy*

E_R= *Reflected energy*

E_A= *Absorbed energy*

E_T= *Transmitted energy*

$$\rho + \alpha + \tau = 1 \qquad \text{Equation 3}$$

ρ= Reflectance

α= Absorbance

τ= Transmittance

A relevant aspect of thermal imaging is that each compound or molecule has a specific signature. This is because each material, depending on its composition, can absorb, transmit and reflect at different frequencies. This is referred to as the spectral signature, the detector (contactless sensor) is pointed at a spot, and it can measure the IR radiation from it and converting in a value of temperature and then correct it for the right value of estimated or measured emissivity of the target (Kaplan, 2007) (Figure 5)

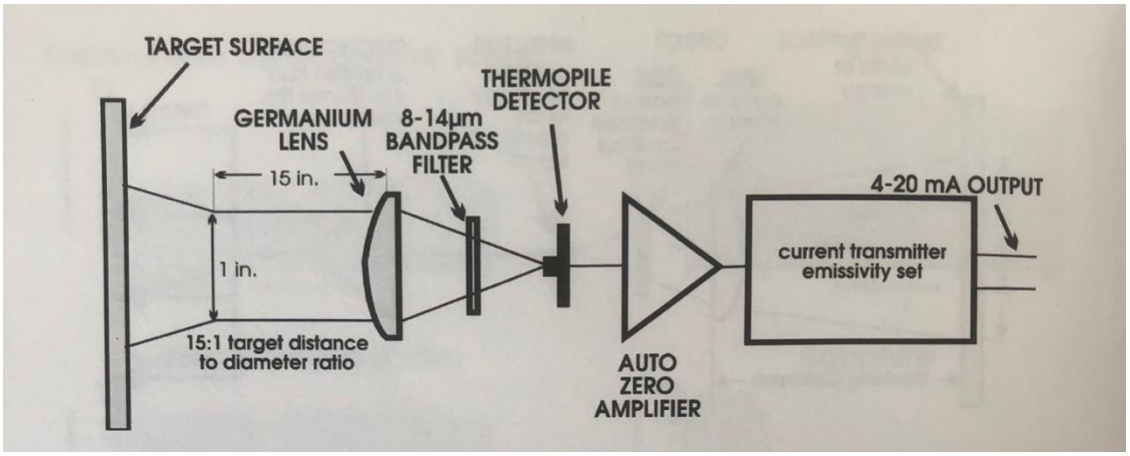

Fig. 5 Schematic functioning of a typical Infrared radiation thermometer (Kaplan, 2007).

2.4.2. Thermography and plants

Plants and leaves interact with the environment via energy exchange processes (Costa et al., 2013). The temperature of plant depends on several factors, such as the surrounding climate conditions (clear or cloudy sky, air temperature, wind speed), time of the day, soil characteristics (soil type, water content, soil covering, soil colour) and leaf morphological characteristics (Jones, 2004). All these parameters can influence the ratio and magnitude of sensible and latent heat fluxes (Costa et al., 2013).

Sensible heat flux (H) is directly determined by the conductivity of the leaf boundary layer, with lower values increasing Tleaf for a given H. For a given Rnet, increased water stress can lead to decreased stomatal conductance and LE, resulting in decreased leaf transpiration and increased Tleaf. In contrast, ΔT (Tair-Tleaf) and H increase (Still et al., 2019).Leaf temperature

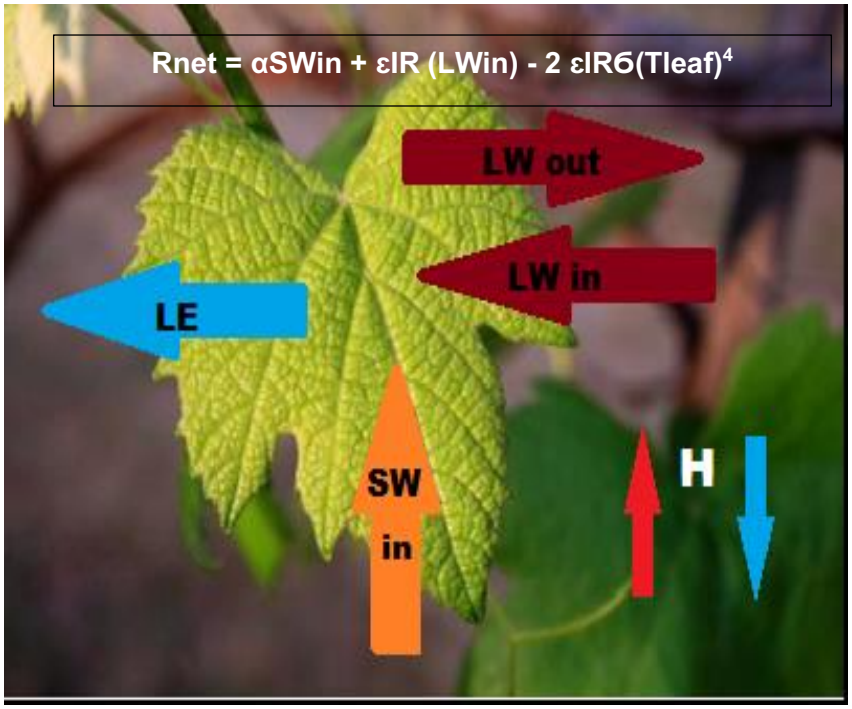

Fig. 6 Energy exchange of a young leaf, where LE = latent heat flux, cooling of the leaf by transpiration, LWin = longwave radiation, i.e., the LW radiation absorbed by the leaf, LWout = longwave radiation emitted by the leaf at Tleaf, SW = longwave radiation, i.e., incoming SW radiation absorbed by the leaf, H = heat detected, where the blue and red colors indicate cooling and heating of the leaf by the environment, respectively the last term in the equation is LWout, which stands for Tleaf and contains the Stefan-Boltzmann constant Ϭ (5.67x 10^{-8} W · 10^{-8} W · m^{-2} · K^{-4}) Source: (Still et al., 2019).

is the result of leaf energy balance. This balance includes energy input and output (Costa et al., 2013; Still et al., 2019). Inputs are related to shortwave (SW) and longwave radiation (LW) absorbed by the leaf. Water-stressed plants usually maintain a fine regulation of stomatal closure and opening to allow metabolic processes such as photosynthesis or to prevent heat damage (Chaves et al., 2016). *Citrullus colocynthis* plants growing in deserts where air temperatures are close to the survival threshold use increased transpiration to cool leaf temperatures (Chaves et al., 2016). Under water stress conditions, one of the short-term responses of plants is to close stomata to balance water loss, evaporative cooling, and photosynthesis. This varies between regions and between genotypes/clones (Chaves et al., 2010, 2016; Simonneau et al., 2017). Therefore, an increase in canopy temperature due to stomatal closure can be a good indicator of water stress, which can be measured with infrared thermometers (Alchanatis et al., 2006). These methods allow non-contact and non-destructive monitoring of crop water stress (Jones, 2004).Under drought or heat stress conditions, higher water use efficiency (WUE) is related to stomatal closure and reduced transpiration, as well as increased leaf temperature (6-7 °C above air temperature) (Chaves et al. 2016). Stomatal closure is linked to the phytohormone ABA (abscisic acid), which sends signals from the roots to the top of the plant, causing a reduction in vigour and subsequent stomatal closure due to osmotic outflow from guard cells (Damour et al. 2010; Chaves et al., 2010). In model plants *Arabidopsis thaliana*, but also in crops water stress was found to trigger ABA biosynthesis in

shoots and subsequent signalling leading to stomatal closure (Chaves et al., 2011; 2016). As reported by Martorell et al. (2015), variations in water potential correlate with ABA concentration in cotyledons: ABA concentrations below 200 g/ml under means no water stress conditions, but ABA concentrations above 300 g/ml under water stress conditions, as drought causes hormonal responses in plants that result in reduced gs. Under drought conditions, the requirement for atmospheric evaporation also increases, stimulating the stomatal response to VPD, which may indicate different mechanisms of water accumulation. In fact, depending on the variety, the sensitivity of stomata to drought varies there are isohydric (pessimistic) and anisohydric (optimistic) varieties. Anisohydric cultivars allow stomata to open to regulate transpiration when leaf water potential decreases whereas isohydric cultivars close their stomata at the first sign of stress in order to maintain high leaf water potential (Simonneau, et al., 2017; Damour, et al., 2010). Drought stress can cause stomata to close, thereby retaining water in the plant and preventing water loss by the leaves but increasing leaf temperature by 6-8°C and an increase in WUE (Chaves et al., 2011; Pou et al., 2008). Stomatal closure and gs correlated with ABA levels in cysts, whereas during water stress, re-hydration correlated only with hydraulic conductance, which was also lower (Pou et al., 2008). Another physiological process that can be altered by stomatal closure during water stress is photosynthesis, which involves a complex metabolic pathway in which carbon dioxide is transported from the atmosphere to the active site of ribulose-1-5-biphosphate carboxylase/oxygenase (Rubisco) in the chloroplast (Chaves et al., 2011). Stomatal defence cells are exposed to endogenous and exogenous signals such as light, CO_2, VPD and hormones (ABA, auxin). Thus, cells can rapidly open and close in response to atmospheric changes (Chaves et al., 2011). In addition to regulating transpiration, stomata also influence leaf temperature: when stomata are close to a water retention site during water stress, leaf temperature usually rises by 5-6 °C, depending on air temperature. This can be important for maintaining a constant leaf temperature (Chaves et al., 2011).

As described by Downton et al. (1987) under sunny conditions, e.g., in summer, carbon CO2 assimilation decreases during the day as temperature rises. According to the same authors a 10°C rise in temperature results in a reduction of about 6 μmol CO_2 m^{-2} s^{-1}. This is in line with Lovisolo and colleagues (2010) that observed a photosynthesis decreases around midday (11:00-15:00h) and that stomatal closure was associated with ABA accumulation in xylem and petiole, increased xylem pH and decreased hydraulic conductivity.Non-state factors are also responsible for this reduction. As reported by Lovisolo et al. (2010), gs is less sensitive to ABA and more sensitive to CO_2 in the afternoon. The main factors are feedback through source-sink interaction, reduction of mesophyll conductance to CO_2, light and light inhibition (Lovisolo et al., 2010) showed that the quantitative efficiency of the PSII (Photosystem 2) is lower in the afternoon at all light intensities. Air temperature also affects the rate of photosynthesis.

Downton et al. (1987) showed that gs and photosynthetic rate are reduced at 39°C. Late in the evening, the leaves begin the process of photosynthetic recovery.

2.5. Thermal indexes and canopy temperature

Canopy temperature has long been considered an indicator of plant water status (Jones, 1999; Jones et al., 2002), as leaf temperature is related to stomatal conductance under constant environmental conditions (Jones, 1999). Furthermore, stomatal regulation is a key factor in photosynthesis and plant water status, affecting plant survival, adaptation, and growth. Stems sense the environment and respond rapidly to abiotic and biotic stress. Therefore, water vapor conductivity (gs) and/or transpiration (E) are valuable physiological parameters to monitor in plant breeding and agricultural sciences. However, the measurement of leaf gas exchange is associated with leaf contact and is often time consuming. Canopy temperature is also affected by changes in environmental conditions (Maes and Steppe, 2012). To alleviate this problem, heat stress indices such as CWSI (Idso et al.,1981) and Ig have been developed to account for the effect of environmental fluctuations on canopy temperature (Jones et al., 2002).
Transpiration affects leaf energy balance and consequently their temperature (T-leaf). It is thus possible to estimate or quantify gs and E using thermal imaging. However, the accuracy of thermal measurements is affected by environmental variability (e.g., light intensity, temperature, relative humidity, wind speed). In this review, the advantages of using thermal imaging in plant production, agriculture, and ecology, as well as the limitations and possible approaches to minimize them, are presented and discussed using examples from previous and current studies.

2.6. Applications of thermography to plant science and viticulture

The use of thermography in viticulture is diverse and can involve academical research or applied research. It has been used for multiple assessments and purposes such as:

- Berry temperature monitoring: temperature influences ripening and thus most of the quality of the berry. Thermography is a system that allows monitoring heat stress and consequently modulates ripening with agronomic techniques (Stoll and Jones, 2007).
- Crop water status monitoring

  Thermography is one of the most effective non-invasive methods for assessing water status in vineyards (Jones et al., 2002; Costa et al., 2010; Shellie and King, 2020). This technology allows producers to determine where and when to irrigate, which can improve water management, yield, and fruit quality. Thermal cameras have been used for manual monitoring of water regimes in vineyards (Fuentes et al., 2012; Pou et al., 2014; Grant et al., 2016;) and for remote irrigation scheduling using aerial platforms such as drones (Baluja et.al; 2012; Bellvert et al., 2014). Recently, ground vehicles have been equipped

with thermal cameras to map water conditions in commercial vineyards (Gutiérrez et al., 2018; 2021)

- Irrigation systems monitoring: Thermal cameras can also detect water leaks during irrigation (Stoll et al., 2007) and thus reduce water loss.
- Detect biotic stress: because a multispectral camera can show the temperature variation within the leaf it is possible to predict through the MTD (maximum temperature difference) index a reliable index to detect an infected leaf tissue from a healthy one in this specific case by P*lasmopara viticola* (Lindenthal et al. 2005; Oerke et al. 2006).
- Detect freezing damage: the vine is a plant that is very sensitive to frost damage, especially as regards the organs with a high-water content. Temperatures below -2 degrees have been found to cause irreversible damage to the affected organs, especially leaves, shoots, and green buds. Thermography comes in handy here, as it can be used to identify when water freezes inside a tissue, generating an exothermic process that heats it. Thermography can detect the temperature variation in a tissue. (Prashar and Jones, 2014).
- Plant selection: Leaf temperature can be a good parameter to select genotypes with different stomatal behaviour in both model plants (*Arabidopsis thaliana*) and crop species e.g., cereals and grapevine (Costa et al. 2013).

2.7. Low-cost sensors in thermography: advantages vs disadvantages

Recent developments in low-cost IR sensors, compatible with smartphones, provide competitive advantages for home-monitoring applications (Neves, 2018). Indeed, thermal technology has become available for smartphones and can be more accessible to all growers. In Australia, (Petrie et al., 2019) used a miniature thermal camera connected to a smartphone to assess water conditions in vineyards. Several commercial IR cameras are currently available and were compared and evaluated in the medical field (Villa et al., 2020). The technical requirements were low, medium, or high cost, low weight, internal optics and electronics, and compatibility with mobile devices. Different cameras were found to meet these requirements, and the characteristics provided by the manufacturers are summarized in Table 4. Nevertheless, there is still the need to validate their measurements for application to viticulture and other field crops.

Table 4 Characteristics of the different low-cost thermal sensor. Prices are taken in commercial information available on the companies or commercial sites (Adapted from Villa et al. 2020)

CHARACTERISTICS	Seek thermal Contact Pro (ST)	Thermal expert TE-Q1 Plus (TE-Q1)	Flir one Pro LT	CAT sS60	Flir TG165X	IRXCAM-640
Spatial resolution (pixels)	320 x 240	384 x 288	80 x 60	80 x 60	80 x 60	640 x 480
Frame rate	>15 Hz	<9 Hz	8.7 Hz	8.7 Hz	8.7 Hz	60 Hz
NETD/MRTD	< 70 mK	< 50 mK	100 mK	150 mK	<70 mK	<50 mK
Price (Euros)	473	832	376	407	451	/
Manufacturer	Seek Thermal Inc. (Santa Barbara, CA, USA)	I3system, Inc. (Daejeon, Republic of Korea)	FLIR System Inc. (Wilsonville, OR, USA)	FLIR System Inc. (Wilsonville, OR, USA)	FLIR System Inc. (Wilsonville, OR, USA)	Canadian corporation INO (National Optics Institute)

Spatial image resolution has traditionally been one of the main drawbacks of low-cost cameras compared to high-end models (Manfreda et al., 2018). The use of IR thermometers with low resolution can be more limited as they provide an average temperature value for all objects in the sensor's field of view, and aspects such as shaded and unshaded parts of the vegetation cover and/or soil may not be easily detected (Neves 2018). The accuracy of these low-resolution sensors is even lower when plants are small and immature (Maes and Steppe, 2012). However, based on the work presented by Villa et al., (2020) the image resolution of the selected inexpensive cameras (384 × 288 pixels and 320 × 240 pixels) appears to be sufficient for the TE-Q1 and INOVASI cameras. The TE-Q1 and INO IRXCAM-640 cameras have a lower noise level and quality similar to the standard configuration. This improvement in image appearance is likely due to the TE-Q1's internal processing, which cannot be altered or controlled by the user. On the other hand, the ST images show high noise levels, which can be due to the lack of internal calibration. The results of the NETD values are consistent with the first visual inspection and show that the TE-Q1 and INO IRXCAM-640 values are similar, but the ST camera values are higher. The electronics of the INO IRXCAM-640 camera are very easy to adjust, which helps to reduce its NETD (Villa et al., 2020).

2.8. Image analyses and open-source software

Image analysis is an important component of the use of imaging systems in plant science and agriculture. Companies such as Flir have their software, but they are quite expensive,

especially the most versatile and complete analysis software (e.g., Therma CAM researcher (see https://www.flir.eu/support-center/Instruments/what-can-thermacam-researcher-2.8-do-and-what-is-the-difference-between-thermacam-researcher-2.8-professional-and-basic/). Therefore, open-source software is ideal for scientific research because it can be freely inspected, modified, and redistributed (Schindelin et al., 2015).

Table 5 Indicative list of open-source and paid software analyses

Software	**Web-source**	***Cost per year (USD)***	***Source***
FIJI	https://fiji.sc	free	
THERMIMGAEJ	https://github.com/gtatters/ThermImageJ	free	(Playà-Montmany &Tattersall, 2021)
IR IMAGE	https://github.com/gpereyrairujo/IRimage	free	(Irujo, 2022)
FLIR TOOLS	https://www.flir.com	free	Neves (2018)
FLIR RESEARCH STUDIO (standard edition)	https://www.flir.com	499	

2.8.1. ImageJ (Fiji distribution)

ImageJ is a widely used tool for scientific image analysis and is considered one of the "computer codes that changed science". (Perkel, 2021) Not only does it provide an accurate understanding of the measurements made to estimate temperature from raw sensor data, but also researchers can use the tool through ImageJ's graphical user interface (no programming required) or modify, customize, and extend the tool's functions using ImageJ's advanced scripting language (Cacciabue et al., 2019). ImageJ (especially the FIJI distribution) offers a large ecosystem of tools.

2.8.2. The IRimage open-source tools

The IRimage is a flexible and proven open-source tool for processing, measuring, and communicating thermal imaging data used in biological and environmental sciences (Irujo, 2022). It is especially useful when using low-cost consumer camera thermal imagery IRimage

processes thermal images by extracting raw data and calculating temperature values according to an open and documented algorithm, allowing further processing of the data with image analysis software. It can reproduce temperature measurements of an object in different images to obtain visual results (images and videos) suitable for scientific reports (Irujo, 2022). IRimage provides tools to extract and analyse temperature data in line with recommendations for working with reconstructed images (Miura and Nørrelykke, 2021) avoiding limitations posed by the analysis of thermal imagery data from household cameras. Software for these cameras is usually only capable of measuring temperatures for manually selected viewpoints or regions (García-Tejero et al., 2018; Nosrati et al., 2020). When dealing with large numbers of images, researchers often need to develop their dedicated software that cannot be reused by others (Van Doremalen et al., 2019; Goel et al., 2020; Mul Fedele et al., 2020), or use advanced methods to extract temperature values from colour data of fake images (Alpar and Krejcar, 2017; Petrie et al., 2019).

The software IRimage aims to improve the performance, accuracy, and reproducibility of thermal imagery, including imagery from low-cost and publicly available cameras. "IRimage" processes thermal images by extracting raw data and calculating temperature values according to an open and documented algorithm, allowing post-processing of the data with image analysis software. It is also possible to reproduce temperature measurements of an object in different images and to produce (Novak, 2000) visual results (images and videos) suitable for scientific reports." IRimage's capabilities are better suited for scientific research than many other currently available solutions, making consumer thermal imaging more accessible and reproducible for scientific research (Irujo, 2022).

2.9. Conclusions and future prospects

Thermography is one of the most used imaging techniques in science and the industry. Thermography emerged also as a tool to support precision agriculture and viticulture, namely, to monitor plant and soil water conditions, is a very useful tool, but one that still needs a great deal of study and optimization for more efficient and wider use in practice.

The use of imaging devices and platforms has brought considerable benefits in terms of technological advancement in this field, but different platforms have different pros and cons and must be used according to the objectives and to the budget available.

The use of thermography and related image analysis software is still prohibitively expensive for small to medium-sized companies or even for the academy that also miss qualified personnel and capital needed to use the instrumentation and mainly to analyse data. The literature review shows that there are several low-cost solutions available in the market and that thermal imaging analysis can be performed by free software. This can help to enlarge the use of thermography in viticulture and agriculture but also in plant selection and phenotyping.

Image analysis software can be expensive and the free options from companies have major limitations in terms of possibilities to analyse images. Therefore, the integration of low-cost imaging with free image analysis tools will be a breakthrough for wider use of thermography in viticulture. ImageJ (Fiji distribution), integrated with thermimageJ, gives the possibility of using more easily images from thermal cameras and reduces time related time-related to image calibration and ROI selection. It also gives the possibility of displaying the image with different LUTs and thus displaying the image with the classic colours of a thermal image (iron bow).

3. MATERIAL AND METHODS

3.1. Location, climate, and soil conditions

The study site was at the “Meia Encosta” vineyard that is located at the campus of Instituto Superior de Agronomia (38°42′24.61″ N 9°11′05.53″ W). The vineyard was planted in 2006 and is composed of seven white *Vitis vinifera* cv: Arinto, Moscatel de Setúbal, Alvarinho, Viosinho (grafted onto 1103 Paulsen rootstock) and the Encruzado, Macabeu, Moscatel Galego (grafted onto 110 Richter rootstock).

Fig. 7 *Vineyards are located in the campus of Instituto Superior de Agronomia. The red line indicates the location of the experimental plot used in the trial. Source (Google Earth).*

Climate normal from ISA’s meteo station indicate that the annual average air temperature (Tair) is 16.4°C with July and August as the warmest months (mean maximum Tair off 27.6°C and 28.0°C, respectively (Ervideiro, 2021). The annual average rainfall is 680.4 mm, concentrated mostly in the months of November, December, and January. In 2022 the season was characterized by 165,2mm of precipitation between January to September.

The soil of the vineyard was classified as clay soil with a pH ranging from 6.3 to 6.6, and with an average organic matter content (about 1.6 to 3%). It contains a very high concentrations of K, Mg, Fe, Mn, Cu, a high concentration of Ca and a medium-high concentration of P, according to a recent analysis report (Ervideiro, 2021). The expandability and the field capacity values are considered high with highly usable capacity in the first 50 cm. The vineyard is drip irrigated and standard cultural practices in the ISA vineyards were applied to all the Alvarinho to plots.

The climate in Lisbon is classified as Csa (C: warm temperature; s: summer dry; a: hot summer) as established by the classification of Köppen and Geiger (Kottek et al. 2006), with

higher precipitation in the winter than in the summer. The annual mean Tair is 15.4 °C and the annual mean precipitation (1973 to 2000) is 725.8 mm (IPMA, 2019).
Soil management and pest control were conducted by the “Gabinete de Espaços Verdes” and were the same as in the rest of the vineyard.

3.2. Plant material

This field experiment used plants of Vitis *vinifera* cv ‘Alvarinho’ a Portuguese white variety grafted onto an 1103 P rootstock. The 1103 P rootstock (*V. berlandieri* Résséguier no. 2 x Rupestris du Lot) is a quite vigorous rootstock, with good resistance to Phylloxera and drought tolerant, with medium salt tolerance and medium tolerance to water-logged soil conditions (Magalhães, 2015). Planting density was 4000 pl/ha (1 x 2,5m spacing) and rows were North-South oriented. (Figure 1). Vines are trained on a vertical shoot position VSP system and spur-pruned on a unilateral Royat cordon system with 10 to 12 nodes on five to six spurs per vine. The trunk high was around 65-70cm. To guide and sustain canopy vegetation growth there are two pairs of movable wires. The vineyard presents a slight 7° to 9° slope oriented from Northwest to South-east is the lowest point at 50 m above sea level and the highest at 70 m (Ervideiro, 2021).

3.3. Soil and canopy management and soil water

The experimental site was subject to similar standard cultural practices during the growing cycle, including water shoot removal, shoot trimming at 1.2 m above the cordon, shoot positioning and fertilization. Regarding soil, the inter-row space was covered with spontaneous vegetation managed periodically with the help of a tractor and a mower. Water was supplied with a drip irrigation system. Irrigation started on 21 of April, and after 1 May irrigation was done weekly. Soil water was monitored with capacitance probes at 10, 20, 30, 40, 50 and 60 cm depth (Figure 7). These probes were located in a contiguous line outside the experimental plots. We have used a sensor located in the middle of the rice straw treatment and data was received via web (https://www.aquacheckweb.com/index.html).

3.4. Experimental set-up and treatments

The experimental set up was originally implemented by Umberto Losana and Francisca Aguiar in Spring 2022, using 4 contiguous rows (23 to 26) of the vineyard located at the Instituto Superior de Agronomia, Lisbon. Each row and portion were divided into 3 sections of 5-6 meters, which were treated in the following way (Francisca Aguiar pers, common.):

- 1) About 25 cm thick rice straw mulch, for which were used around 500 kg per plot (2000 kg total), making it 104 ton/ha treatment.

- 2) About 15 cm thick Eucalyptus leaves mulch for which were used around 625 kg per plot (2500 kg total), making it 130 ton/ha treatment.
- 3) Control, natural soil covers similar to the remaining vineyard area

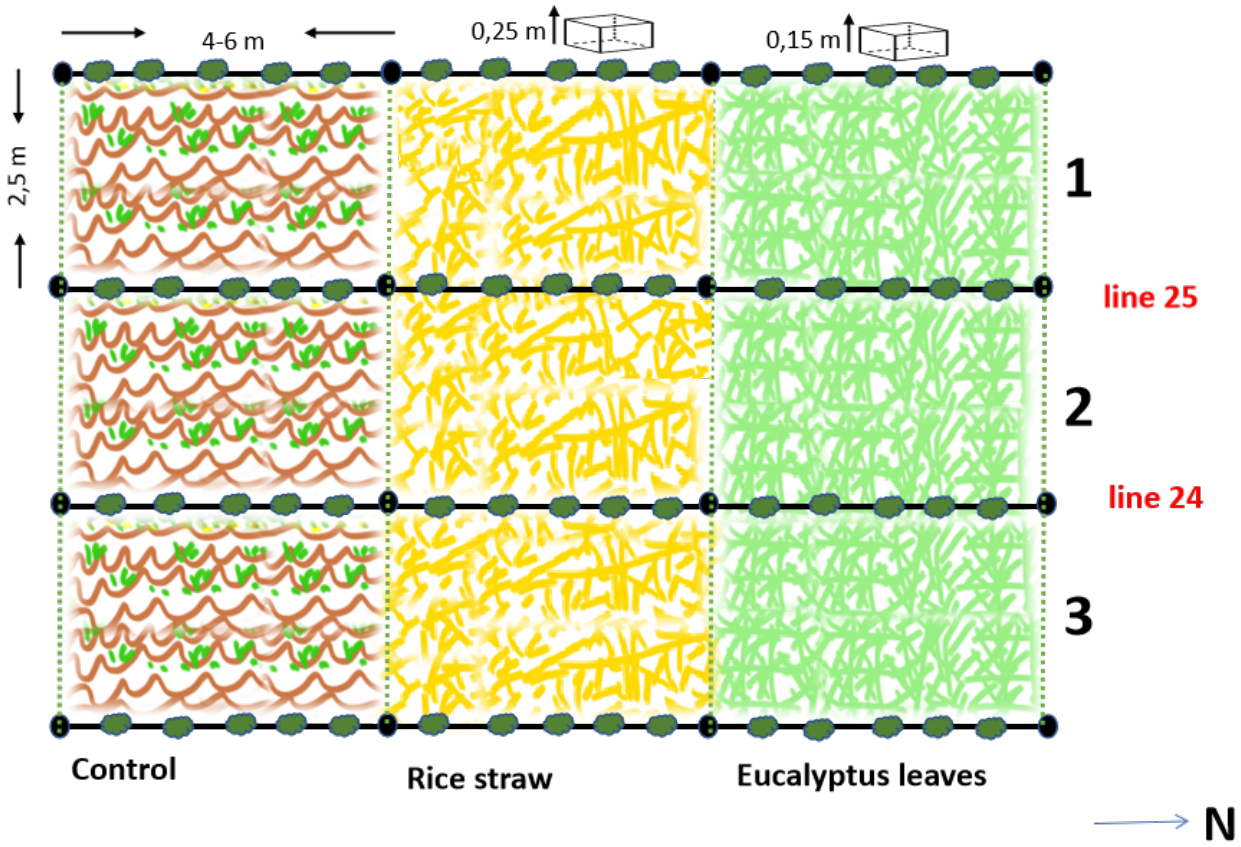

Fig. 8 Diagram of the experimental set up showing the filed plots with the different treatments (control, eucalyptus mulch and rice straw mulch). The two central rows (lines 24 and 25) were used in the trial described in this thesis. We used a total of 10 vines per treatment (5 vines per row per treatment). Losana, (2022)

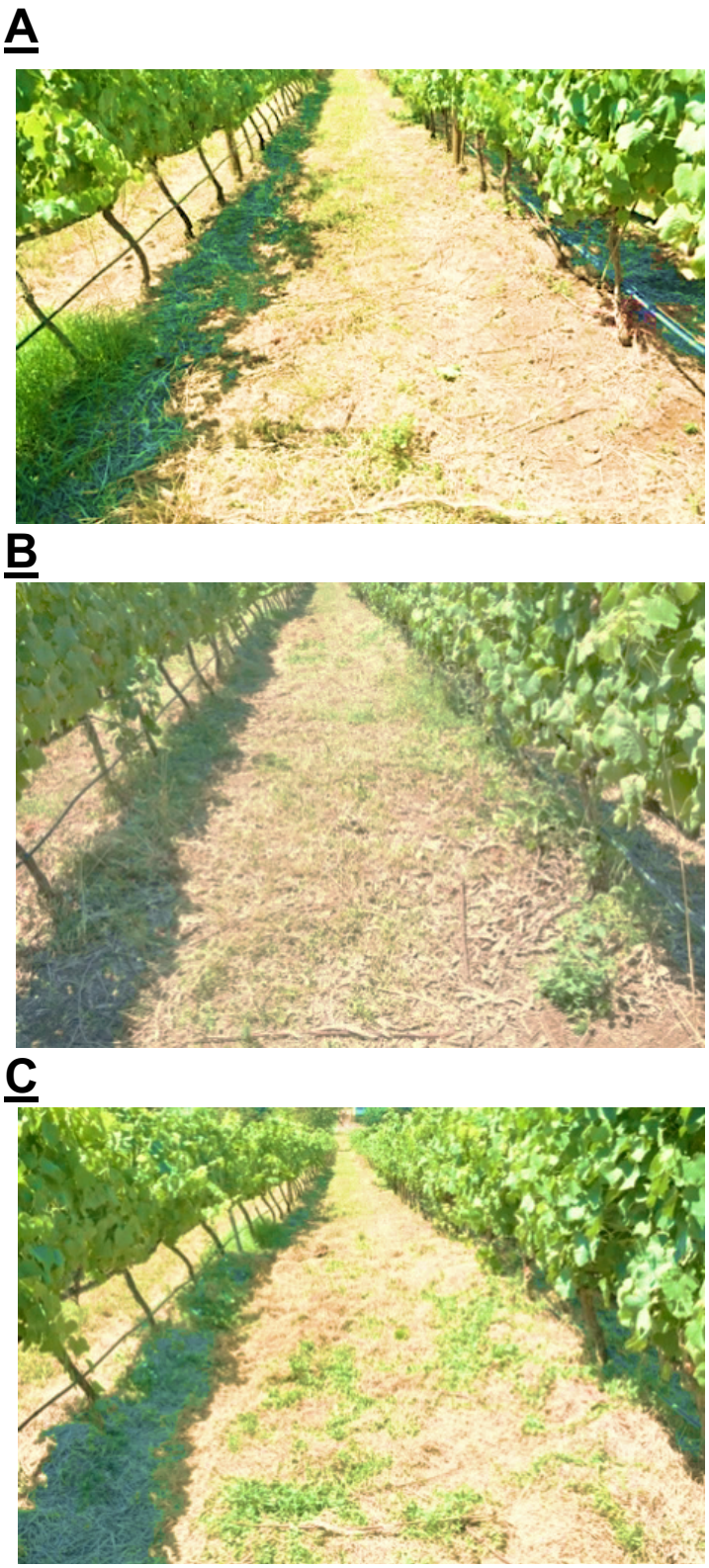

Fig. 9 *The three different treatments; a) control with natural soil cover; b) the eucalyptus mulch and c) the rice straw mulch. Images were taken during the first measurement on the 9June*

3.5. Visible RGB and Thermal imaging

3.5.1. Thermal sensors

Visible RGB images (Nikon ,,,,,,,,,,) were done from the soil (sunlit and shadow) and from the sunlit side of the canopies. Two thermal imagers, the FLIR A35 (Flir systems, USA) and the low-cost Flir One Pro LT (Flir, Systems, USA) were used. The FLIR A35, is a thermal imager often used for condition monitoring, process control/quality assurance, and fire prevention applications and it has been used in plant science/phenotyping and remote sensing (Ludovisi et al., 2017). The image sensor is a Focal Plane Array (FPA) based on uncooled microbolometers with spectral response in the range of 7.5–13 μm. The camera field of view is equal to 48° (horizontally) × 39° (vertically), it has an IR resolution of 320 × 256 pixels, and an acquisition frequency of 60 Hz. This camera requires an external power supply using two Ethernet cables, one input to the PC and one input to the power supply. It is a medium-high resolution thermal camera. The Flir One Pro LT is a thermal imaging low-cost (around 450 Euros) and low-resolution thermal sensor (80 x 60 pixels) that can be coupled to a mobile phone. It is used for condition monitoring, process control/quality assurance, and fire prevention application but there are also reports of sues in plant science and phenotyping (Neves, 2021). The FlirOne has less resolution than the A35 (Table 6) but stands out for its convenience of use, connecting to the smartphone plug being equipped with USB-C.

Fig. 10 Flir A35 (on the left) and Flir One Pro LT (on the right)

Table 6 Resume of the characteristics of the two thermal cameras used in the trial (Flir A35 and Flir One). NETD - Noise Equivalent Temperature Difference.

	FLIR A35	FLIR ONE PRO LT
IMAGE FREQUENCY	60 Hz	8,7 Hz
IR RESOLUTION	320x256 pixels	80 x 60 pixels
SPECTRAL RANGE	7,5-13 μm	8-14 μm
NETD	50 mK	70 mK

Thermal imaging was performed by making use of a robot (Vinbot) (Lopes et al.2016) punctually as a mobile ground platform and mainly as power source for the thermal camera Flir A35 via Ethernet power cable. The Vinbot platform is based on a Summit XL HL commercial robot, capable of carrying a payload of up to 65 kg (Lopes et al. 2016). Image acquisition was done in series, starting by the control, then the ice straw and finally the Eucalyptus mulch Images were taken from the row 24 and then from row 25 (See Fig. 10).

3.5.2. Imaging set-up

Because the RGB camera and the two thermal cameras had different field of view (FOV), this required to optimize distances between the cameras and the objects (soil and canopy). Once this distance to objects was set and the tripod location was defined, this permitted to speed up data acquisition by all the 3 cameras (first the Flir A35, then the Flir One Pro LT and at last the RGB camera). Overall, it took about 1-1.30h to collect the full set of images at each time of observation (morning and afternoon). The standardisation of the set-up of cameras with different FOVs made it possible to obtain very similar images and greatly facilitated the inclusion of multiple ROIs via the ImageJ ROI manager (Fiji) tool in the analysis of images taken by Flir A35 and Flir One PRO.The RGB and thermal imaging set up enable us to retrieve images with a field view (FOV) that included a total of 5 vines from each treatment for images from the soil/mulching covering (Figure 12 A and B). We used two plastic bars covered with aluminium to georeference the limits of the treatments and in order to have a representative image of the treatment. First, we measure 130 cm from the axis that determines the start of the treatment and position the camera at this point in the centre of the row. Maximum tripod opening at a height of 1.40m (See Figure 13 A and B).

For images from the sunlit side of the canopy, we have set up the equipment so that we have a 60 cm distance from the starting point of the first vine and a 1.80 m distance from the canopy as shown in (Figure 13 C and D). Both thermal imagers were able to image a total of 4-5 vines in the row as shown in Fig.13.

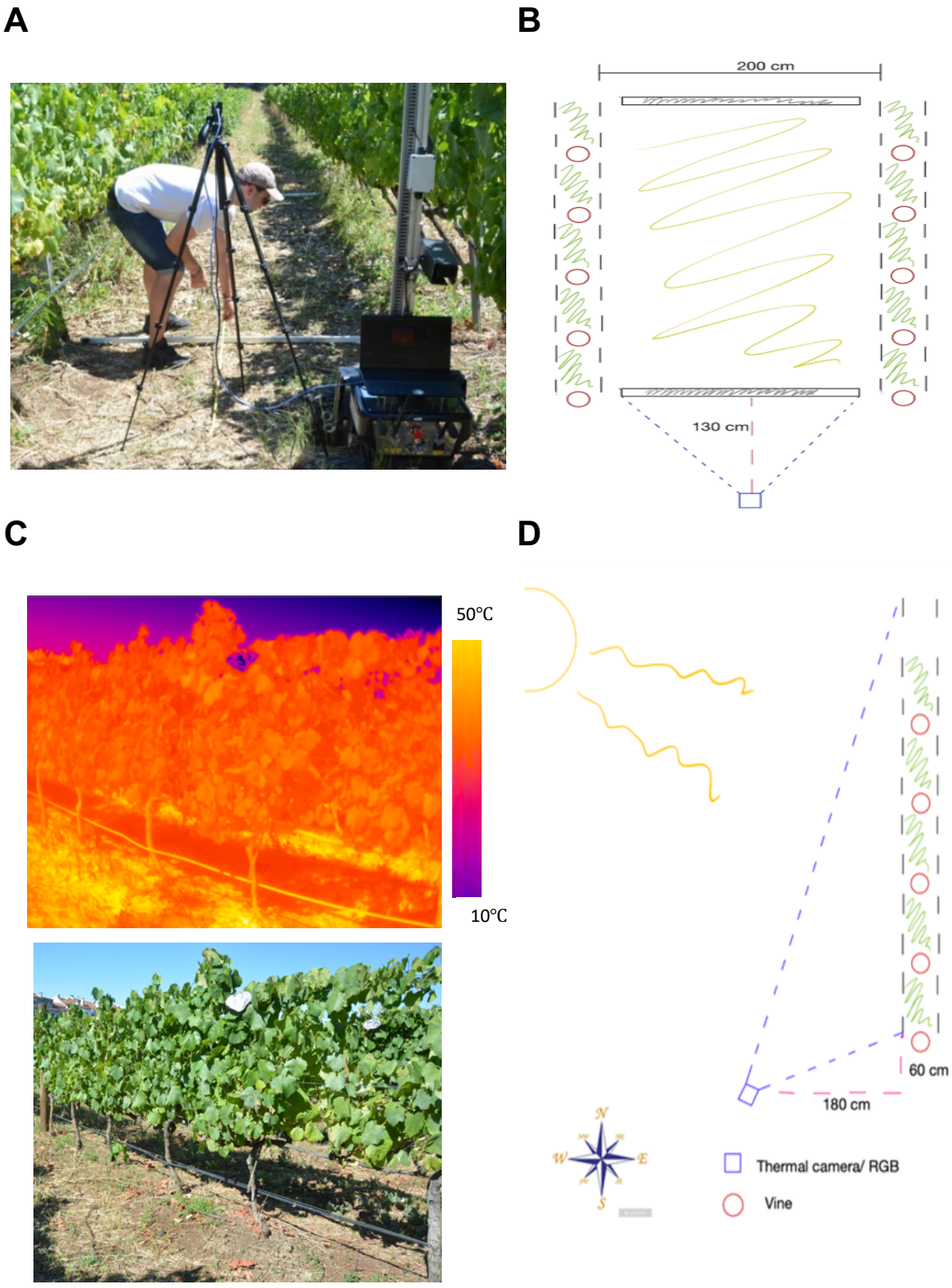

Fig. 11 Overall view of the imaging set up in the vineyards. RGB and thermal images were taken from the sunlit side of the canopy. Each RGB and thermal image contained a total of 5 vines per row. Images were taken in the morning (9-10.30h) and in the afternoon (15-16.30h).

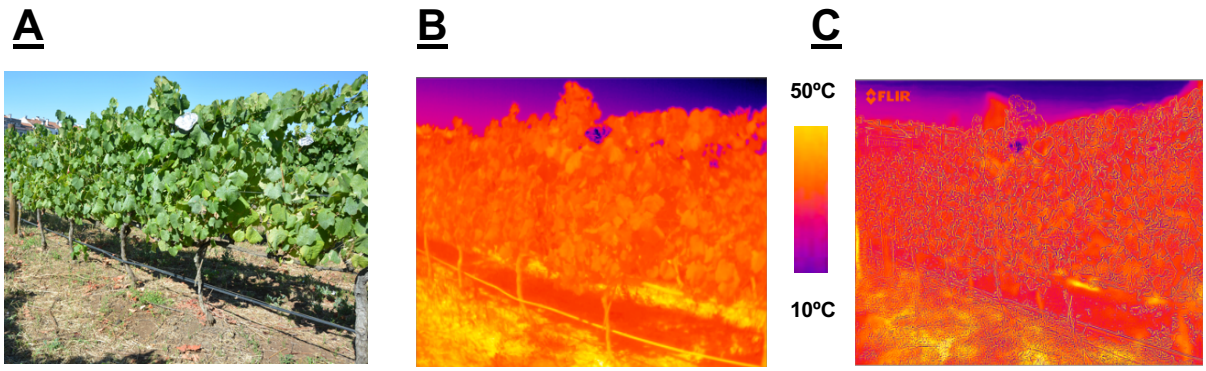

Fig. 12 Example of a set of RGB and respective thermal images for canopy measurement taken with the Flir A35 (320x256 pixels) (B) and the Flir One (80x60 pixels) (C).

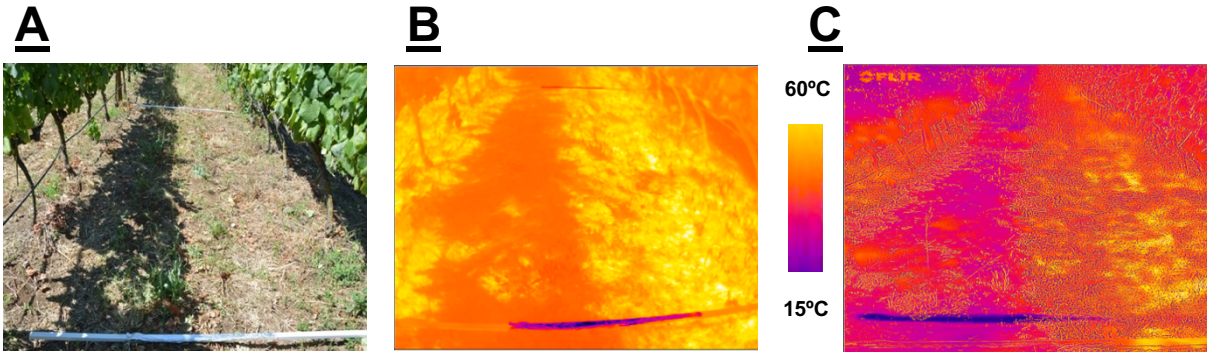

Fig. 13 *Example of a set of RGB and respective thermal images for ground-surface measurement taking with the Flir A35 (320x256 pixels) (**B**) and the Flir One (80x60 pixels) (**C**)*

3.6. Measurements

For measurements we used side by side rows in the vineyard (rows 24 and 25). In each row, we selected a total of 5 vines per treatment which resulted in a total of 10 vines observed per treatment at each time of observation. Observations were done along the growing cycle, on 9 June (flowering), 1 July (veraison), and 12 August (maturation/pre-harvest) and at different times of the day, in the morning (9.00-10.30h) and in the afternoon (15-16.30h). Temperature of soil surface was measured by taking thermal and RGB images were taken from the soil surface and from the sunlit side of the grapevine canopy. Measurements were done under clean sky conditions and under low wind speed conditions (4-7km/h). A total of 3 operators was needed to implement measurements for a period of 1,5, hours (9,00-10.30 in the morning and 15-16.30 in the afternoon). Thermal data was also used to calculate the thermal index CWSI which was also estimated based on the formula CWSI= (Tc-Twet) / (Tdry-Twet) (Jones and Vaughan, 2010). This formula considers two base values or thresholds: a base value without water stress and representing the temperature of a fully transpiring leaf/ or fully irrigated crop (Twet), and a base value with maximum stress / no transpiration (Tdry), CWSI values can range from 0 to 1, indicating zero water stress and water stress (no carry-over)

conditions, respectively. Furthermore, it is a useful method to represent the water potential of a strain, as confirmed at (Poblete-Echeverría et al., 2017) where the correlation is 0.88. Twet and Tdry were obtained in the following way: we sprayed a randomly selected leaf with water and apply grease (Vaseline) to another one on (both sides of the leaf). An addition leaf with aluminium foil was used to geo-reference the canopies/leaves in the thermal images. Wait 5-10 m after applying water and the Vaseline.

Climatic conditions were monitored with a meteorological station installed in the vineyard (https://www.orm.pt/servicos/3/meteoagri) during the measurements namely in terms of radiation, air temperature and wind speed (Table 7).

3.7. Imaging analyses protocol development

The purpose of the image analysis is to identify representative ROIs (Regions of Interest), in order to determine the canopy temperature for each treatment. In the case of canopy temperature measurements, we have divided the canopy into two parts: “high canopy “and “low canopy – cluster zone”, as previously described by Costa et al., (2019) for field measurements. Images were analysed by using the image analysis software Fiji (ImageJ distribution) (https://imagej.net/software/fiji/) and implemented with a ThermimageJ package of macros and plugins (https://tattersalllab.com).

Regarding image acquisition by the two thermal cameras, once images were taken, files are saved in two different formats. In the case of the Flir A35, the images were saved as a radiometric Jpeg and analysed with the Fiji software. Images from the Flir One Pro LT camera were saved in the RGB format and further analysed using the Flir tools thermal image processing software (https://www.flir.com). Next we present the steps adopted to analyse images retrieved by the two thermal cameras .

3.7.1. Protocol steps to analyse Flir A35 Images using the Fiji software

Step 1. Activating ThermimageJ

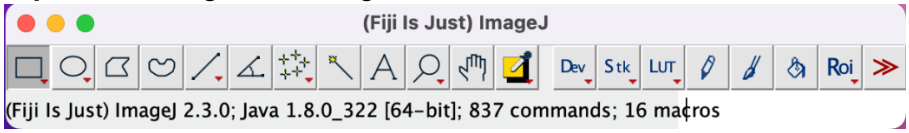

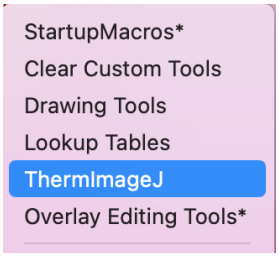

Step 2. Once is activated press “FILE” and “import the image file you want to analyse (FLIR JPG)”

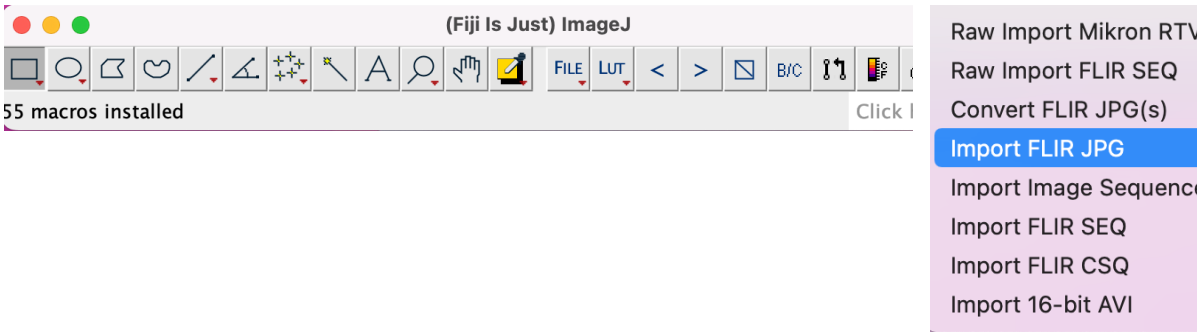

Step 3. Configuration of Parameters

Once the image is chosen from the directory the configuration layout appears, set the temperature ranges for the image (main and max temperatures), atmospheric and reflected temperature and the emissivity (we considered a value of 0.96) (Jones and Vaughan, 2010). Once the values have been set, the image with the selected palette type will appear (if necessary, this can always be changed using the LUT function in Fiji. Fiji multifunctional bar. At this point, to analyse the image, it is necessary to use the tools called Roi manager, which allows us to modify and move the various ROI. It is also possible to save the ROI and open them directly in the ROI manager if necessary. The programme does not give the scale of temperature, so it was subsequently added manually.

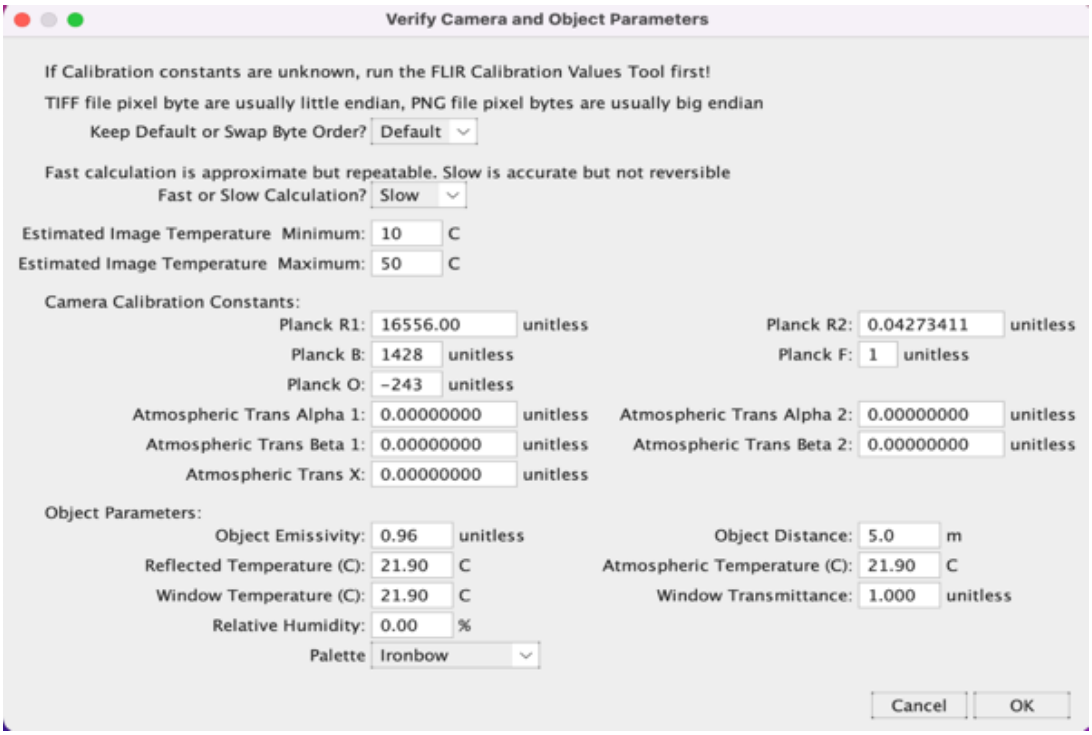

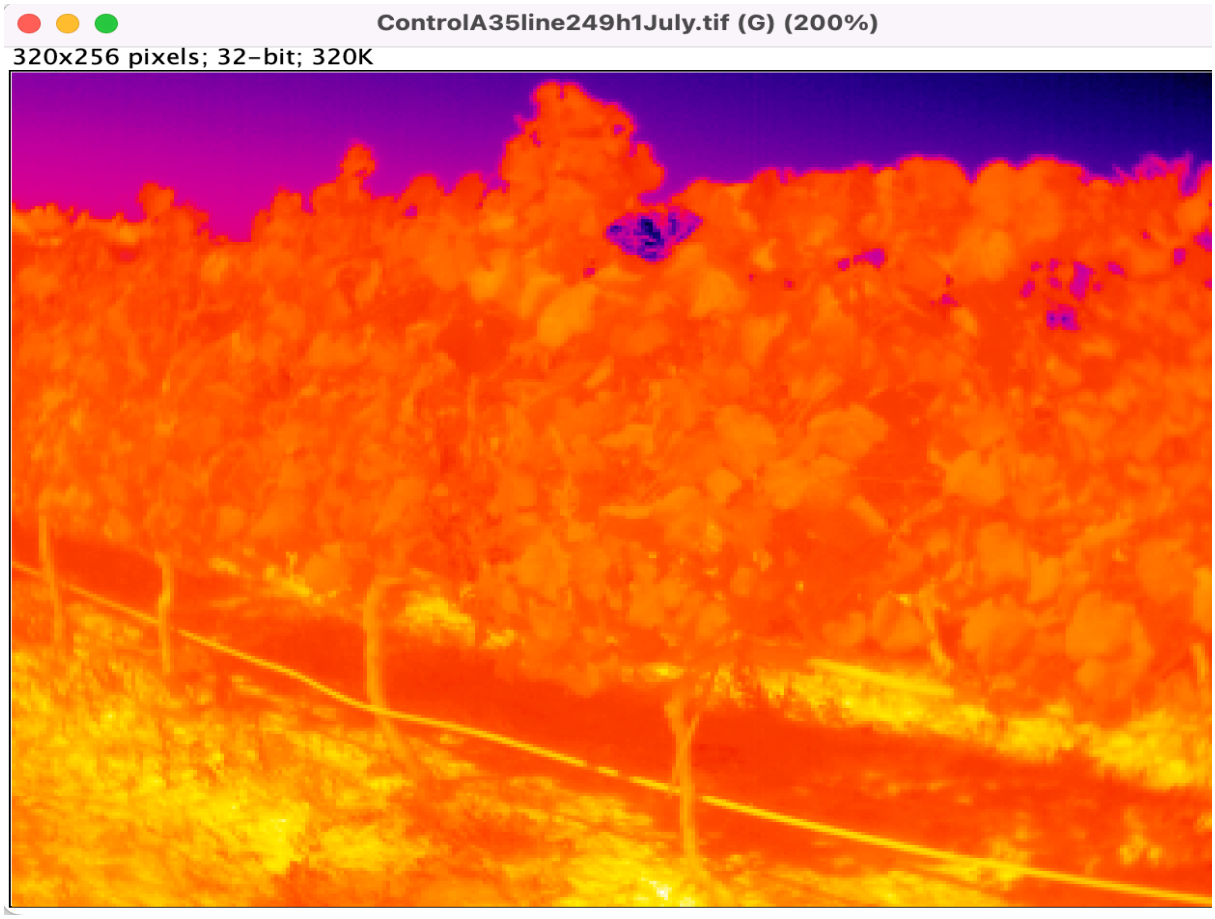

Step 4. Using of ROI manager

Activate ROI Manager from “Tools” found in “Analyse” to determine the type and the number of ROIS to select in the image to extract the temperature values form the image

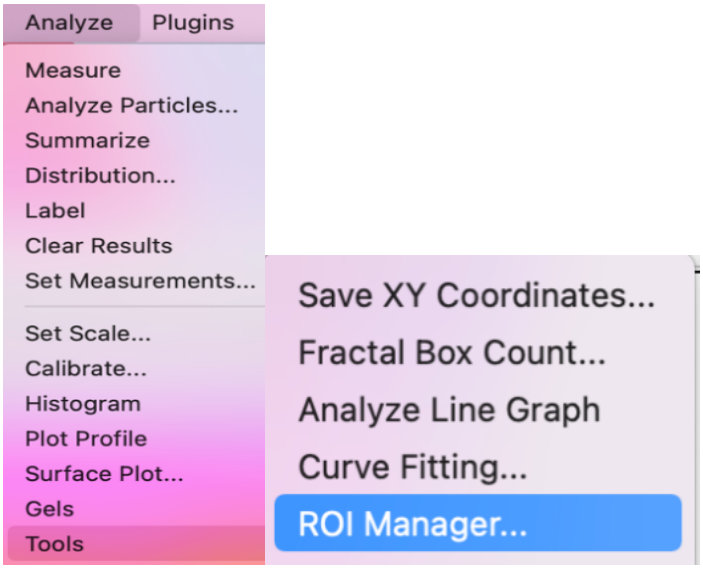

Step 5 Choose the ROI.zip previously make in the same way that it will be showed

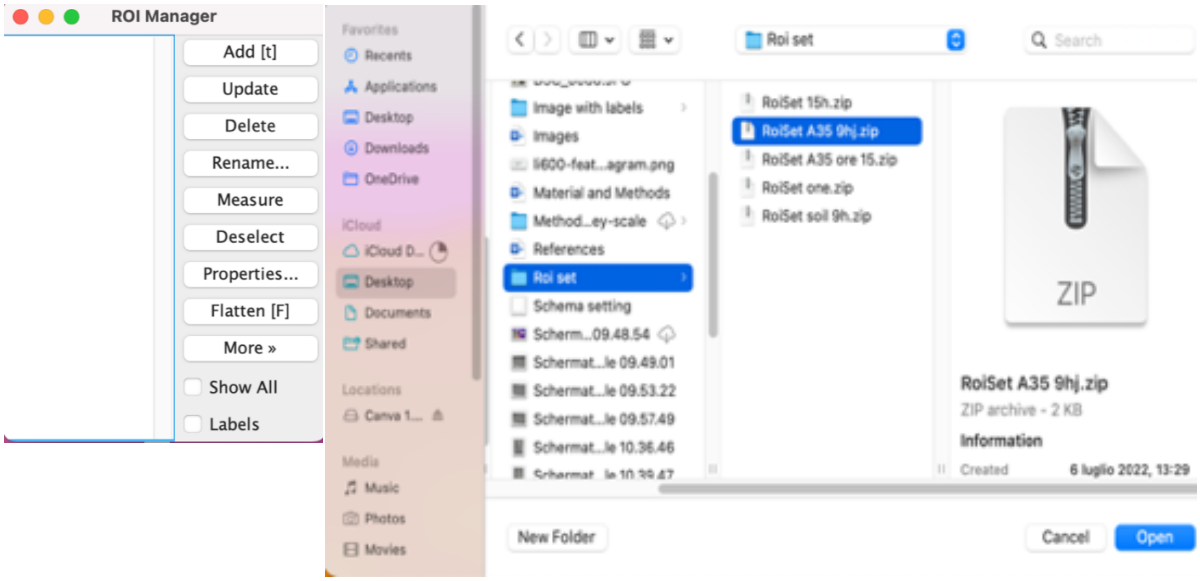

Step 6. Make and position the ROIS.

We have selected a total of 10 ROIS (5 on the top of the canopy and other five on the basal part/bunch zone). Each time a ROI is created, it must be added to the ROI manager by pressing add or the quick key t

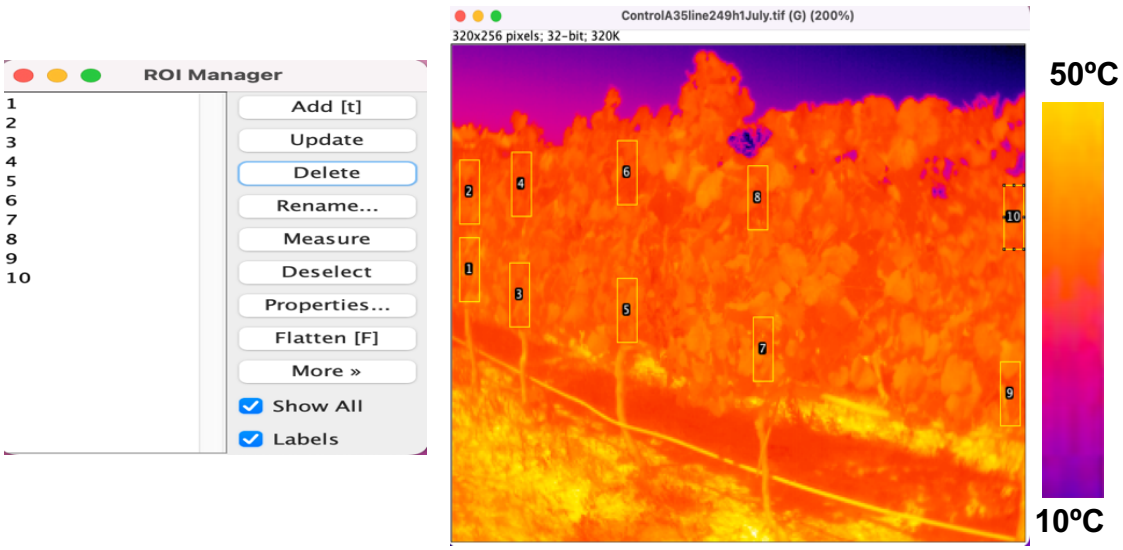

Step 7 Use the Multi Measure operation to obtain the average temperature value of the corresponding ROI.

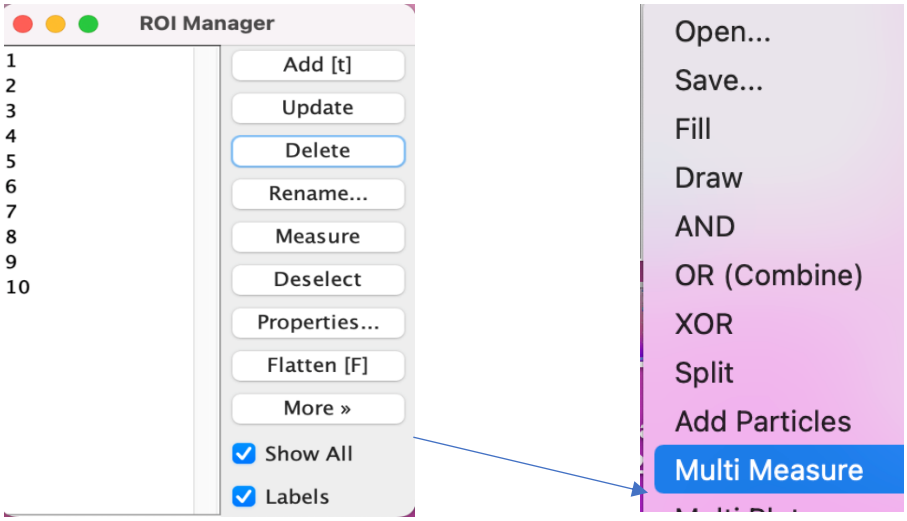

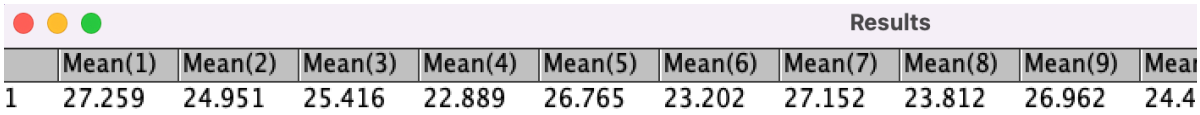

3.7.2. Protocol steps to analyse Flir One Images with FIJI (ImageJ Distribution)

Analysing images acquired with the Flir One Pro LT ne thermal camera using FIJI (ImageJ Distribution) software (https://imagej.nih.gov/ij/index.html) has some differences. Because images are saved as RGB and not as radiometric Jpegs, images were first converted into an 8 bit-grey format image. In an 8-bit image each pixel occupies 1 byte, which means that each pixel has 256 (2^8) possible numerical values, from 0 to 255. As result the color palette for an 8-bit image has 256 entries, defining color 0 through color 255. As consequence, and because the Flir One Pro LT images are 8 bit not radiometric we had to calibrate the image and match each pixel value (0 to 255) with the corresponding temperature value (10-50 ℃) for canopy and (15-60℃) for the soil images. To that extent we use the Calibrate (find in Analyse option) and use for calibration. Following this, all steps (Fig. 16) are identical to the protocol used for A35 images except that since the resolution is different from the images acquired with the A35, the same ROIs could not be used because they will be smaller due to the fact that Flir One Pro LT images have more pixels being RGB images.

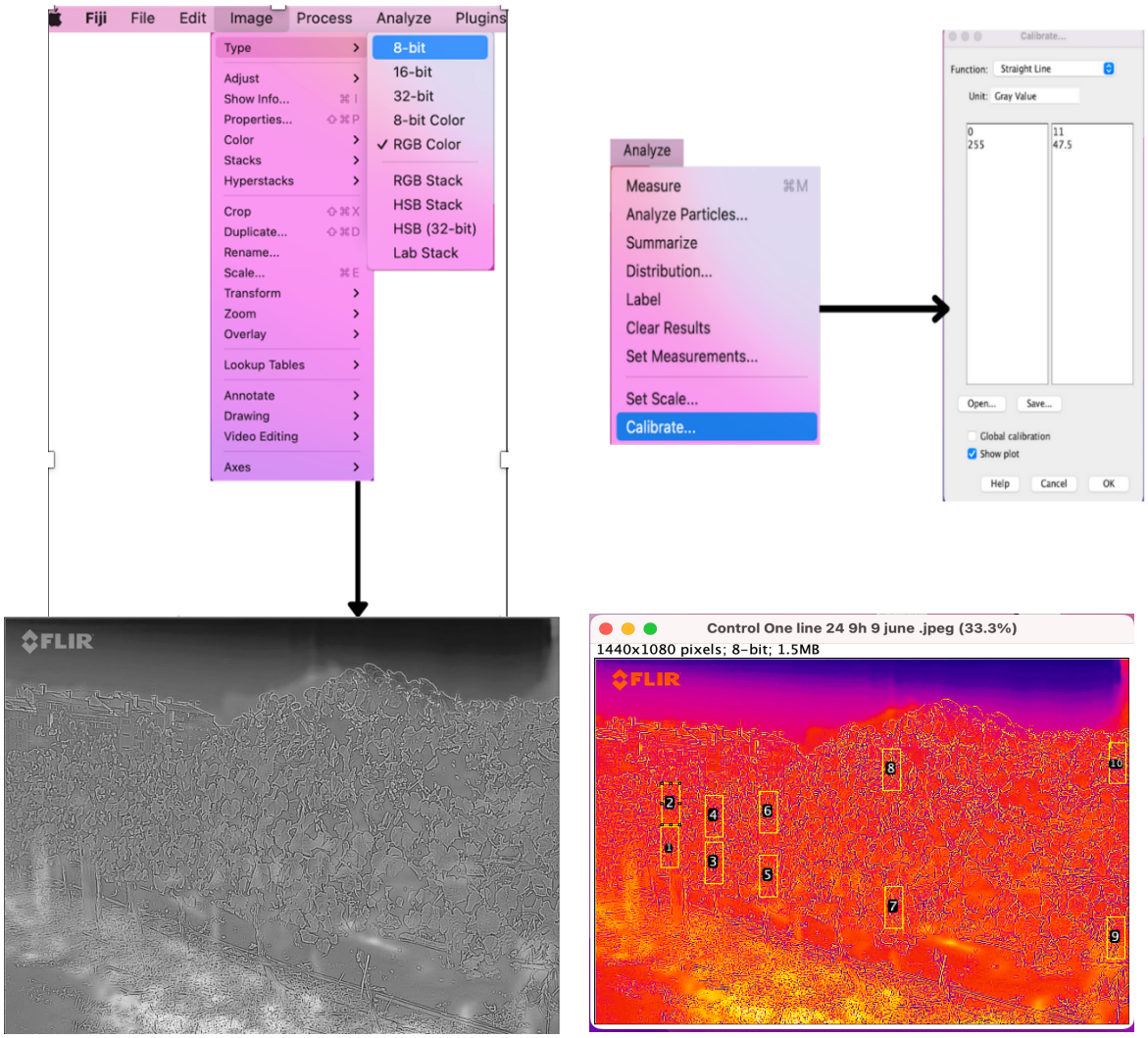

Fig. 14 All steps required to image analyses for Flir One Pro LT using FIJI software

What is stated in the previous paragraphs (3.5.1; 3.5.2) is also valid for the thermal analysis of the soil surface, with the only difference being that instead of there being two ROIs, one for the sunlit side and the other for the shadow (Fig.17)

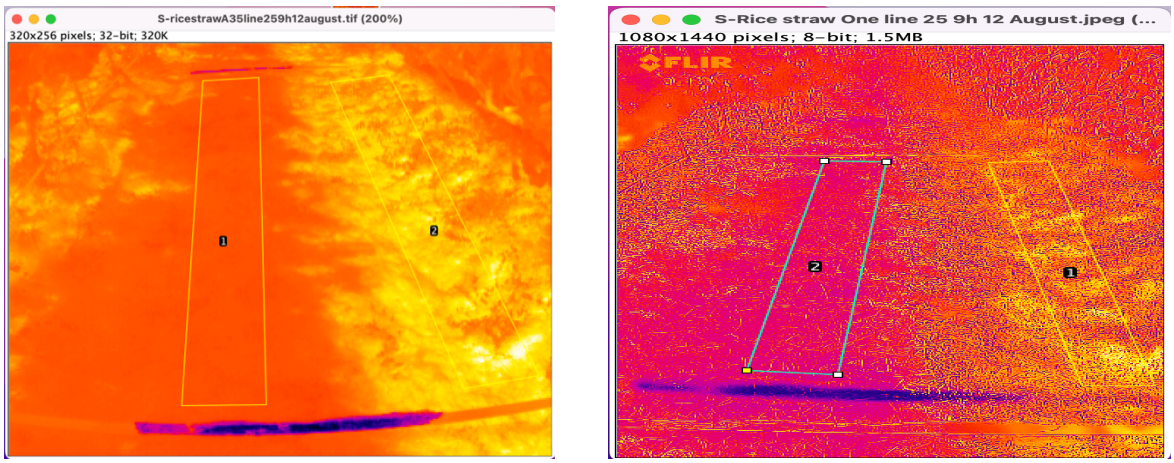

Fig. 15 ROIs selected for ground-surface measurement using Fiji software

3.8. Leaf gas exchange and chlorophyll fluorescence measurements

Thermal imaging measurements were combined with individual leaf gas exchange and chl fluorescence measurements on 1 July and 12 of August. While two operators were taking RGB and thermal images other operator was measuring leaf gas exchange with a porometer LI-600, Licor, Biosystems, USA). Measurements were done on the sunlit side of the canopy. The LI-600 equipment permits to measures stomatal conductance to water vapor (gs) and chl fluorescence over the same leaf area. The LI-600 uses an open flow-through differential measurement to quantify transpiration (E) and stomatal conductance. First, E is quantified by measuring the flow rate and water vapor mole fraction of air that enters and leaves the chamber. Meanwhile, total conductance to water vapor (gtw) is computed as a function of E and vapor pressures in the leaf and cuvette. Finally, stomatal conductance to water (gsw) is computed as a function of gtw and the boundary layer conductance to water vapor (gbw) (https://www.licor.com).

For light-adapted leaves, the LI-600 measures the quantum yield of fluorescence (ΦPSII), or the proportion of light absorbed by PSII used in biochemistry based on the equation

$$\Phi_{PSII} = \frac{F_m' - F_s}{F_m'} \qquad \text{Equation 4}$$

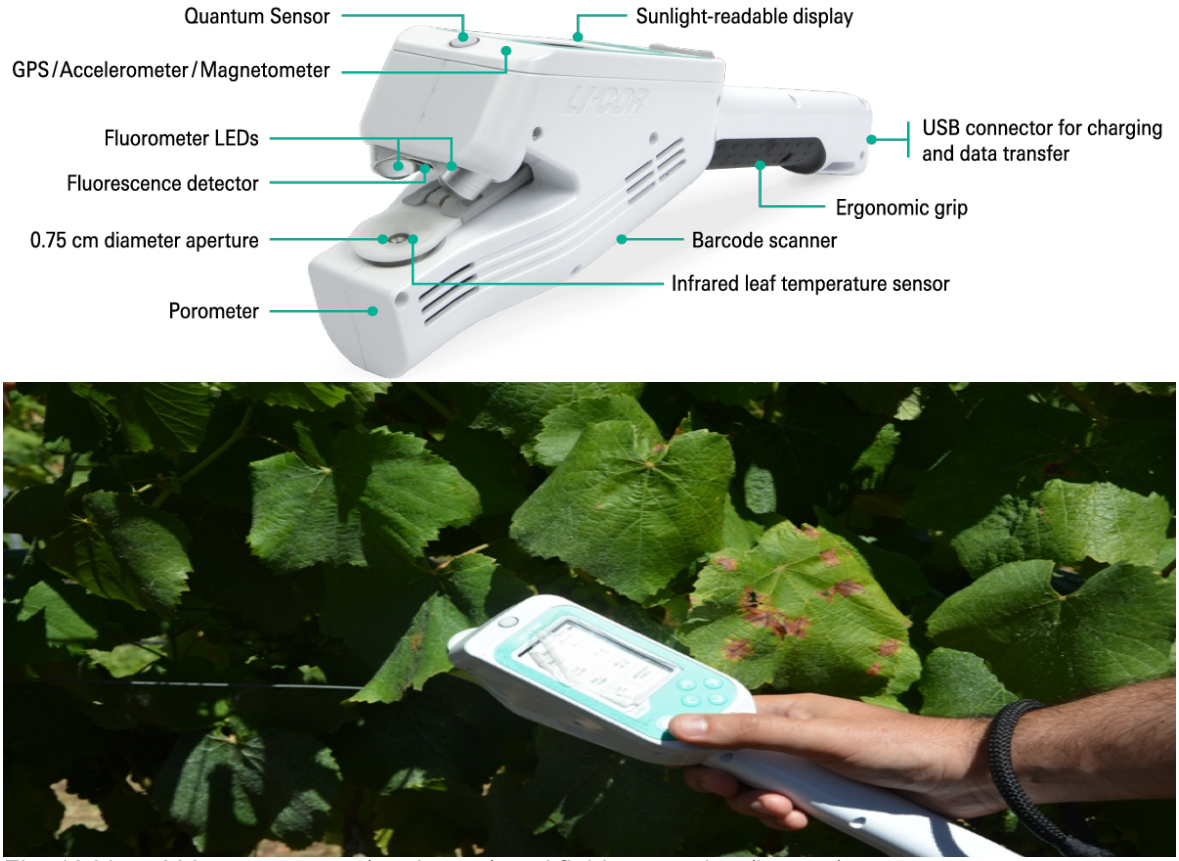

Fig. 16 Licor 600 components (on the top) and field measuring (bottom)

where, Fm' is maximum fluorescence yield in a light-adapted leaf; Fs is steady-state fluorescence yield in a light-adapted leaf. The Electron transport Rate was estimated based on the equation given by Baker (2008) [1]: ETR = 0.5 × 0.84 × PPFD × ΦPSII.

A total of 3 measurements were done per vine (one measurement per leaf), from the intermediate zone between the bunch zone and the top of the canopy. Measurements were done from the sunlit side of the canopy, under full light conditions. Data on the PSII efficiency and the Electron Transport Rate was also calculated be the equipment based on the chlorophyll fluorescence measurement, A total of 30 measurements were done for the 10 vines considered in the trial

3.9. Statistical analysis

Canopy temperature measured along the season (morning and afternoon) were analysed using Microsoft Excel (Microsoft 365). A two-tailed paired sample comparison (having the same sample number) was performed with a 95% confidence level ($p < 0.05$) to assess the significance of differences between the three treatments (control, eucalyptus mulch and Rice straw mulch).

4. RESULTS

4.1. Climate conditions and soil water

Data on the climate conditions was measured along the trial. Data was obtained via the website of the company Meteoagri (https://www.orm.pt/servicos/3/meteoagri) (Table 7). All measurements were done under no precipitation conditions. The 9 of June and 1 July were the times of observation showing the highest evaporative demand (higher ETo), especially in the afternoon. In terms of wind conditions, the 9 June was the windiest, and mainly in the afternoon (Table 7).

Table 7 Climate conditions and soil moisture measured along the season and during the day (9.00-10.30 and 15-16.30h)

Time of observation		Tair (ºC)	Radiation (W/m^2)	Eto (mm)	VPD (Kpa)	RH (%)	Wind (km/h)	Soil moisture (mm)
9th June	**a.m.**	23,7	878	0,38	0,92	68,70	7,12	235.88
	p.m.	29,9	1237	0,63	2,26	46,40	7,47	250.35
1st July	**a.m.**	23,3	865	0,39	1,19	58,30	4,70	254.78
	p.m.	29,5	1219	0,65	2,38	42,30	6,11	241.30
12th August	**a.m.**	24,5	762	0,44	0,96	68,9	3,61	250.56
	p.m.	29.1	1171	0,50	1,87	53,60	8,89	245.05

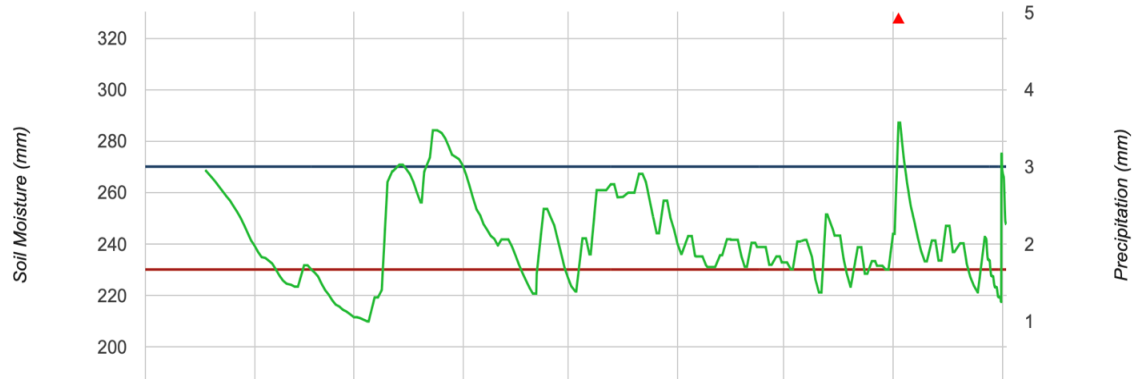

Fig. 17 Soil moisture data from 2022 season (JAN-SEP) collected by the soil capacitance probe located at "Meia Encosta" vineyard. Blue bars represent LRAW, red bar URAW. (Source: https://www.aquacheckweb.com/index.html)

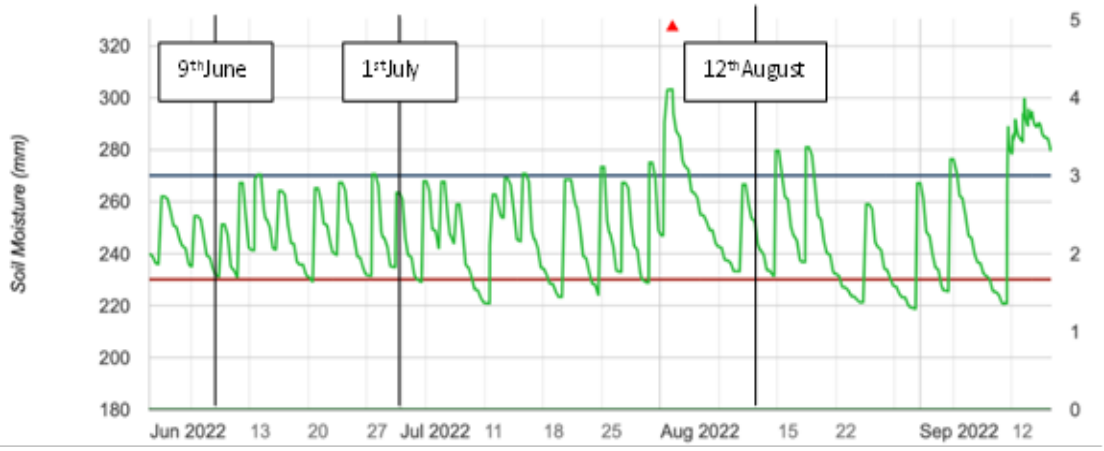

Fig. 18 Soil moisture data from 2022 season (JUNE-SEP) with the treatments indicated with black lines, collected by the soil capacitance probe located at "Meia Encosta" vineyard Blue bar represent LRAW, red bar URAW. (Source: https://www.aquacheckweb.com/index.html).

4.2. Soil surface temperature

The temperature of soil surface (soil and mulch surface) was measured along the season in the morning and in the afternoon The lowest temperatures values were found during the morning period, and under shadowing conditions and varied between 18 and 24 ºC. The highest values were found in the afternoon period and in the sunlight exposed parts and varied between 39 and 54 ºC (Fig.19). The high values of soil T observed in the morning measurements of 9 June can be related to the fact that measurements were delayed (till 12h) making the temperature results more similar to the afternoon values. The effect of the organic mulches was clearer in the afternoon specially when using the Flir A35 camera. Results show a decreasing trend in both sunlit and shadow side of the interrow, with less 2 to 5 ºC in straw as compared to the control surface (Fig. 19), The lower temperatures of the shadow side were also detected in the afternoon. The surface of the rice straw presented 3-4 ºC less than the control.

The control had the lowest temperature on the sunlit side in the morning but in the afternoon showed the highest surface reaching a maximum of 54 ºC in July (Fig. 19 D). This suggests that a larger diurnal variation in temperatures is occurring for control conditions. Nevertheless, we cannot exclude the fact that the control was always the first treatment to be assessed in the morning period.

The Flir One Pro LT camera was not able to detect any differences between treatments nor between morning and afternoon measurements (Fig. 20) but even so was able to distinguish between shadow and sunlit zones of the ground (Fig. 20).

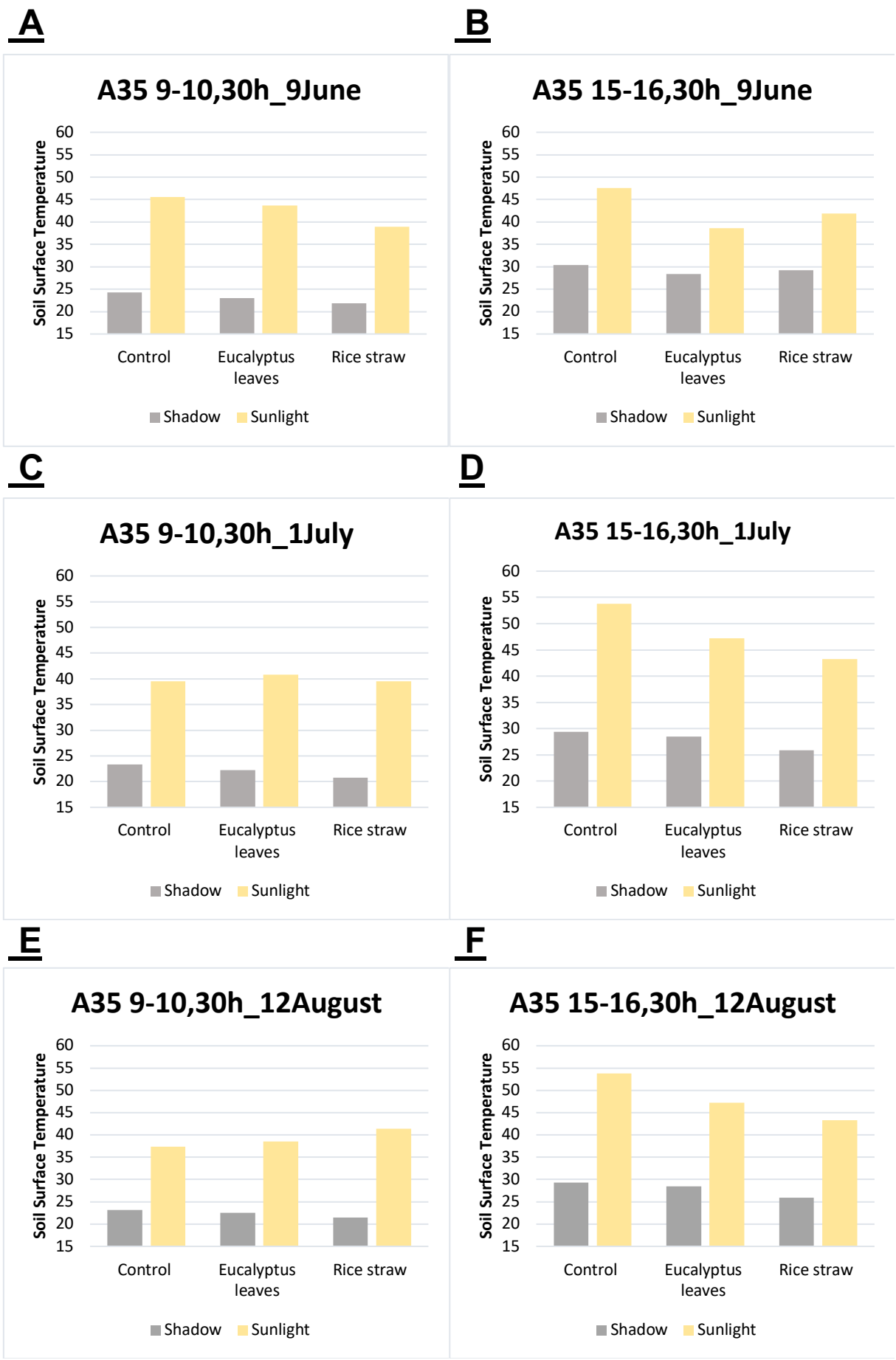

Fig. 19 Ground-surface temperature values obtained by Flir A35 thermal camera along the season and at two times of the day (morning-afternoon). *Values are means from two ROI areas selected in the thermal images (see M&M).*

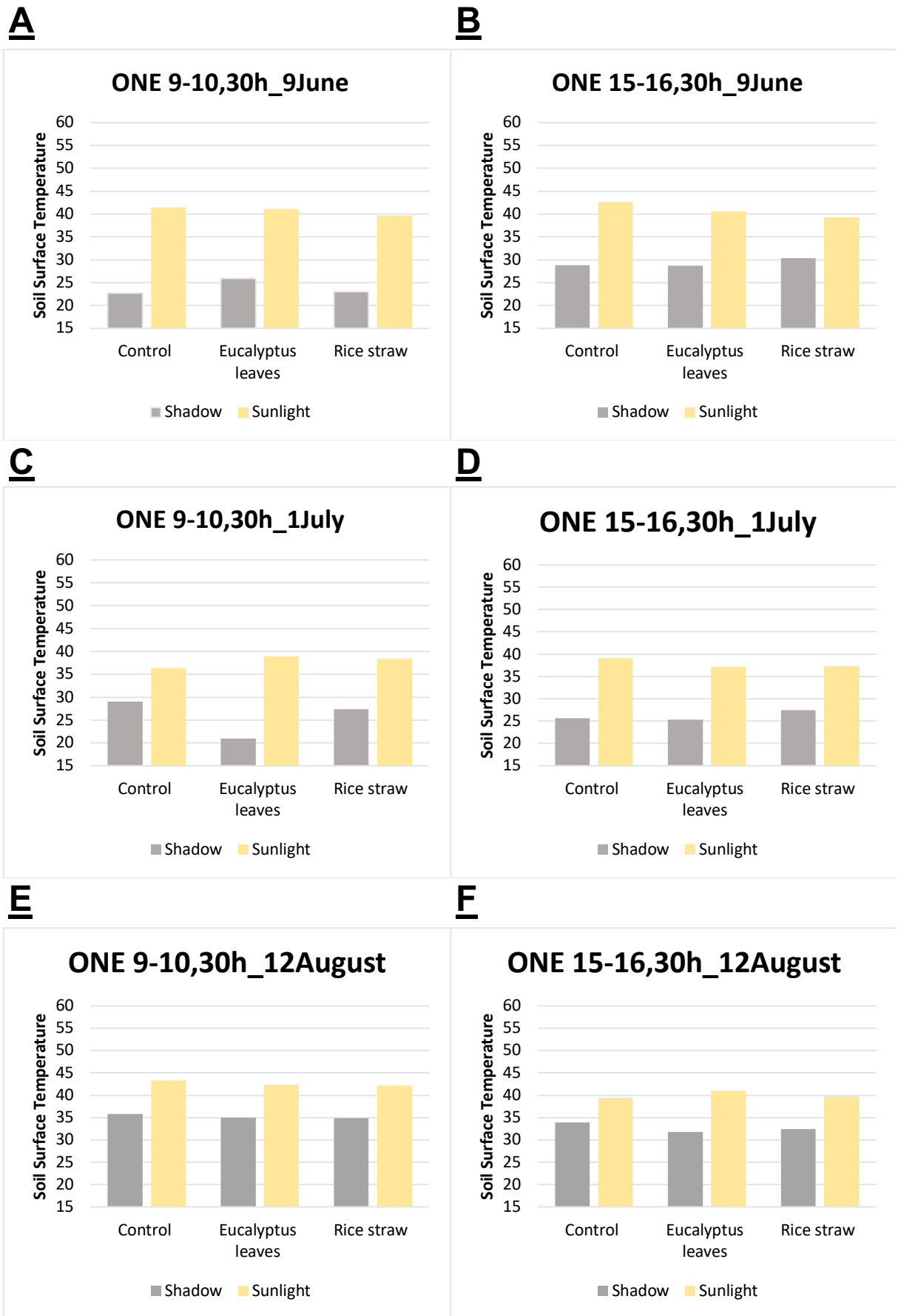

Fig. 20 *Ground-surface temperature values obtained by the Flir One Pro LT thermal camera during the season and at two times of the day (morning-afternoon). Values are means from two ROI areas selected in the thermal images (see M&M)*

4.3. Canopy and vertical temperature profile

Regarding the sunlit canopy temperature, thermal measurements helped to visualize differences between the morning period and the afternoon period, with the tendency for a slightly higher canopy temperatures in the afternoon in all treatments (Fig. 21). Thermal measurements with the higher resolution camera A35 permitted as well to visualize vertical profiles of canopy. Indeed, data from the Flir A35 show that the canopy temperature of the lower part (at the cluster zone) was on average 2-3 ºC higher than the upper part of the canopy except in the case of plants subjected to 'Eucalyptus' mulching observed on 12 August. (Fig.21 E). This tendency for a vertical temperature profile was again observed in the afternoon (Fig 21 B; D and F) but less markedly with smaller temperature differences between the cluster zone and the upper part of the canopy (see Fig. 21 B; D; F). On average the cluster zone has a temperature value of about 1-1.5 ºC larger than the upper part of the canopy. Results obtained with the A35 camera, show as well that mulching had no effect on canopy temperature. (Fig. 21).

On the contrary, the time of the day had an effect, and the highest temperatures are achieved for mulching treatments in the afternoon. In addition, the control was the one that showing more variable canopy temperature values along the season, in opposite to the mulching treatments that showed greater variations in temperature, in particular "Eucalyptus leaves".

Regarding the thermal sensor the Flir One Pro LT camera was again unable to distinguish between the temperatures of the cluster zone and top of the canopy (differences of about 1 ºC or less). The same applies to the identification of temperature differences due to the time of the day (Fig. 22)

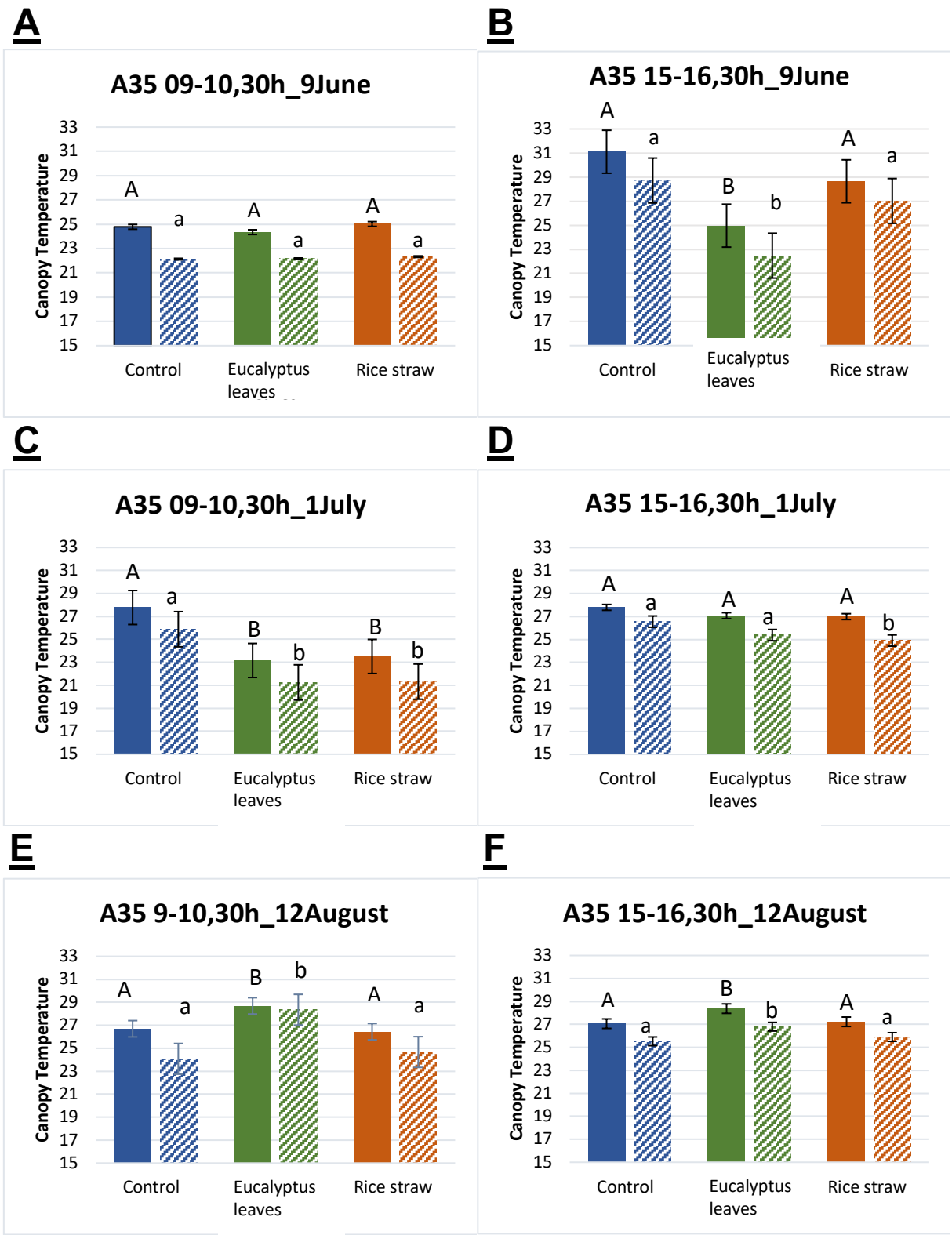

Fig. 21 *Canopy temperatures obtained by using a Flir A35 thermal camera during the season and at two times of the day (morning-afternoon). Full filled coloured bars indicate the lower part of the canopy (cluster zone) while the pattern bars indicate the top part of the canopy. Values are means of (n= 10) 12 August rice straw 9h (n=5). Different letters indicate significant differences between treatments considering a p-value (0.05). Upper caps letter refers to cluster zone and small size to the top part of the canopy.*

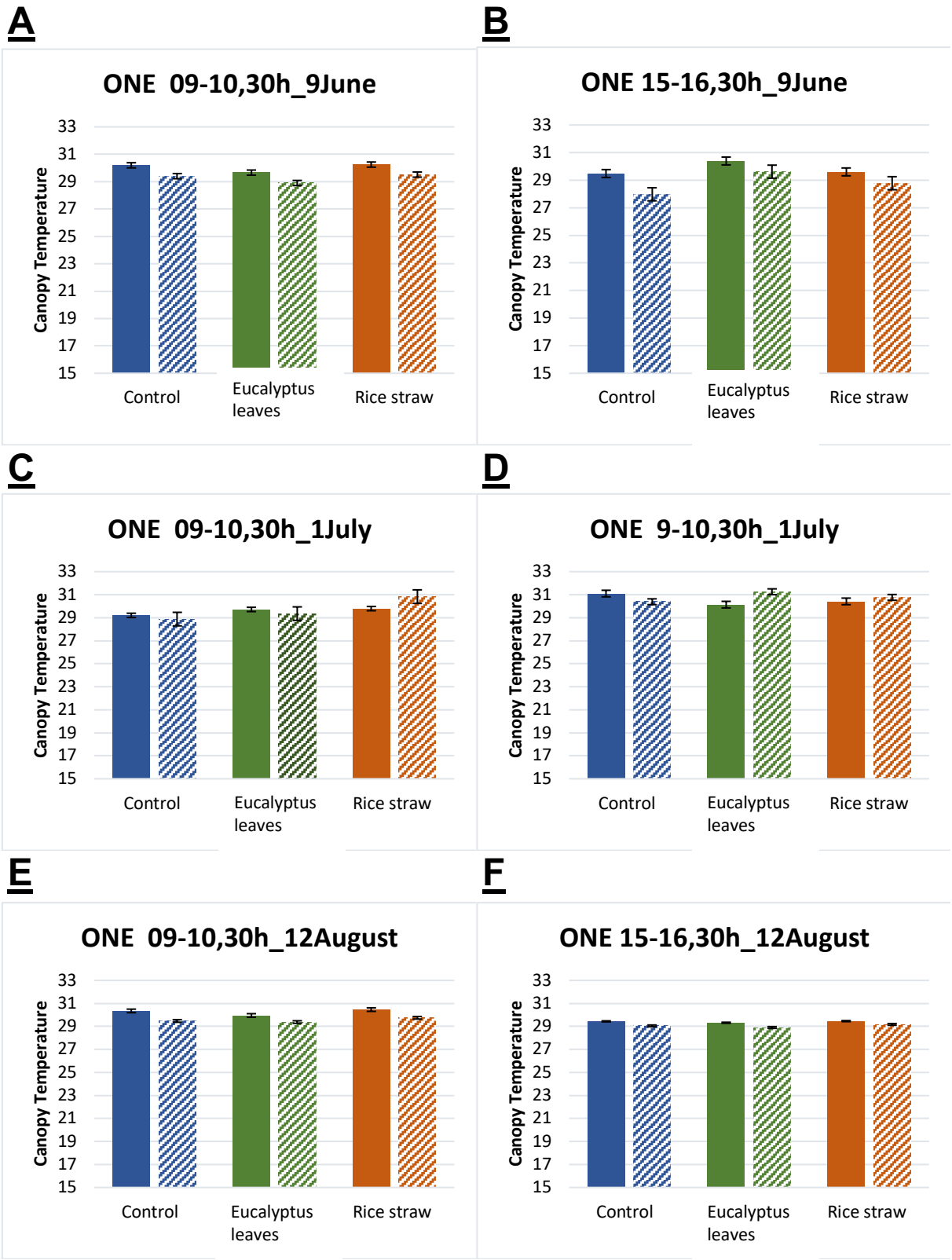

Fig. 22 *Canopy temperatures obtained by using a Flir One ProLT thermal camera during the season and at two times of the day (morning-afternoon). Fuller bars indicate the cluster zone of the canopy while drawn bars indicate the higher part. Values are means n=10*

4.4. Thermal index CWSI

Thermal indices allow a non-destructive assessment of the water status of a plant under variable climate conditions permitting to minimize the impact of variation in the environmental conditions during the observations. Thus, calculation of these indices is often combined with the measurement of leaf water potential or leaf gas exchange in order to obtain both soil water status and plant water status based on temperature measurements (Costa et al., 2012; Katimbo et al, 2022; Tejero et al., 2016). We calculated the CWSI based on the equation presented in M&M and on the calculation of the Tdry and Twet values also described in M&M (Table 8)

The CWSI values for the morning periods varied between 0,3 and 0,8 and were slightly smaller than the ones found for afternoon which varied between 0,1 and 0,9 indicating less stress during the morning period. The CWSI estimated for the vines subjected to the different treatments indicate values lower or around 0.8 suggesting that mild to moderate water stress was experienced by Fig. 23. CWSI values around 0,4-0,8 is suggested for mild water stress conditions under deficit irrigation (Costa et al. 2012; Also, the threshold of 0.8, has been considered the limit value for plants not incurring severe water stress (Belfiore et al., 2019; Pagay & Kidman, 2019; Sepúlveda-Reyes et al., 2016). Results from 9 June may differ from the other dates because of the delay in finalizing the morning measurements. Overall and if we consider the July and August observation our results indicate higher CWSI values (near 1) in the afternoon, which corresponds to the higher stress condition.

We have also calculated the Delta T index, but results are less clear than the CWSI output. Nevertheless, it indicates that on 9 June (the most stressful day) canopy temperatures were clearly above air T which could be related to the higher radiation load. (Appendix)

Table 8 Twet and Tdry values obtained by Flir A35 camera along the season. Twet – Fully transpiring leaf; Tdry no transpiration

Time of observation		Twet (℃)	Tdry (℃)
9th June	**a.m.**	16,57	25,85
	p.m.	22,86	32,67
1st July	**a.m.**	22,51	31,91
	p.m.	21,38	28,52
12th August	**a.m.**	23,08	29,67
	p.m.	22,45	28,76

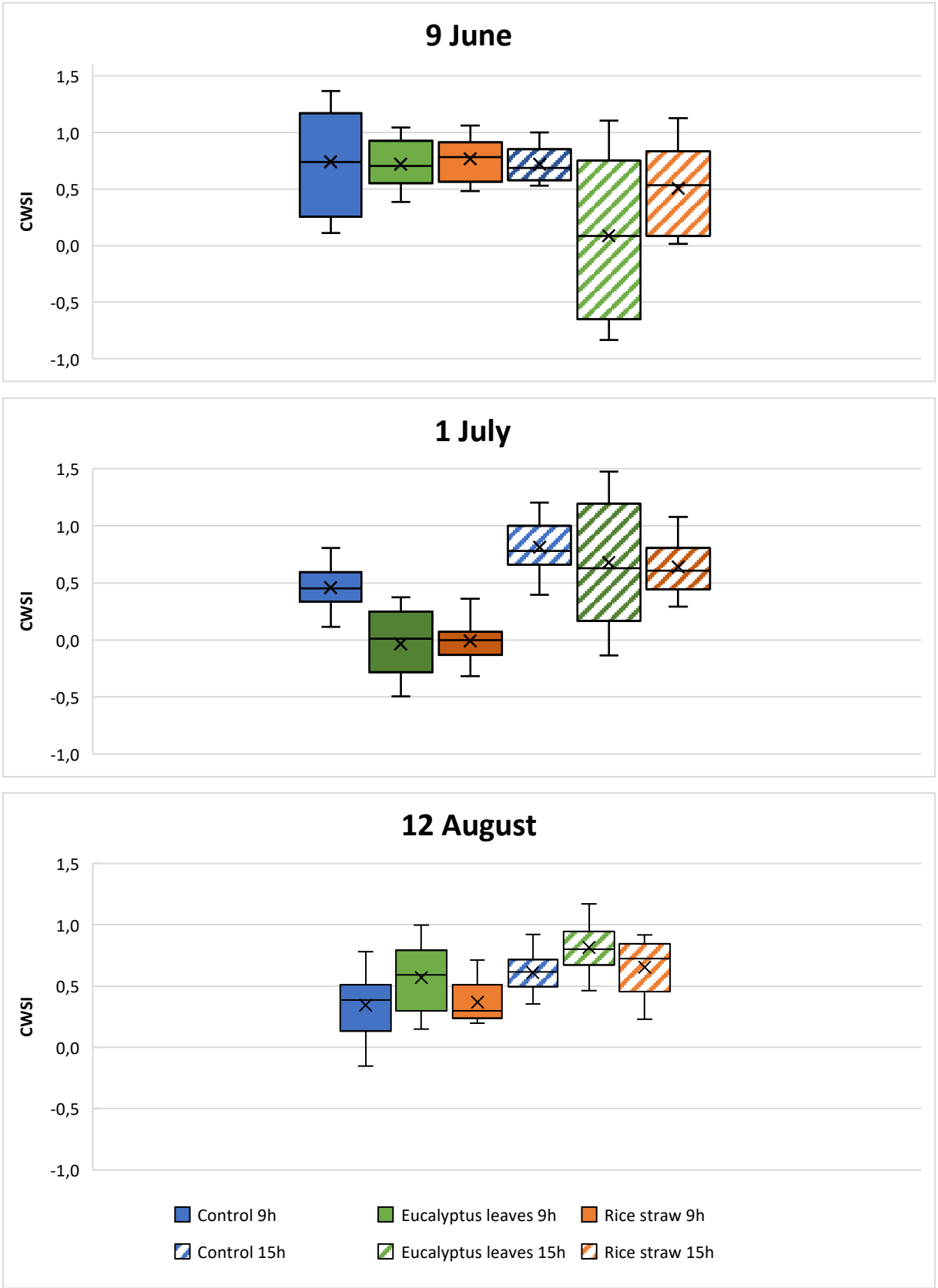

Fig. 23 *Value of the Crop Water Stress Index (CWSI) measured for the three treatments (soil cover – control., Eucalyptus leaves and Rice straw) along the season and based on the data retrieved by the Flir A35 camera*

4.5. Stomatal conductance to water vapour and PSII efficiency

Porometry measurements showed that stomatal conductance to water vapour varied between 0.1.and 0,16 mmol H_20 m^{-2} s^{-1}, in the morning and 0.08 and 0.15 H_20 m^{-2} s^{-1} in the afternoon. (Figures 23 A and C). Vines subjected to “Rice straw” mulching treatment had the highest gs values in the morning and in the afternoon except for the morning measurement on 12 August (Fig. 23 C). It can also be seen that the control vines and vines subjected to the Eucalyptus mulch have fairly similar gs values, with the exception of the morning survey of 12 August. (Fig. 23C). In addition, stomatal conductance of control plants measured in the morning is higher than 'eucalyptus leaves' (Fig 23 A: C). In the case of the observations done on 1 July by 0.01 $mol \cdot m^{-2} \cdot s^{-1}$ and by 0.05 $mol \cdot m^{-2} \cdot s^{-1}$ on 12 August. Meanwhile values of 'Eucalyptus leaves' remain more or less constant at around 0.1 $mol \cdot m^{-2} \cdot s^{-1}$ along the season.

By the contrary, during the afternoon period vines subjected to the mulching treatment with the ‘Eucalyptus leaves' had the tendency to show values how much, albeit slightly lower than the 'Control'.

As shown in Fig 24, stomatal conductance was similar along the period of observation (July and August) and there was a reduction in the gs observed in the afternoon (See Fig. 24 B; D)

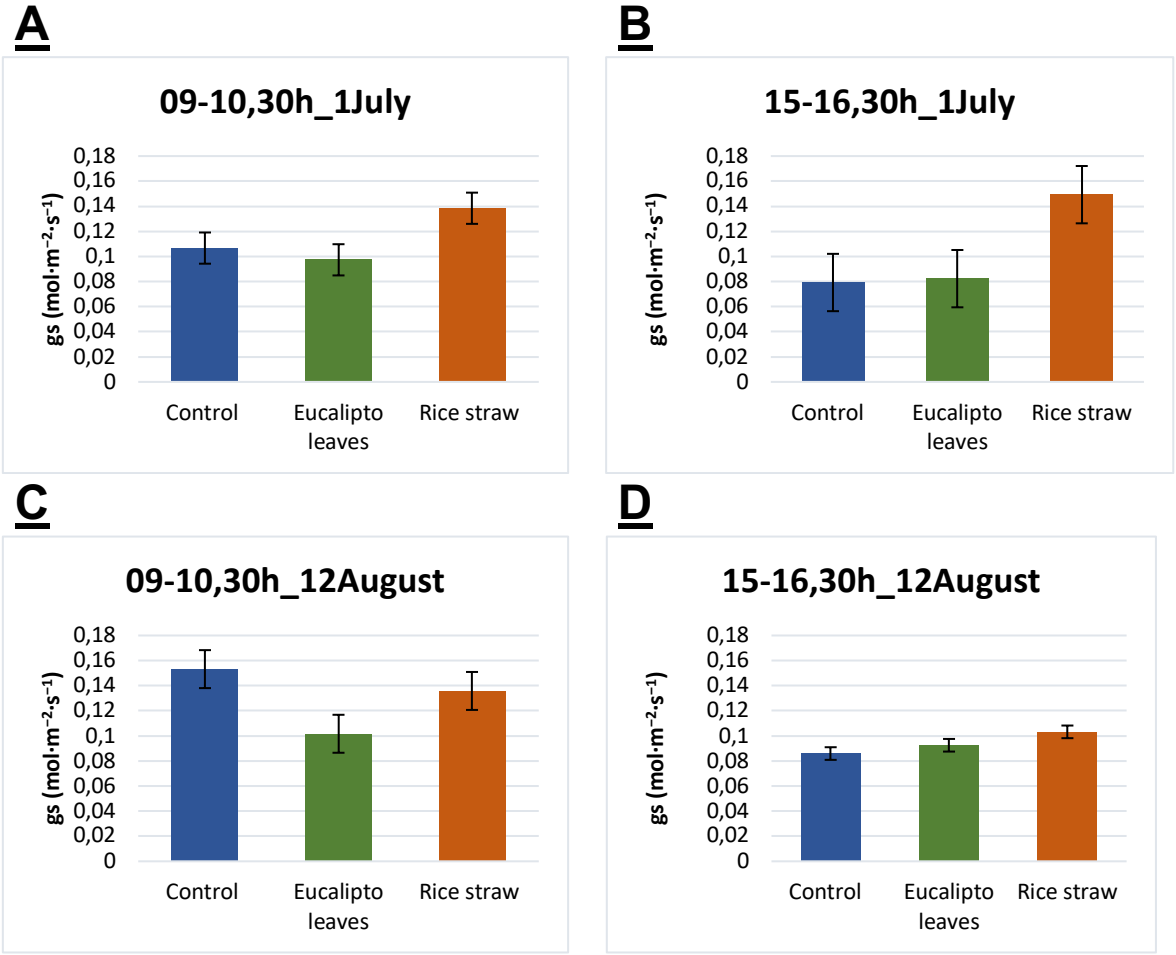

Fig. 24 Value of Stomatal conductance obtained by the porometer LI-600 (Licor Biosystems). Values are means ± SE (n=30)

which can be related with more stressful conditions. This is visible in the measurements of 1July (A; B) that showed a drop of about of almost 0,1 mmol H_20 m^{-2} s^{-1}. Vines under "control" and "Eucalyptus leaves" mulching conditions while vines subjected to “rice straw" it is around 0,12 mmol H_20 m^{-2} s^{-1}. The opposite was verified on 12 August (Fig.24 C; D), where an increase in values was observed from the morning to the afternoon measurements, although less markedly.

The LI_600 permitted also to measure Chlorophyll fluorescence as an indicator of photosynthetic functioning of the grapevine plants. The PSII efficiency values obtained under light conditions showed no particular trend as regards to the PSII efficiency measured with the LI-600. (Fig. 25). The range of values varied from a minimum of 0.3 in the afternoon survey of 1July (Fig. 25 B) to a maximum of 0.5-rice straw in the morning of 1July (Fig. 25 A).

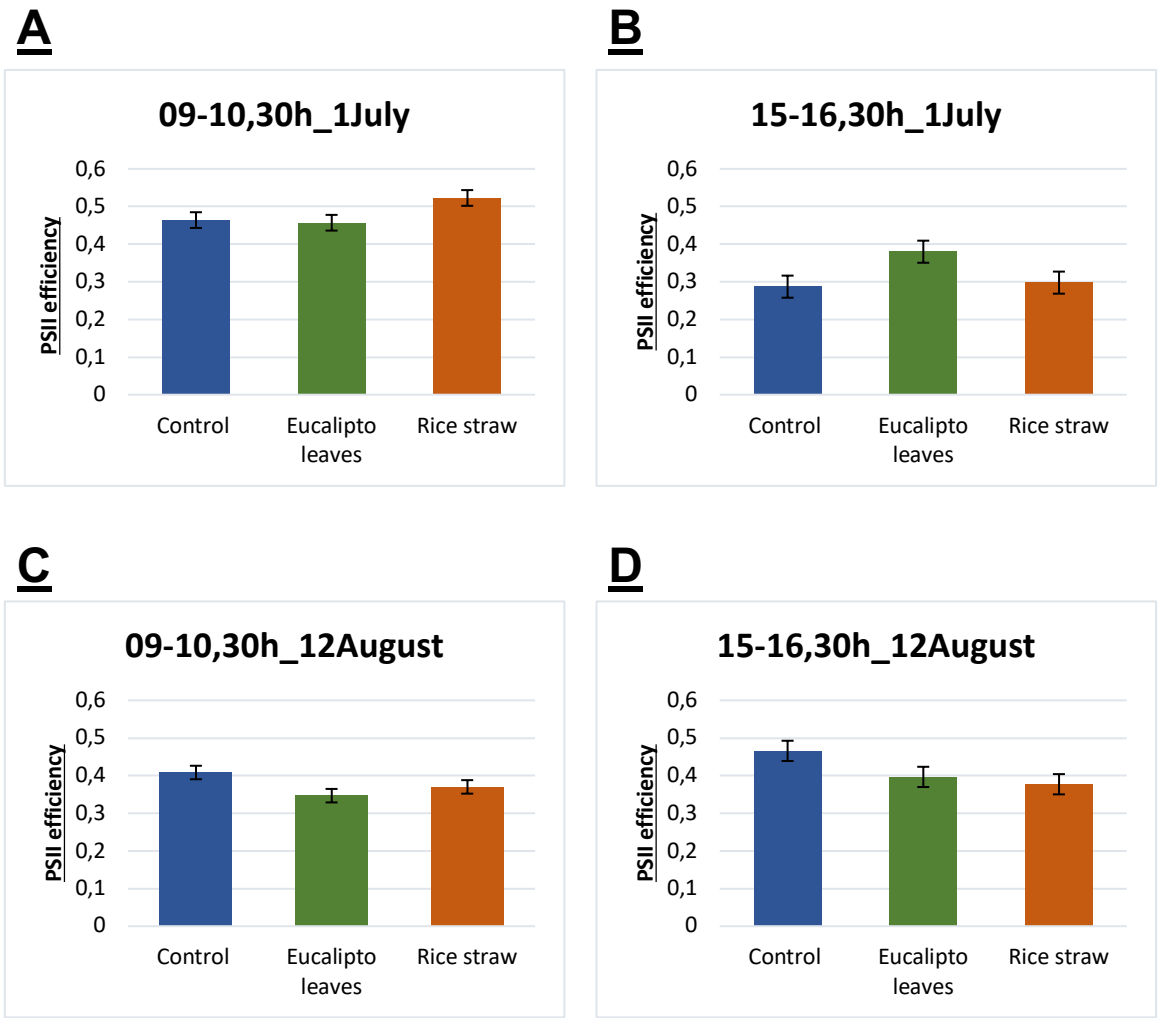

Fig. 25 PSII efficiency measured under light conditions by using LI-600 (Licor Biosystems). Values are means (n=30)

The values obtained for PSII values were lower in the afternoon period in July suggesting some decreased efficiency under more stressful environmental conditions. However, the same trend

was not observed in August afternoon. However, overall, there is no particular trend observed for the PSII efficiency (Fig. 25).

5. DISCUSSION

Soil is a very important component of agriculture and viticulture and the use of imaging technologies (e.g. thermography) in viticulture has become increasingly relevant and common due to lower price solutions and light weight equipment making imaging a tool to support soil and plant management.

Soil characteristics can largely influence yield and berry quality. Moreover, in row crops like grapevine the influence of the soil in terms of heat fluxes is amplified especially under extreme conditions (heat and drought stress) (Costa et al., 2018; 2019). This becomes more relevant if we consider that drought and high temperatures are expected to become more severe in the Mediterranean region, which can negatively affect sector's performance and its sustainability (Costa et al., 2020; Fraga et al., 2020).

Soil temperature can be also soil relevant because it may affect leaf and berry physiology and berry composition (Costa et al., 2019; Burg et al., 2022). Therefore, measurements of soil temperature and vertical temperature profiles are relevant in the context of the viticulture sector located in typically warm and dry areas such as the Mediterranean areas (Costa et al. 2019; Gutierrez-Gamboa et al, 2020)

Soil temperature influences root metabolism, root growth, respiration, the uptake of water and nutrients, microbial activity, decomposition of organic matter, soil chemistry, and soil moisture levels (Gliessman, 1998; Akter et al. 2015). In addition, it may also affect the microclimate of leaves and berries (Costa et al., 2018; 2019). For this reason, more studies on soil management and the impacts of short-term strategies (e.g., mulching) and long-term strategies (e.g., varieties) is crucial to reduce the effects of climate change (Santos et al., 2020),

In this thesis, we have carried out a very preliminary study to evaluate the relevance and robustness of thermal information retrieved in vineyard conditions by two low to medium cost thermal cameras We have tested the use of thermal imaging to monitor soil and canopy temperature under conditions of natural soil cover and under mulch conditions (Eucalyptus and Rice Straw) along the summer season of 2022. In addition, this study aimed to test the use of open-source image processing software to develop an accessible and repeatable protocol to support image analysis retrieved by medium- low-cost thermal cameras.

5.1. Imaging set up and image analysis

Together with the testing of low-cost thermal sensors as we have also tested the use of free software for basic image analysis and processing. In this way, free software was also tested

to process and analyses the thermal images retrieved along the trial. The planting spacing/density characteristics, and especially the inter row spacing (2.5m), of the vineyard used (Fig.7-10) made it possible to carry out this study and to elaborate a basic protocol to retrieve and analyse thermal images obtained in field conditions. Since distances between rows of less than 2.5 m would make it impossible to acquire 5 vines per image, as they would not be included in the optical field of both thermal cameras, a distance of at least 1.80 m to the object (the vine's row) plus 30-50 cm was required for the setting.

The setting up was affected by several technical and important difficulties that were related with the different cameras and computer characteristics and incompatibilities. Indeed, there were problems when using the two thermal cameras connected to the Pc MacBook pro 2016 2 USB-C inputs. In the case of Flir A35, this camera is equipped with an ethernet cable for both power and data transfer. This obliged to purchase two adapters, one from USB-C to USB 2.0 and another from USB 2.0 to ethernet. In turn, the Flir One Pro LT, is equipped with a USB-C connection which is not compatible with the iPhone 8, and which obliged to used other phone Honor X8 to capture images with this camera. This issues emphasis the limitations posed by technology especially when using different types of cameras in field conditions

In addition to the testing of low-cost imagers, we aimed at creating a low cost and user-friendly image analysis protocol that could reduce the time required to analyse images retried by the two thermal cameras and based on open source and simple software tools.

One of the main steps that led to thinking about how to do this was the size of the ROIs to be used to analyse the thermal images. The initial idea was to have a set of large ROIs that could identify a large part of the canopy region per vine, and get more information form a large number of pixels. This idea was however abandoned because: 1) it showed down of the analysis process: the use of large ROIs meant that every time the ROIs saved with ROI manager (Step 4-5 section 3.7.1) were added, it was needed to edit each individual ROI to better frame vine's leaf canopy making the protocol long and complex, which was contrary to the initial aim. Therefore, and attending to the homogeneity of the canopy temperatures we tested the use of small, and always identical ROI which allowed them to be moved in the images without the need to changes in the ROI area. Nevertheless, we must consider that this option loses pixel information and generates small but still significant differences in the average temperatures (e.g., about 0,6C between the large and small ROIs. (See Appendix). In addition, the use of small regions of interest (ROIs) (9-10 pixels) made it possible to standardise the number of pixels without the need to modify or adjust all images using FIJI (ImageJ distribution). It is clear that having acquired images in diagonal perspective, we will find that it can exist some distortion in the borders of the due to different pixel dimensions. This means that the ROI for the first vine is about half of the canopy size in the case of the last one is only about 2 leaves. This option, however, was the preferred in to speed up image analysis and to

have a roughly similar number of pixels analysed for all images, i.e., the same number of pixels for all images.

It is also important to point out that during the trials and set up there was a set of issues related to the image analysis process and related to the combination of different hardware and non-compatible characteristics.

Using a computer with a Windows operating system we could run the Flir Tools software (Flir Systems, USA) (https://www.flir.com/support/products/flir-tools/#Overview) and then transfer images to a Macintosh computer to implement an analyst by using the ImageJ software. However, other problem emerged as the Flir tools, software only runs on a Windows operating system. The Flir Systems company released a unique software available for Mac called *Flir Research Studio* (https://www.flir.com/products/flir-research-studio/), which allows to analyse both images and videos but unfortunately it is a paid software. As consequence we tested the use of the open-source free Fiji (ImageJ) software (https://imagej.net/software/fiji/).

Initially, we proceeded by downloading thermal image macros and plugins, called ThermimageJ, allowing the direct transfer of radiometric JPEGS. We then proceeded by validating the use of ImageJ with this macro package: Transferring a non-radiometric JPEG image to ImageJ, then transforming it into 8bit format, calibrating it so that each pixel value was given a certain value corresponding to the temperature. We then compared for the same ROI of the two images whether the maximum minimum and average temperature values corresponded, giving us a positive result.

When comparing the two methodologies for image analysis (see sections 3.7.1 and 3.7.2), the use of ThermimageJ permitted a faster analysis than only using exclusively the Fiji (ImageJ distribution) as configured when downloaded. This saved time once the functioning was understood. No particularly limiting factors presented themselves when using this software for analysing thermal images. The only limiting factor (not only in the use of this software, but also in the use of the analysis method for the Flir One ProLT thermal camera), is the fact that it is impossible to add a thermal scale with adapted values to those pre-set in the image characteristics setting (step 3 section 3.7.1).

5.2. Image analysis and processing

Image retrieval is important, but imaging processing is another very important aspect of imaging applied to plant/crop monitoring, phenotyping and remote sensing of crops (Costa et al., 2019. Image analysis can be done by using different types of software, but to make the process cheaper and user-friendly low cost or free software is required

In this study we have found several critical issues related with the three software packages and the ImageJ has emerged as, the most suitable free software for our purpose. We have used the Fiji software (image distribution) that is an open-source image processing

package based on ImageJ2. The ImageJ2 is a rewrite of ImageJ for multidimensional image data, with a focus on scientific imaging and the major goal of such software is to broaden the paradigm of ImageJ beyond the limitations of the original ImageJ application, to support the next generation of multidimensional scientific imaging. (https://imagej.net/software/imagej2/)

Fiji's main purpose is to provide a distribution of ImageJ2 with many bundled plugins. This is because this software is able to be implemented with ThermimageJ, (Tattersall; 2019) a package of macros and plugins (see https://github.com/gtatters/ThermImageJ)Thanks to ThermimageJ, images can be imported directly in radiometric Jpeg so that the image does not have to be calibrated, saving time. However, this approach revealed only to apply to Flir A35 images because images taken with the Flir One ProLT were recognized as an RGB image requiring a more time-consuming procedure as they are not in the form of a radiometric jpeg.

5.3. Soil and canopy temperature vs mulching treatments

Thermal images were taken in series: first the control, then the rice straw mulch, and the eucalyptus mulch, first row 24 and then row 25. The fact that the temperatures observed for the control during the morning hours (Fig. 19 C and E) were lower, contrary to what is shown in images 19D and 19F, may be related with the fact that the images were not taken at the same time and therefore the effect of higher air temperatures and sun radiation (approaching midday) would have positively influenced the surface temperatures measured for the eucalyptus and rice straw mulches.

Because the control was the first treatment to be analysed at 09.30 hours (line 24), it had not yet been significantly affected by the morning climatic conditions. The same applies to line 25. Obviously, we have to consider it shifted by 45m, therefore at a different time, but as the image acquisitions were always carried out in series and not at the same time, we found ourselves with lower temperature and irradiation conditions for the control line 25. This is confirmed by the trend on the shaded side, which instead confirms the afternoon trend, showing in both cases a linear decrease in temperature from the control to the rice straw.

Our results show that the temperature of the upper part of the canopy is lower than that of the lower part (Figure 21). This can be due to several reasons including, for the higher part, the greater influence from the wind and leaf morphology (Jones, 1992a; Teixeira et al., 2018; Costa et al. 2019) which means leaves with less surface area have better control in temperature. For the lower part we may consider the influence of the soil in heating the basal leaves it so also a different soil composition (Cellier 1991; Ressèguier et al., 2020; Costa et al., 2019). This suggests that vertical profiles found, and their variation are greatly influenced by the dominant atmospheric conditions (Ressèguier et al., 2020). If fact, the soil water factor could be discarded from this condition because all the three treatments have very similar

temperature variation as well identical values of stomatal conductance, with exception of the rice straw plants that showed higher gs value.

Comparing the three treatments and considering the fact that mulching would help soil to retain more water at the upper levels of the soil due to limited evaporation, (Yang et al., 2021) vines were supposed to perform better in terms of gs and as consequence to show lower canopy Ts (Medrano et al., 2003; Costa et al. 2013). However, that seems not to occur and more extended observation (in time and in number of repetitions) would be needed to conclude about the effects of the mulching on plants water status and leaf gas exchange. It would be also necessary to optimize measurements of plant water status and include in the future trials measurements of leaf water potential (ex. pre-dawn and midday) to assess eventual variation in plant water status.

5.4. Canopy temperature and CWSI

In contrast to previous literature (Neves 2021; Tejero et al., 2018), the canopy temperature values measured using the low-cost thermal camera (Flir One ProLT) showed major limitations. The FlirOne was not able to identify patterns nor major differences contrary to the Flir A35 camera (see Figures 21-22). It is possible that Flir One measurements need more repetitions and other type of image analyses that takes advantage of larger ROIs.

Because of the limitations of the Flir One, the thermal index CWSI was calculated only by using data from the Flir A35. The CWSI estimated for the vines subjected to the different treatments indicate a range of values around 0.8 suggesting that no severe water stress was being experienced by our vines during the trial (Belfiore et al., 2019; Pagay & Kidman, 2019; Sepúlveda-Reyes et al., 2016). This relates with the fact that vines were irrigated. Furthermore, it can be observed that there is an increase in the CWSI values along the season, especially during the afternoon hours indicating a progressive increase in the conditions of stress. In this trial, the atmospheric climatic conditions (air T, Radiation and VPD) seem to play here a more important role than the soil water status, cause soil water availability has been kept quite similar along the season due to irrigation. Indeed, partial stomata closure could be promoted by higher air temperature and higher VPD conditions during the afternoon period (Costa et al., 2012; Simonneau et al., 2017; Paul and Foyer, 2001; Farquhar and Sharkey, 1982) (see section 5.4).

5.5. Leaf gas exchange and Chl fluorescence

Reduced stomatal conductance in the afternoon hours is confirmed by higher CWSI values revealing less favourable conditions to leaf gas exchange in the noon period making the plants to reduce stomatal conductance (Speirs et al., 2013). Leaf gas exchange is mostly affected by climate condition as discussed by (Rahimi-Eichi et al., 2013) and it follows that the values shown in Table 7 suggest a typical daily course of stomatal conductance, such as: the increase in VPD from daytime to afternoon hours that causes a decrease in gs values (Chaves et al., 2010; Broughton et al., 2021),

5.6. Flir One Pro LT vs Flir A35

In this study, an attempt was made to identify the potential usefulness of the low cost and low resolution Flir One Pro LT in the agricultural sector, and in this specific to monitor soil and plant temperature. This low-cost thermal camera using the protocol shown in (section 3.5.2) is unable to detect significant differences in canopy temperatures (Fig.22). On the contrary, it proved to be useful as it was particularly accurate, compared to the Flir A35, when detecting temperature differences between the sunlit and shadow sides of the ground surface, which can be related with the larger delta Ts between shadow and sunlit soil (Fig. 20). It is possible that for such a large delta Ts the Flir One is suitable and high precision is not required, but only a preliminary evaluation has been made in this study. We may suggest the detection of irrigation leaks in the soil, which would generate major temperature differences between dry and wet sides (Krapez et al., 2022). The use of the temperature values resulting from less precise cameras may pose limitations to the calculation of thermal indexes and may result in misinterpretations of the situation. Our results are not in line with previous studies (Neves 2018; Blaya-Ros et al., 2020) but it is possible that the set-up, the limited number and small size of the selected ROIs and also the reduced number of repetitions may have limit the robustness of the results derived from the Flir One.

The positive aspects are that it is easy to use, pocket-sized, does not require bulky tools for its operation, does not require external power supply. Another major disadvantage of the Flir One is the energy issue. If the time interval between one image and the next is greater than 1 minute and the quantity of thermal images to be acquired is high (over a dozen), you are forced to switch off the camera to save the battery for about an hour at full power. The problem is that switching on and connecting takes at least 10-15 seconds, which creates an unpleasant condition with considerable waiting time. So, if we are looking to optimise the process and reduce image acquisition time, this camera is somewhat ill-advised. On the other hand, if we need to evaluate a few samples and in series, it could be an economical and quick-use alternative as we do not have to carry other tools with us, which would require the use of a high-resolution thermal camera such as the Flir A35.

In the agricultural sphere, Flir One ProLT**,** it could be used in the monitoring of irrigation systems to determine whether, for example, we have leaks in an irrigation system, but even in this case, since it is a camera that has to be attached to a mobile phone, it is assumed that the operator in the field, given that the loss of water to cause an increase in the temperature of the plastic irrigation pipe must be considerable, would notice it without the use of the camera. Maybe other models could be more adequate to that such as the Cat S60, which is a mobile phone with an integrated thermal camera.

Moreover, as it is not an automatable, proximity process, it would not make sense to employ it in this manner. On the other hand, it could be the use of this camera with machines or objects that make heat absorption or emission their main purpose, and thus assess whether there is a large temperature difference in the process due to a component malfunction or leakage, as in the case of solar panels.

The Flir A35 has potential to field monitoring but we must still optimize the measuring protocols and the limitations posed by the equipment. The use of the image software analyses should be improved in order to take the advantage of the maximum number pixels while guaranteeing a fast data analysis and processing.

6. CONCLUSION AND FUTURE

In the context of precision viticulture and aiming at using thermal cameras to measure both canopy and soil temperature, it is certainly necessary to validate these thermal data over time and ultimately to combine them with soil moisture data and plant water status using an increased number of sensors in the soil and an algorithm that can relate soil and plant water values with leaf temperature and soil moisture values.

More information is also needed about the true impact of the organic mulch on the longer term in terms of soil and plant temperature but also in terms of plant water status. It will be relevant to study the effects of mulching on keeping the canopy at optimal temperatures for photosynthesis (e.g., below 30 ºC) in order to promote photosynthesis throughout the growing season by counteracting heat peaks and drought and thus being able to irrigate more efficiently by increasing water use efficiency values. Also, a better characterization of the soil should be done as means to know better the structure and texture of the soil to be able to better modulate irrigation and to better understand soil temperature and soil water status variation. Even these studies require considerable effort to see how the canopy responds to the amount of irrigation water supplied and soil water status changes.

Finally low-cost thermal sensors could be a useful alternative to considerably reduce costs and time for data collection, as they are very simple to use and do not need to be used by particularly skilled operators. On the other hand, they are not as accurate as a medium- and high-cost sensors and one of the main objectives of this work is to determine whether these types of sensors are useful for field surveying and whether the values determined by these instruments are not too different from high-resolution ones without compromising subsequent operations.

In addition to optimising the set-up and creating a protocol that could be valid for detecting leaf and soil temperatures by means by ground-based measurements with thermal cameras one of the main objectives was to evaluate an effective effect of mulching compared to an untreated 'control' treatment. In some cases, the effect of mulching: on increasing the stomatal conductance, reducing leaf and soil surface temperature and improving water status condition of the vines was observed using “rice straw”, but the data recorded were sometimes discordant and variable and without the presence of particularly significant trends. This leads us to reflect that the mulching actually could be a useful strategy for improving the eco-physiological conditions of the vine not in a single season, evaluating its effects after 3-4 years considering it as a medium to long term strategy.

More studies are needed to properly evaluate the performance of low-cost devices and optimize image analysis and protocols. The set up also has limitations in terms of the number

of observations and the image analysis was based not only in few plants but also in reduced number of ROIs. This can affect the conclusions with regards to the performance of the Flir One and explain some differences to previous literature (Neves, 2018; Tejero et al, 2018).

REFERENCES

Abbas, A. K., Heimann, K., Blazek, V., Orlikowsky, T., & Leonhardt, S. (2012). Neonatal infrared thermography imaging: Analysis of heat flux during different clinical scenarios. *Infrared Physics & Technology*, *55*(6), 538–548. https://doi.org/10.1016/j.infrared.2012.07.001

Alchanatis, V., Cohen, Y., Cohen, S., Moller, M., Meron, M., Tsipris, J., Orlov, V., Naor, A., & Charit, Z. (2006). *Fusion of IR and Multispectral Images in the Visible Range for Empirical and Model Based Mapping of Crop Water Status*. https://doi.org/10.13031/2013.20652

Akbar H., Silva, J. A., Lozovskayaa, M. V., & Zvolinsky, V. P. (2012). High temperature combined with drought affect rainfed spring wheat and barley in South-Eastern Russia: I. Phenology and growth. Journal of Biosciences, 19(4), 473-487.

Akter, M., Miah, M., Hassan, M., Mobin, M., & Baten, M. (2016). Textural Influence on Surface and Subsurface Soil Temperatures under Various Conditions. *Journal of Environmental Science and Natural Resources*, *8*(2), 147–151. https://doi.org/10.3329/jesnr.v8i2.26882

Alpar, O., & Krejcar O. (2017). Quantization and equalization of pseudo colour images in hand thermography. In: Rojas I, Ortuo F, eds. Bioinf. and biom. engin. Lecture notes in computer science, 397-407.

Atkinson, C. J., Brennan, R. M., & Jones, H. G. (2013). Declining chilling and its impact on temperate perennial crops. *Environmental and Experimental Botany*, *91*, 48–62. https://doi.org/10.1016/j.envexpbot.2013.02.004

Baluja, J., Diago, M. P., Balda, P., Zorer, R., Meggio, F., Morales, F., & Tardaguila, J. (2012). Assessment of vineyard water status variability by thermal and multispectral imagery using an unmanned aerial vehicle (UAV). *Irrigation Science*, *30*(6), 511–522. https://doi.org/10.1007/s00271-012-0382-9

Belfiore, N., Vinti, R., Lovat, L., Chitarra, W., Tomasi, D., de Bei, R., Meggio, F., et al. (2019). Infrared Thermography to Estimate Vine Water Status: Optimizing Canopy Measurements and Thermal Indices for the Varieties Merlot and Moscato in Northern Italy. *Agronomy*, *9*(12), 821. http://dx.doi.org/10.3390/agronomy9120821

Bellvert, J., Zarco-Tejada, P. J., Girona, J., & Ferrers, E. (2014). Mapping crop water stress index in a «Pinot-noir» vineyard: Comparing ground measurements with thermal remote sensing imagery from an unmanned aerial vehicle. *Precision Agriculture*, *15*(4), 361–376.

Bellvert, J., Zarco-Tejada, P. j., Marsal, J., Girona, J., González-Dugo, V., & Fereres, E. (2016). Vineyard irrigation scheduling based on airborne thermal imagery and water potential thresholds. *Australian Journal of Grape and Wine Research*, *22*(2), 307–315. https://doi.org/10.1111/ajgw.12173

Bendel, N., Backhaus, A., Kicherer, A., Köckerling, J., Maixner, M., Jarausch, B., Biancu, S., Klück, H.-C., Seiffert, U., Voegele, R. T., & Töpfer, R. (2020). Detection of Two Different Grapevine Yellows in Vitis vinifera Using Hyperspectral Imaging. Remote Sensing, 12(24), 4151. https://doi.org/10.3390/rs12244151

Benelli, A., Cevoli, C., Ragni, L., & Fabbri, A. (2021). In-field and non-destructive monitoring of grapes maturity by hyperspectral imaging. Biosystems Engineering (207), 59.agg

Bernardo, S., Dinis, L.-T., Machado, N., & Moutinho-Pereira, J. (2018). Grapevine abiotic stress assessment and search for sustainable adaptation strategies in Mediterranean-like climates. A review. Agronomy for Sustainable Development, 38(6), 66. https://doi.org/10.1007/s13593-018-0544-0

Berni, J., Zarco-Tejada, P. J., Suarez, L., & Fereres, E. (2009). Thermal and Narrowband Multispectral Remote Sensing for Vegetation Monitoring From an Unmanned Aerial Vehicle. *IEEE Transactions on Geoscience and Remote Sensing*, *47*(3), 722–738. https://doi.org/10.1109/TGRS.2008.2010457

Bhandari, A. K., Kumar, A., & Singh, G. K. (2012). Feature Extraction using Normalized Difference Vegetation Index (NDVI): A Case Study of Jabalpur City. *Procedia Technology*, *6*, 612–621. https://doi.org/10.1016/j.protcy.2012.10.074

Blancquaert, E. H., Oberholster, A., Ricardo-da-Silva, J. M., & Deloire, A. J. (2019). Effects of Abiotic Factors on Phenolic Compounds in the Grape Berry – A Review. *South African Journal of Enology and Viticulture*, *40*(1), Article 1. https://doi.org/10.21548/40-1-3060

Broughton, K. J., Payton, P., Tan, D. K. Y., Tissue, D. T., & Bange, M. P. (2021). Effect of vapour pressure deficit on gas exchange of field-grown cotton. *Journal of Cotton Research*, *4*(1), 30. https://doi.org/10.1186/s42397-021-00105-4

Brown, S. J. (2020). Future changes in heatwave severity, duration, and frequency due to climate change for the most populous cities. *Weather and Climate Extremes*, *30*, 100278. https://doi.org/10.1016/j.wace.2020.100278

Bruce, W. B., Edmeades, G. O., & Barker, T. C. (2002). Molecular and physiological approaches to maize improvement for drought tolerance. *Journal of Experimental Botany*, *53*(366), 13–25. https://doi.org/10.1093/jexbot/53.366.13

Burg, P., Čížková, A., Mašán, V., Sedlar, A., Matwijczuk, A., & Souček, J. (2022). The Effect of Mulch Materials on Selected Soil Properties, Yield and Grape Quality in Vineyards under Central European Conditions. *Agronomy*, *12*(8). https://doi.org/10.3390/agronomy12081862

Cacciabue, M., Currá, A., & Gismondi, M. I. (2019). ViralPlaque: A Fiji macro for automated assessment of viral plaque statistics. *PeerJ*, *7*, e7729. https://doi.org/10.7717/peerj.7729

Campos, J., García-Ruíz, F., & Gil, E. (2021). Assessment of Vineyard Canopy Characteristics from Vigour Maps Obtained Using UAV and Satellite Imagery.*Sensors*, *21*(7), 2363. https://doi.org/10.3390/s21072363

Cellier, P., 1991. La prévision des gelées de printemps. Comptes Rendus de l'Académie d'Agriculture de France, 77: 55–64.

Chan, K. Y., Fahey, D. J., Newell, M., & Barchia, I. (2010). Using Composted Mulch in Vineyards—Effects on Grape Yield and Quality. *International Journal of Fruit Science*, *10*(4), 441–453. https://doi.org/10.1080/15538362.2010.530135

Chaves, M. M., Costa, J. M., & Saibo, N. J. M. (2011). Chapter 3—Recent Advances in Photosynthesis Under Drought and Salinity. In I. Turkan (A c. Di), *Plant Responses to Drought and Salinity Stress* (Vol. 57, pp. 49–104). Academic Press. https://doi.org/10.1016/B978-0-12-387692-8.00003-5

Chaves, M. M., Santos, T. p., Souza, C. R., Ortuño, M. f., Rodrigues, M. l., Lopes, C. M., Maroco, J. p., & Pereira, J. s. (2007). Deficit irrigation in grapevine improves water-use efficiency while controlling vigour and production quality. *Annals of Applied Biology*, *150*(2), 237–252. https://doi.org/10.1111/j.1744-7348.2006.00123.x

Chaves, M. M., Zarrouk, O., Francisco, R., Costa, J. M., Santos, T., Regalado, A. P., Rodrigues, M. L., & Lopes, C. M. (2010). Grapevine under deficit irrigation: Hints from physiological and molecular data. *Annals of Botany*, *105*(5), 661–676. https://doi.org/10.1093/aob/mcq030

Chen, S. y., Zhang, X. y., Pei, D., Sun, H. y., & Chen, S. l. (2007). Effects of straw mulching on soil temperature, evaporation and yield of winter wheat: Field experiments on the North China Plain. *Annals of Applied Biology*, *150*(3), 261–268. https://doi.org/10.1111/j.1744-7348.2007.00144.x

Costa, J. M., Egipto, R., Sánchez-Virosta, A., Lopes, C. M., & Chaves, M. M. (2019). Canopy and soil thermal patterns to support water and heat stress management in vineyards. *Agricultural Water Management*, *216*, 484–496. https://doi.org/10.1016/j.agwat.2018.06.001

Costa, J.M., Grant, O., Chaves, M. (2010). Use of Thermal Imaging in Viticulture: Current Application and Future Prospects. In: Delrot, S., Medrano, H., Or, E., Bavaresco, L., Grando, S. (eds) Methodologies and Results in Grapevine Research. Springer, Dordrecht. https://doi.org/10.1007/978-90-481-9283-0_10

Costa, J. M., Grant, O. M., & Chaves, M. M. (2013). Thermography to explore plant–environment interactions. *Journal of Experimental Botany*, *64*(13), 3937–3949. https://doi.org/10.1093/jxb/ert029

Costa, J. M., Ortuño, M. F., Lopes, C. M., & Chaves, M. M. (2012). Grapevine varieties exhibiting differences in stomatal response to water deficit. *Functional Plant Biology*, *39*(3), 179. https://doi.org/10.1071/FP11156

Costa, J. M., Marques da Silva, J., Pinheiro, C., Barón, M., Mylona, P., Centritto, M., Haworth, M., Loreto, F., Uzilday, B., Turkan, I., & Oliveira, M. M. (2019). Opportunities and Limitations of Crop Phenotyping in Southern European Countries. *Frontiers in Plant Science*, *10*. https://doi.org/10.3389/fpls.2019.01125Costa

Costa, J. M., Egipto, R., Silvestre, J., Lopes, C. M., & Chaves, M. M. (2018). Chapter 10—Water and Heat Fluxes in Mediterranean Vineyards: Indicators and Relevance for Management. In I. F. G. Tejero & V. H. D. Zuazo (A c. Di), *Water Scarcity and Sustainable Agriculture in Semiarid Environment* (pp. 219–245). Academic Press. https://doi.org/10.1016/B978-0-12-813164-0.00010-7

Costa, J. M., Vaz, M., Escalona, J., Egipto, R., Lopes, C., Medrano, H., & Chaves, M. M. (2016). Modern viticulture in southern Europe: Vulnerabilities and strategies for adaptation to water scarcity. *Agricultural Water Management*, *164*, 5–18. https://doi.org/10.1016/j.agwat.2015.08.021

Crameri, F., Shephard, G. E., & Heron, P. J. (2020). The misuse of colour in science communication. *Nature Communications*, *11*(1), 5444. https://doi.org/10.1038/s41467-020-19160-7

Crawford, A. J., McLachlan, D. H., Hetherington, A. M., & Franklin, K. A. (2012). High temperature exposure increases plant cooling capacity. *Current Biology*, *22*(10), R396–R397. https://doi.org/10.1016/j.cub.2012.03.044

Damour, G., Simonneau, T., Cochard, H., & Urban, L. (2010). An overview of models of stomatal conductance at the leaf level. *Plant, Cell & Environment*, *33*(9), 1419–1438. https://doi.org/10.1111/j.1365-3040.2010.02181.x

De Rosas, I., Ponce, M. T., Malovini, E., Deis, L., Cavagnaro, B., & Cavagnaro, P. (2017). Loss of anthocyanins and modification of the anthocyanin profiles in grape berries of Malbec and Bonarda grown under high temperature conditions. *Plant Science*, *258*, 137–145. https://doi.org/10.1016/j.plantsci.2017.01.015

DeVetter, L. W., Dilley, C. A., & Nonnecke, G. R. (2015). Mulches Reduce Weeds, Maintain Yield, and Promote Soil Quality in a Continental-Climate Vineyard. *American Journal of Enology and Viticulture*, *66*(1), 54–64. https://doi.org/10.5344/ajev.2014.14064

Downton, W. J. S., Grant, W. J. R., & Loveys, B. R. (1987). Diurnal Changes in the Photosynthesis of Field-Grown Grape Vines. *New Phytologist*, *105*(1), 71–80. https://doi.org/10.1111/j.1469-8137.1987.tb00111.x

Duchêne, E., Huard, F., Dumas, V., Schneider, C., & Merdinoglu, D. (2010). The challenge of adapting grapevine varieties to climate change. *Climate Research*, *41*(3), 193–204. https://doi.org/10.3354/cr00850

Ervideiro, J.M. (2021) Inoculation of mycorrhizal fungi on a vineyard. The impact of a mycorrhiza-inoculated under-vine cover crop on grapevine performance and soil quality in a Portuguese vineyard. *Dissertação de Mestrado em Engenharia Agronomica*. Instituto Superior de Agronomia, Universidade de Lisboa, Lisboa

Farquhar, G.D. and Sharkey, T.D. (1982) Stomatal Conductance and Photosynthesis. Annual Review of Plant Physiology, 33, 317-345. http://dx.doi.org/10.1146/annurev.pp.33.060182.001533

Feller, U., & Vaseva, I. I. (2014). Extreme climatic events: Impacts of drought and high temperature on physiological processes in agronomically important plants. *Frontiers in Environmental Science*, https://www.frontiersin.org/articles/10.3389/fenvs.2014.00039

Ferrini, F., Mattii, G. B., & Nicese, F. P. (1995). Effect of temperature on key physiological responses of grapevine leaf *American Journal of Enology and Viticulture*.

Fraga, H., Malheiro, A. C., Moutinho-Pereira, J., & Santos, J. A. (2012). An overview of climate change impacts on European viticulture. *Food and Energy Security*, *1*(2), 94–110. https://doi.org/10.1002/fes3.14

Fraga, H., Molitor, D., Leolini, L., & Santos, J. A. (2020). What Is the Impact of Heatwaves on European Viticulture? A Modelling Assessment. *Applied Sciences*, *10*(9), 3030. https://doi.org/10.3390/app10093030

Fraga, H., & Santos, J. A. (2018). Vineyard mulching as a climate change adaptation measure: Future simulations for Alentejo, Portugal. *Agricultural Systems*, *164*, 107–115. https://doi.org/10.1016/j.agsy.2018.04.006

Fuentes, S., De Bei, R., Pech, J., & Tyerman, S. (2012). Computational water stress indices obtained from thermal image analysis of grapevine canopies. *Irrigation Science*, *30*(6), 523–536. https://doi.org/10.1007/s00271-012-0375-8

Gambetta, J. M., Holzapfel, B. P., Stoll, M., & Friedel, M. (2021). Sunburn in Grapes: A Review. *Frontiers in Plant Science*, *11*. https://doi.org/10.3389/fpls.2020.604691

García-Tejero, I. F., Ortega-Arévalo, C. J., Iglesias-Contreras, M., Moreno, J. M., Souza, L., Tavira, S. C., & Durán-Zuazo, V. H. (2018). Assessing the Crop-Water Status in Almond (*Prunus dulcis* Mill.) Trees via Thermal Imaging Camera Connected to Smartphone. *Sensors*, *18*(4), 1050. https://doi.org/10.3390/s18041050

Giorgi, F. (2006). Climate change hot-spots. *Geophysical Research Letters*, *33*(8). https://doi.org/10.1029/2006GL025734

Goel, J., Nizamoglu, M., Tan, A., Gerrish, H., Cranmer, K., El-Muttardi, N., Barnes, D., & Dziewulski, P. (2020a). A prospective study comparing the FLIR ONE with laser Doppler imaging in the assessment of burn depth by a tertiary burns unit in the United

Kingdom. *Scars, Burns & Healing*, *6*, 2059513120974261. https://doi.org/10.1177/2059513120974261

Goel, J., Nizamoglu, M., Tan, A., Gerrish, H., Cranmer, K., El-Muttardi, N., Barnes, D., & Dziewulski, P. (2020b). A prospective study comparing the FLIR ONE with laser Doppler imaging in the assessment of burn depth by a tertiary burns unit in the United Kingdom. Scars, Burns & Healing, 6, 2059513120974261. https://doi.org/10.1177/2059513120974261

Grahn, H., & Geladi, P. (2007). Techniques and applications of hyperspectral image analysis. John Wiley and Sons.

Grant, O. M. (2012, 03 22). Thermography in Viticulture. Book of Proceedings – Appendix 1 of Thermology international.

Grant, O. M., Ochagavía, H., Baluja, J., Diago, M. P., & Tardáguila, J. (2016). Thermal imaging to detect spatial and temporal variation in the water status of grapevine (*Vitis vinifera* L.). The Journal of Horticultural Science and Biotechnology, 91(1), 43–54. https://doi.org/10.1080/14620316.2015.1110991

Gutiérrez, S., Diago, M. P., Fernández-Novales, J., & Tardaguila, J. (2018). Vineyard water status assessment using on-the-go thermal imaging and machine learning. *PLOS ONE*, *13*(2), e0192037. https://doi.org/10.1371/journal.pone.0192037

Gutiérrez, S., Diago, M. P., Fernández-Novales, J., & Tardaguila, J. (2018). On-The-Go Hyperspectral Imaging Under Field Conditions and Machine Learning for the Classification of Grapevine Varieties. *Frontiers in Plant Science*, *9*. https://www.frontiersin.org/articles/10.3389/fpls.2018.01102

Gutiérrez, S., Tardaguila, J., Fernández-Novales, J., & Diago, M. p. (2019). On-the-go hyperspectral imaging for the in-field estimation of grape berry soluble solids and anthocyanin concentration. *Australian Journal of Grape and Wine Research*, *25*(1), 127–133. https://doi.org/10.1111/ajgw.12376

Gutiérrez-Gamboa, G., Zheng, W. and Martínez de Toda, F. (2021), Strategies in vineyard establishment to face global warming in viticulture: a mini review. J Sci Food Agric, 101: 1261-1269. https://doi.org/10.1002/jsfa.10813

Hall, A., Lamb, D. w., Holzapfel, B., & Louis, J. (2002). Optical remote sensing applications in viticulture—A review. *Australian Journal of Grape and Wine Research*, *8*(1), 36–47. https://doi.org/10.1111/j.1755-0238.2002.tb00209.x

Hall, A., Lamb, D. W., Holzapfel, B. P., & Louis, J. P. (2011). Within-season temporal variation in correlations between vineyard canopy and winegrape composition and yield. *Precision Agriculture*, *12*(1), 103–117. https://doi.org/10.1007/s11119-010-9159-4

Hossain, A., Teixeira da Silva, J. A., Lozovskaya, M. V., & Zvolinsky, V. P. (2012). High temperature combined with drought affect rainfed spring wheat and barley in South-Eastern Russia: I. Phenology and growth. *Saudi Journal of Biological Sciences*, *19*(4), 473–487. https://doi.org/10.1016/j.sjbs.2012.07.005

Horton, R., Bristow, R.I., Rluitenberg, G.J. and Sauer, T.J. (1996). Crop residue effects on surface radiation and energy-balance review: Theoretical and applied climatology, 54: 27-37.

Idso, S. B., Jackson, R. D., Pinter, P. J., Reginato, R. J., & Hatfield, J. L. (1981). Normalizing the stress-degree-day parameter for environmental variability. *Agricultural Meteorology (Netherlands)*.

Ingvordsen, C. H., Lyngkjær, M. F., Peltonen-Sainio, P., Mikkelsen, T. N., Stockmarr, A., & Jørgensen, R. B. (2018). How a 10-day heatwave impacts barley grain yield when superimposed onto future levels of temperature and CO2 as single and combined factors. *Agriculture, Ecosystems & Environment*, *259*, 45–52. https://doi.org/10.1016/j.agee.2018.01.025

IPCC, 2021: Climate Change 2021: The Physical Science Basis. Contribution of Working Group I to the Sixth Assessment Report of the Intergovernmental Panel on Climate Change [Masson-Delmotte, V., P. Zhai, A. Pirani, S.L. Connors, C. Péan, S. Berger, N. Caud, Y. Chen, L. Goldfarb, M.I. Gomis, M. Huang, K. Leitzell, E. Lonnoy, J.B.R.

Matthews, T.K. Maycock, T. Waterfield, O. Yelekçi, R. Yu, and B. Zhou (eds.)]. Cambridge University Press, Cambridge, United Kingdom and New York, NY, USA, In press, doi:10.1017/9781009157896

Irujo, G. P. (2022). IRimage: Open source software for processing images from infrared thermal cameras. *PeerJ Computer Science*, *8*, e977. https://doi.org/10.7717/peerj-cs.977

Jiang, H., Howell, G. S., & Flore, J. A. (1999). Efficacy of chlorophyll fluorescence as availability test for freeze-stressed woody grape tissues. Canadian journal of plant science. 401-409

Jiang, X., & Li, X. G. (2015). Assessing the effects of plastic film fully mulched ridgef furrow on rainwater distribution in soil using dye tracer and simulated rainfall. *Soil and Tillage Research*, *152*, 67–73. https://doi.org/10.1016/j.still.2015.04.002

Jones, H. G. (1999). Use of infrared thermometry for estimation of stomatal conductance as a possible aid to irrigation scheduling. *Agricultural and Forest Meteorology*, *95*(3), 139–149. https://doi.org/10.1016/S0168-1923(99)00030-1

Jones H. G., & Vaughan, A. R. (2010). Remote Sensing of Vegetation: Principles, Techniques, and Applications. Oxford university press.

Jones, H. G., & Grant, O. M. (2015). Remote sensing and other imaging technologies to monitor grapevine performance. In *Grapevine in a Changing Environment* (pagg. 179–201). John Wiley & Sons, Ltd. https://doi.org/10.1002/9781118735985.ch8

Jones, H. G., Stoll, M., Santos, T., Sousa, C. de, Chaves, M. M., & Grant, O. M. (2002). Use of infrared thermography for monitoring stomatal closure in the field: Application to grapevine. *Journal of* Experimental Botany, 53(378), 2249–2260. https://doi.org/10.1093/jxb/erf083

Kaplan H (2007) Practical applications of infrared thermal sensing and image equipment. SPIE Publications, Bellingham.

Katimbo, A., Rudnick, D. R., DeJonge, K. C., Lo, T. H., Qiao, X., Franz, T. E., Nakabuye, H. N., & Duan, J. (2022). Crop water stress index computation approaches and their sensitivity to soil water dynamics. *Agricultural Water Management*, *266*, 107575. https://doi.org/10.1016/j.agwat.2022.107575

Keller, M. T., & Keller, M. E., Elsevier Academic Press: London, U. 2., & 400., p. (n.d.).

Kottek, M., Grieser, J., Beck, C., Rudolf, B., & Rubel, F. (2006). World Map of the Köppen-Geiger Climate Classification Updated. *Meteorologische Zeitschrift*, *15*, 259–263. https://doi.org/10.1127/0941-2948/2006/0130

Krapez, J.-C., Sanchis Muñoz, J., Mazel, C., Chatelard, C., Déliot, P., Frédéric, Y.-M., Barillot, P., Hélias, F., Barba Polo, J., Olichon, V., Serra, G., Brignolles, C., Carvalho, A., Carreira, D., Oliveira, A., Alves, E., Fortunato, A. B., Azevedo, A., Benetazzo, P., … Le Goff, I. (2022). Multispectral Optical Remote Sensing for Water-Leak Detection. *Sensors*, *22*(3). https://doi.org/10.3390/s22031057

Krizhevsky, A., Sutskever, I., & Hinton, G. E. (2012a). ImageNet Classification with Deep Convolutional Neural Networks. *Advances in Neural Information Processing Systems*, *25*. https://proceedings.neurips.cc/paper/2012/hash/c399862d3b9d6b76c8436e924a68c45b-Abstract.html

Krizhevsky, A., Sutskever, I., & Hinton, G. E. (2012b). ImageNet classification with deep convolutional neural networks. *Proceedings of the 25th International Conference on Neural Information Processing Systems - Volume 1*, 1097–1105.

Leeuwen, C. van, & Darriet, P. (2016a). The Impact of Climate Change on Viticulture and Wine Quality*. *Journal of Wine Economics*, *11*(1), 150–167. https://doi.org/10.1017/jwe.2015.21

Lereboullet, A.-L., Bardsley, D., & Beltrando, G. (2013). Assessing vulnerability and framing adaptive options of two Mediterranean wine growing regions facing climate change:

Roussillon (France) and McLaren Vale (Australia). *EchoGéo*, *23*, Article 23. https://doi.org/10.4000/echogeo.13384

Levin, A. D., Deloire, A., & Gambetta, G. A. (2020). Does water deficit negatively impact wine grape yield over the long term? : Original language of the article: English. *IVES Technical Reviews, Vine and Wine*. https://doi.org/10.20870/IVES-TR.2020.4029

Lionello, P., Abrantes, F., Gacic, M., Planton, S., Trigo, R., & Ulbrich, U. (2014). The climate of the Mediterranean region: Research progress and climate change impacts. *Regional Environmental Change*, *14*(5), 1679–1684. https://doi.org/10.1007/s10113-014-0666-0

Lopes, C., Graça, J., Sastre, J., Reyes, M., Guzman, R., Braga, R., Monteiro, A., & Pinto, P. (2016, Luglio). VINEYARD YIELD ESTIMATION BY VINBOT ROBOT -PRELIMINARY RESULTS WITH THE WHITE VARIETY VIOSINHO. https://doi.org/10.13140/RG.2.1.3912.0886

Losana, U. (2022). Evaluation of organic mulching for weed management in vineyards. *Dissertação de Mestrado em Engenharia de Viticultura e Enologia*. Instituto Superior de Agronomia, Universidade de Lisboa, Lisboa.

Ludovisi, R., Tauro, F., Salvati, R., Khoury, S., Mugnozza Scarascia, G., & Harfouche, A. (2017). UAV-Based Thermal Imaging for High-Throughput Field Phenotyping of Black Poplar Response to Drought. Frontiers in Plant Science, 8. https://doi.org/10.3389/fpls.2017.01681

Maes, W. H., & Steppe, K. (2012). Estimating evapotranspiration and drought stress with ground-based thermal remote sensing in agriculture: A review. *Journal of Experimental Botany*, *63*(13), 4671–4712. https://doi.org/10.1093/jxb/ers165

Manfreda, S., McCabe, M. F., Miller, P. E., Lucas, R., Pajuelo Madrigal, V., Mallinis, G., Ben Dor, E., Helman, D., Estes, L., Ciraolo, G., Müllerová, J., Tauro, F., De Lima, M. I., De Lima, J. L. M. P., Maltese, A., Frances, F., Caylor, K., Kohv, M., Perks, M., … Toth, B. (2018). On the Use of Unmanned Aerial Systems for Environmental Monitoring. *Remote Sensing*, *10*(4), Art. 4. https://doi.org/10.3390/rs10040641

Mangus, D. L., Sharda, A., & Zhang, N. (2016). Development and evaluation of thermal infrared imaging system for high spatial and temporal resolution crop water stress monitoring of corn within a greenhouse. *Computers and Electronics in Agriculture*, *121*, 149–159. https://doi.org/10.1016/j.compag.2015.12.007

Marques da Silva, J., Correia, P., Calejo Pires, M., Soares Augusto, J., & Miguel Costa, J. (2020). Interdisciplinarity in action: Using infrared thermography to teach plants' energy balance in secondary education. *Proceedings of the 2020 International Conference on Quantitative InfraRed Thermography*. https://doi.org/10.21611/qirt.2020.062

Matese, A., Toscano, P., Di Gennaro, S. F., Genesio, L., Vaccari, F. P., Primicerio, J., Belli, C., Zaldei, A., Bianconi, R., & Gioli, B. (2015). Intercomparison of UAV, Aircraft and Satellite Remote Sensing Platforms for Precision Viticulture. *Remote Sensing*, *7*(3), 2971–2990. https://doi.org/10.3390/rs70302971

Medrano, H., Escalona, J. M., Cifre, J., Bota, J., & Flexas, J. (2003). A ten-year study on the physiology of two Spanish grapevine cultivars under field conditions: Effects of water availability from leaf photosynthesis to grape yield and quality. *Functional Plant Biology: FPB*, *30*(6), 607–619. https://doi.org/10.1071/FP02110

Miura, K., & Nørrelykke, S. F. (2021). Reproducible image handling and analysis. *The EMBO Journal*, *40*(3), e105889. https://doi.org/10.15252/embj.2020105889

Molitor, D., Junk, J., Evers, D., Hoffmann, L., & Beyer, M. (2014). A High-Resolution Cumulative Degree Day-Based Model to Simulate Phenological Development of Grapevine. *American Journal of Enology and Viticulture*, *65*(1), 72–80. https://doi.org/10.5344/ajev.2013.13066

Molitor, D., Schultz, M., Mannes, R., Pallez-Barthel, M., Hoffmann, L., & Beyer, M. (2019). Semi-Minimal Pruned Hedge: A Potential Climate Change Adaptation Strategy in Viticulture. *Agronomy*, *9*(4), 173. https://doi.org/10.3390/agronomy9040173

Mori, K., Goto-Yamamoto, N., Kitayama, M., & Hashizume, K. (2007). Loss of anthocyanins in red-wine grape under high temperature. *Journal of Experimental Botany*, *58*(8), 1935–1945. https://doi.org/10.1093/jxb/erm055

Moutinho-Pereira, J. M., Correia, C. M., Gonçalves, B. M., Bacelar, E. A., & Torres-Pereira, J. M. (2004). Leaf Gas Exchange and Water Relations of Grapevines Grown in Three Different Conditions. *Photosynthetica*, *42*(1), 81–86. https://doi.org/10.1023/B:PHOT.0000040573.09614.1d

Mul Fedele, M. L., Aiello, I., Caldart, C. S., Golombek, D. A., Marpegan, L., & Paladino, N. (2020). Differential Thermoregulatory and Inflammatory Patterns in the Circadian Response to LPS-Induced Septic Shock. Frontiers in Cellular and Infection Microbiology, 10. https://www.frontiersin.org/articles/10.3389/fcimb.2020.00100

Nave, C. (2016, 01 1). Hyperphysics. Retrieved from Hyperphysics.phy: http://hyperphysics.phy-astr.gsu.edu/ hbase/index.html

Neethling, E. B. (2016). Adapting viticulture to climate change: guidance manual to support winegrowers´ decision-making.

Neethling, E., Barbeau, G., Bonnefoy, C., & Quénol, H. (2012). Change in climate and berry composition for grapevine varieties cultivated in the Loire Valley. Climate Research, 53(2), 89–101. https://doi.org/10.3354/cr01094

Neves, E. B., Leal, S., Melo, D., Filgueiras, M., & Dantas, E. (2019). Pain perception and thermographic analysis in patients with chronic lower back pain submitted to osteopathic treatment. Motricidade, 15(2–3). https://doi.org/10.6063/motricidade.17662

Neves, E. B., Salamunes, A. C. C., & Stadnik, A. M. W. (2018). Mathematical Model for Body Fat Percentage in Military using Thermal Imaging and Circumferences. 40th Annual International Conference of the IEEE Engineering in Medicine and Biology Society (EMBC), 790–793. https://doi.org/10.1109/EMBC.2018.8512280

Neves, M.M.S.R. (2021). Uso de dados térmicos para melhor compreensão das respostas da videira ao stress e apoio à decisão. Lisboa: ISA, 2021, 109 p.

Ngosong, C., Okolle, J.N., Tening, A.S. (2019). Mulching: A Sustainable Option to Improve Soil Health. In: Panpatte, D., Jhala, Y. (eds) Soil Fertility Management for Sustainable Development. Springer, Singapore. https://doi.org/10.1007/978-981-13-5904-0_11

Nosrati, Z., Bergamo, M., Rodríguez-Rodríguez, C., Saatchi, K., & Häfeli, U. O. (2020). Refinement and validation of infrared thermal imaging (IRT): A non-invasive technique to measure disease activity in a mouse model of rheumatoid arthritis. *Arthritis Research & Therapy*, *22*(1), 281. https://doi.org/10.1186/s13075-020-02367-w

Novak, M.D., Chen, W., Orchansky, A.L., & Ketler, R. (2000). Turbulent exchange processes within and above a straw mulch. Part II: Thermal and moisture regimes. Agric. For. Meteorol., 102, 155-171.

Nuñez, J. R., Anderton, C. R., & Renslow, R. S. (2018). Optimizing colormaps with consideration for color vision deficiency to enable accurate interpretation of scientific data. PLOS ONE, 13(7), e0199239. https://doi.org/10.1371/journal.pone.0199239

Onvuka, B.; Mang B. (2018). Effects of soil temperature on some soil properties and plant growth. Review Article. Advances in Plants & Agricultural Research 881):34-37.

Pagay, V., & Kidman, C. M. (2019). Evaluating Remotely-Sensed Grapevine (Vitis vinifera L.) Water Stress Responses Across a Viticultural Region. *Agronomy*, *9*(11), 682. https://doi.org/10.3390/agronomy9110682

Paul, M. J., & Foyer, C. H. (2001). Sink regulation of photosynthesis. *Journal of Experimental Botany*, *52*(360), 1383–1400. https://doi.org/10.1093/jexbot/52.360.1383

Perkel, J. M. (2021). Ten computer codes that transformed science. *Nature*, *589*(7842), 344–348. https://doi.org/10.1038/d41586-021-00075-2

Petrie, P. R., YeNiu, W., Liu, S., Lam, S., Whitty, M. A., & Skewes, M. A. (2019). The accuracy and utility of a low cost thermal camera and smartphone-based system to assess grapevine water status. *Biosystems Engineering*, *179*, 126–139.

Pisciotta, A., Di Lorenzo, R., Santalucia, G., & Barbagallo, M. G. (2018). Response of grapevine (Cabernet Sauvignon cv) to above ground and subsurface drip irrigation under arid conditions. *Agricultural Water Management*, *197*, 122–131. https://doi.org/10.1016/j.agwat.2017.11.013

Playà-Montmany, N., & Tattersall, G. (2021). Spot size, distance, and emissivity errors in field applications of infrared thermography. *Methods in Ecology and Evolution*, *12*. https://doi.org/10.1111/2041-210X.13563

Poblete-Echeverría, C., Olmedo, G. F., Ingram, B., & Bardeen, M. (2017). Detection and Segmentation of Vine Canopy in Ultra-High Spatial Resolution RGB Imagery Obtained from Unmanned Aerial Vehicle (UAV): A Case Study in a Commercial Vineyard. Remote Sensing, 9(3). https://doi.org/10.3390/rs9030268

Pou, A., Diago, M. P., Medrano, H., Baluja, J., & Tardaguila, J. (2014). Validation of thermal indices for water status identification in grapevine. *Agricultural Water Management*, *134*, 60–72. https://doi.org/10.1016/j.agwat.2013.11.010

Pou, A., Flexas, J., Alsina, M.d.M., Bota, J., Carambula, C., De Herralde, F., Galmés, J., Lovisolo, C., Jiménez, M., Ribas-Carbó, M., Rusjan, D., Secchi, F., Tomàs, M., Zsófi, Z. and Medrano, H. (2008), Adjustments of water use efficiency by stomatal regulation during drought and recovery in the drought-adapted *Vitis*hybrid Richter-110 (*V. berlandieri* × *V. rupestris*). Physiologia Plantarum, 134: 313-323. https://doi.org/10.1111/j.1399-3054.2008.01138.x

Prashar, A., & Jones, H. G. (2014). Infra-Red Thermography as a High-Throughput Tool for Field Phenotyping. *Agronomy*, *4*(3), 397–417. https://doi.org/10.3390/agronomy4030397

Rahimi-Eichi, V. (2013). Water Use Efficiency in Almonds (Prunus Dulcis (Mill.) D.A. Webb). Dissertation for a Master's degree in Master of Philosophy. School of Agriculture, Food and Wine, Faculty of Science, University of Adelaide

Rességuier, L., Mary, S., Renan, L. R., Petitjean, T., Quénol, H., & van Leeuwen, C. (2020). Temperature Variability at Local Scale in the Bordeaux Area. Relations With Environmental Factors and Impact on Vine Phenology. Frontiers in Plant Science, 11, 515. https://doi.org/10.3389/fpls.2020.00515

Rizhsky, L., Liang, H., Shuman, J., Shulaev, V., Davletova, S., & Mittler, R. (2004). When Defense Pathways Collide. The Response of Arabidopsis to a Combination of Drought and Heat Stress. *Plant Physiology*, *134*(4), 1683–1696. https://doi.org/10.1104/pp.103.033431

Rogiers, S.Y., Greer, D.H., Hutton, R.J. & Clarke, S.J. (2011), Transpiration efficiency of the grapevine cv. Semillon is tied to VPD in warm climates. Annals of Applied Biology, 158: 106-114. https://doi.org/10.1111/j.1744-7348.2010.00446.x

Rogiers, S. Y., & Clarke, S. J. (2013). Nocturnal and daytime stomatal conductance respond to root-zone temperature in «Shiraz» grapevines. *Annals of Botany*, *111*(3), 433–444. https://doi.org/10.1093/aob/mcs298

Salvador Gutiérrez, Juan Fernández-Novales, María-Paz Diago, Rubén Iñiguez, & Javier Tardaguila. (2021). Assessing and mapping vineyard water status using a ground mobile thermal imaging platform. *Irrigation Science*, *39*(4), 457–468. https://doi.org/10.1007/s00271-021-00735-1

Santesteban, L. G. (2019). Precision viticulture and advanced analytics. A short review. *Food Chemistry*, *279*, 58–62. https://doi.org/10.1016/j.foodchem.2018.11.140

Santesteban, L. G., Di Gennaro, S. F., Herrero-Langreo, A., Miranda, C., Royo, J. B., & Matese, A. (2017). High-resolution UAV-based thermal imaging to estimate the instantaneous and seasonal variability of plant water status within a vineyard. *Agricultural Water Management*, *183*, 49–59.

https://doi.org/10.1016/j.agwat.2016.08.026

Santos, J. A., Fraga, H., Malheiro, A. C., Moutinho-Pereira, J., Dinis, L.-T., Correia, C., Moriondo, M., Leolini, L., Dibari, C., Costafreda-Aumedes, S., Kartschall, T., Menz, C., Molitor, D., Junk, J., Beyer, M., & Schultz, H. R. (2020). A Review of the Potential Climate Change Impacts and Adaptation Options for European Viticulture. *Applied Sciences*, *10*(9), 3092.

https://doi.org/10.3390/app10093092

Santos, J. A., Yang, C., Fraga, H., Malheiro, A. C., Moutinho-Pereira, J., Dinis, L.-T., Correia, C., Moriondo, M., Bindi, M., Leolini, L., Dibari, C., Costafreda-Aumedes, S., Bartoloni, N., Kartschall, T., Menz, C., Molitor, D., Junk, J., Beyer, M., & Schultz, H. R. (2021a). Short-term adaptation of European viticulture to climate change: An overview from the H2020 Clim4Vitis action: Original language of the article: English. *IVES Technical Reviews, Vine and Wine*.

https://doi.org/10.20870/IVES-TR.2021.4637

Santos, J. A., Yang, C., Fraga, H., Malheiro, A. C., Moutinho-Pereira, J., Dinis, L.-T., Correia, C., Moriondo, M., Bindi, M., Leolini, L., Dibari, C., Costafreda-Aumedes, S., Bartoloni, N., Kartschall, T., Menz, C., Molitor, D., Junk, J., Beyer, M., & Schultz, H. R. (2021b). Long-term adaptation of European viticulture to climate change: An overview from the H2020 Clim4Vitis action: Original language of the article: English. *IVES Technical Reviews, Vine and Wine*. https://doi.org/10.20870/IVES-TR.2021.4644

Schindelin, J., Rueden, C. T., Hiner, M. C., & Eliceiri, K. W. (2015). The ImageJ ecosystem: An open platform for biomedical image analysis. *Molecular Reproduction and Development*, *82*(7–8), 518–529.

https://doi.org/10.1002/mrd.22489

Schirrmann, M., Gebbers, R., & Kramer, E. (2013). Performance of Automated Near-Infrared Reflectance Spectrometry for Continuous in Situ Mapping of Soil Fertility at Field Scale. *Vadose Zone Journal*, *12*(4), vzj2012.0199. https://doi.org/10.2136/vzj2012.0199

Sepúlveda-Reyes, D., Ingram, B., Bardeen, M., Zúñiga, M., Ortega-Farías, S., & Poblete-Echeverría, C. (2016). Selecting Canopy Zones and Thresholding Approaches to Assess Grapevine Water Status by Using Aerial and Ground-Based Thermal Imaging. *Remote Sensing*, *8*(10), 822. https://doi.org/10.3390/rs8100822

Shah, N. H., & Paulsen, G. M. (2003). Interaction of drought and high temperature on photosynthesis and grain-filling of wheat. *Plant and Soil*, *257*(1), 219–226. https://doi.org/10.1023/A:1026237816578

Shellie, K. C., & King, B. A. (2020). Application of a Daily Crop Water Stress Index to Deficit Irrigate Malbec Grapevine under Semi-Arid Conditions. *Agriculture*, *10*(11), 492. https://doi.org/10.3390/agriculture10110492

Shiners, K.J., Nelson, W.S. and Wang, R. (1994). Effects of residue free band width on soil temperature and water content. Transactions of the ASAE, 37(1): 39-49

Simonneau, T., Lebon, E., Coupel-Ledru, A., Marguerit, E., Rossdeutsch, L., & Ollat, N. (2017). Adapting plant material to face water stress in vineyards: Which physiological targets for an optimal control of plant water status? *OENO One*, *51*(2), 167–179. https://doi.org/10.20870/oeno-one.2017.51.2.1870

Speirs, J., Binney, A., Collins, M., Edwards, E., & Loveys, B. (2013). Expression of ABA synthesis and metabolism genes under different irrigation strategies and atmospheric VPDs is associated with stomatal conductance in grapevine (Vitis vinifera L. cv Cabernet Sauvignon). *Journal of Experimental Botany*, *64*(7), 1907–1916. https://doi.org/10.1093/jxb/ert052

Stoll, M., & Jones, H. G. (2007). Thermal imaging as a viable tool for monitoring plant stress. OENO One, 41(2), 77–84. https://doi.org/10.20870/oeno-one.2007.41.2.851

Stroppiana, D., (2019). Estimating crop density from multi-spectral uav imagery in maize crop," Int. Arch. Photogramm. Remote Sens. Spat. Inf. Sci., 42(2W13), 619-624.

Tardaguila, J., Stoll, M., Gutiérrez, S., Proffitt, T., & Diago, M. P. (2021). Smart applications and digital technologies in viticulture: A review. *Smart Agricultural Technology*, *1*, 100005. https://doi.org/10.1016/j.atech.2021.100005

Teixeira, G., Monteiro, A., Santos, C., & Lopes, C. M. (2018). Leaf morphoanatomy traits in white grapevine cultivars with distinct geographical origin. Ciência e Técnica Vitivinícola. https://doi.org/10.1051/ctv/20183301090

Tejero-Garcia, I. F., Costa, J. M., Egipto, R., Durán-Zuazo, V. H., Lima, R. S. N., Lopes, C. M., & Chaves, M. M. (2016). Thermal data to monitor crop-water status in irrigated Mediterranean viticulture. Agricultural Water Management, 176, 80–90. https://doi.org/10.1016/j.agwat.2016.05.008

Tejero-Garcia, I. F., Ortega-Arévalo, C. J., Iglesias-Contreras, M., Moreno, J. M., Souza, L., Tavira, S. C., & Durán-Zuazo, V. H. (2018). Assessing the Crop-Water Status in Almond (Prunus dulcis Mill.) Trees via Thermal Imaging Camera Connected to Smartphone. Sensors, 18(4), 1050. https://doi.org/10.3390/s18041050

Teskey, R., Wertin, T., Bauweraerts, I., Ameye, M., Mcguire, MA., & Steppe, K. (2014). Responses of tree species to heat waves and extreme heat events. Plant Cell Environ., 1699-1712.

Thyng, K., Greene, C., Hetland, R., Zimmerle, H., & DiMarco, S. (2016). True Colors of Oceanography: Guidelines for Effective and Accurate Colormap Selection. *Oceanography*, *29*(3), 9–13. https://doi.org/10.5670/oceanog.2016.66

Van Doremalen, R. F. M., van Netten, J. J., van Baal, J. G., Vollenbroek-Hutten, M. M. R., & van der Heijden, F. (2019). Validation of low-cost smartphone-based thermal camera for diabetic foot assessment. Diabetes Research and Clinical Practice, 149, 132–139. https://doi.org/10.1016/j.diabres.2019.01.032

Van Leeuwen, C. (2016). The Impact of Climate Change on Viticulture and Wine Quality. Journal of Wine Economics.

Verbilya, D. (1995). Satellite remote sensing of natural resources. Boca Raton: Lewis Publishers.

Villa, E., Arteaga-Marrero, N., & Ruiz-Alzola, J. (2020). Performance Assessment of Low-Cost Thermal Cameras for Medical Applications. *Sensors (Basel, Switzerland)*, *20*(5), 1321. https://doi.org/10.3390/s20051321

Whitehead, K., & Hugenholtz, C. H. (2014). Remote sensing of the environment with small unmanned aircraft systems (UASs), part 1: A review of progress and challenges. Journal of Unmanned Vehicle Systems, 02(03), 69–85. https://doi.org/10.1139/juvs-2014-0006

WoS. (2021). WoS abstract & citation database. 2021. Retrieved July 2022, from https:/apps.webofknowledge.com/WOS_GeneralSearch_input.do?product=WOS&search_mode=GeneralSearch&SID=E1CuPGLUVGqBNwL4Z6x&preferencesSaved

Yang, Y., Wu, J., Du, Y.-L., Gao, C., Pan, X., Tang, D. W. S., & van der Ploeg, M. (2021). Short- and Long-Term Straw Mulching and Subsoiling Affect Soil Water, Photosynthesis, and Water Use of Wheat and Maize. *Frontiers in Agronomy*, *3*. https://doi.org/10.3389/fagro.2021.708075

APPENDIX

Figure A1 Comparison between big and small ROIs that show a small variation of Temperature values

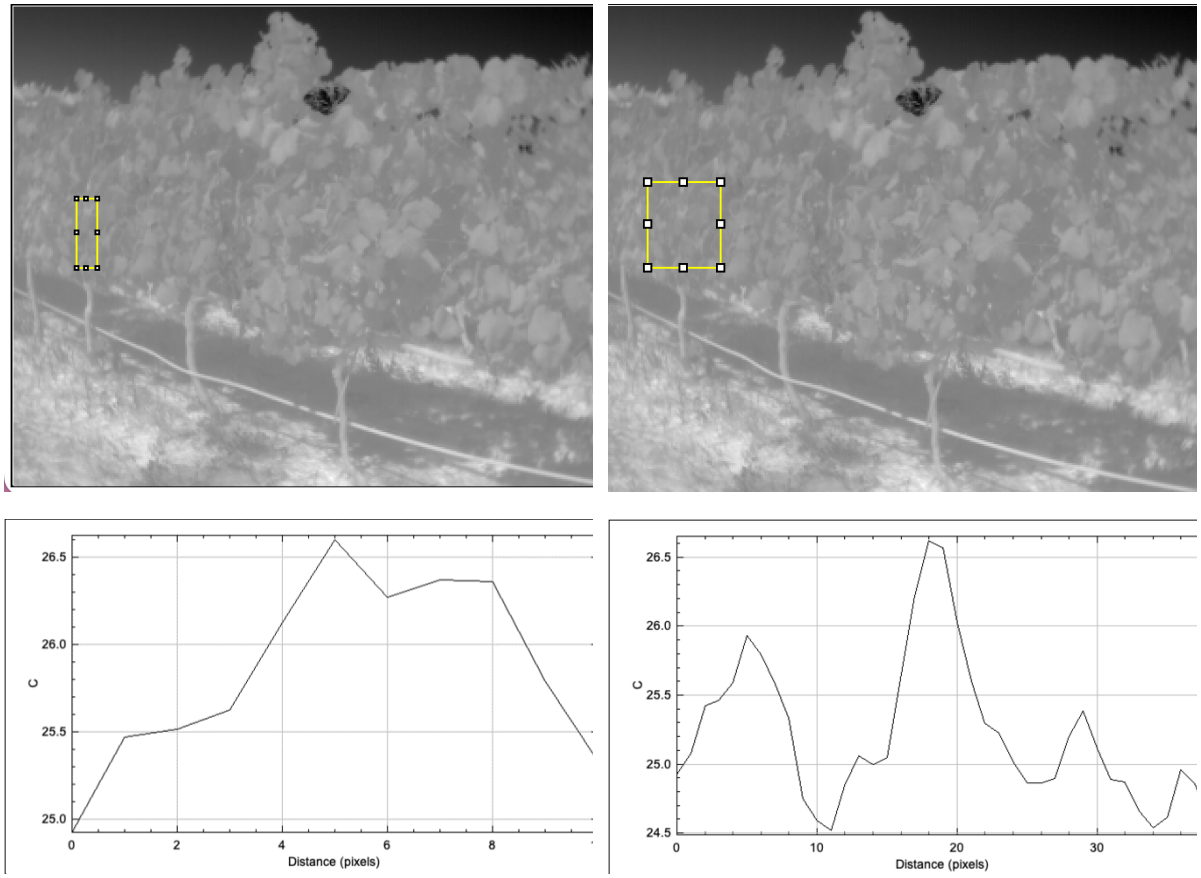

Average Temperature value = 25.2 ºC

Average Temperature value = 25.9 ºC

Figure A2 “Control” thermal images captured by Flir A35 along the season.

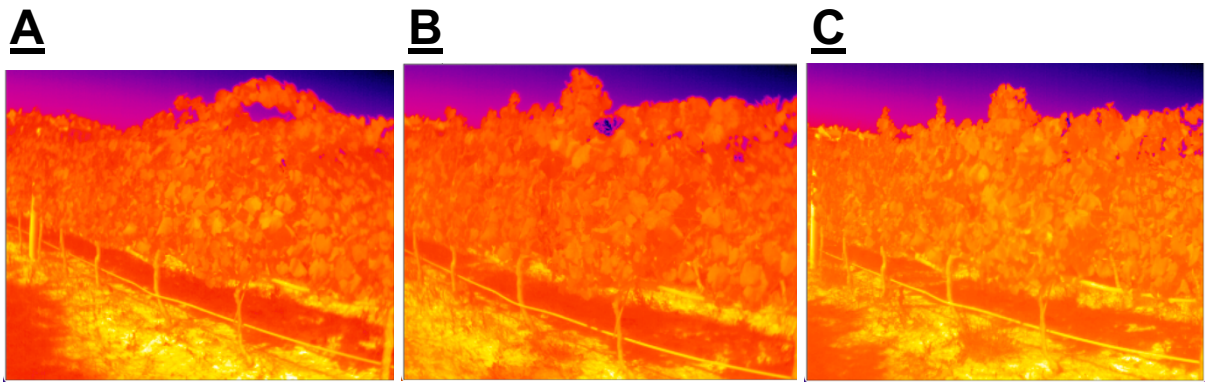

Figure A3 “Control” soil surface thermal images captured by Flir A35 camera along the season

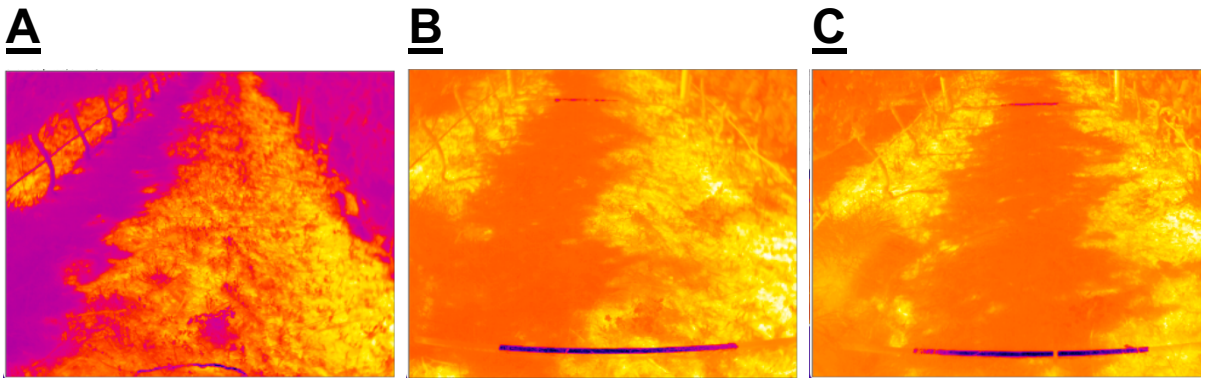

Figure A4, Air temperature (top) and precipitation (bottom) variation along the season along the season (Jan-Sept) (Source: METEOAGRI http://www.meteoagri.com)

Figure A6 VPD (Vapour pressure deficit) values *obtained by using LI-600 (Licor Biosystems)*

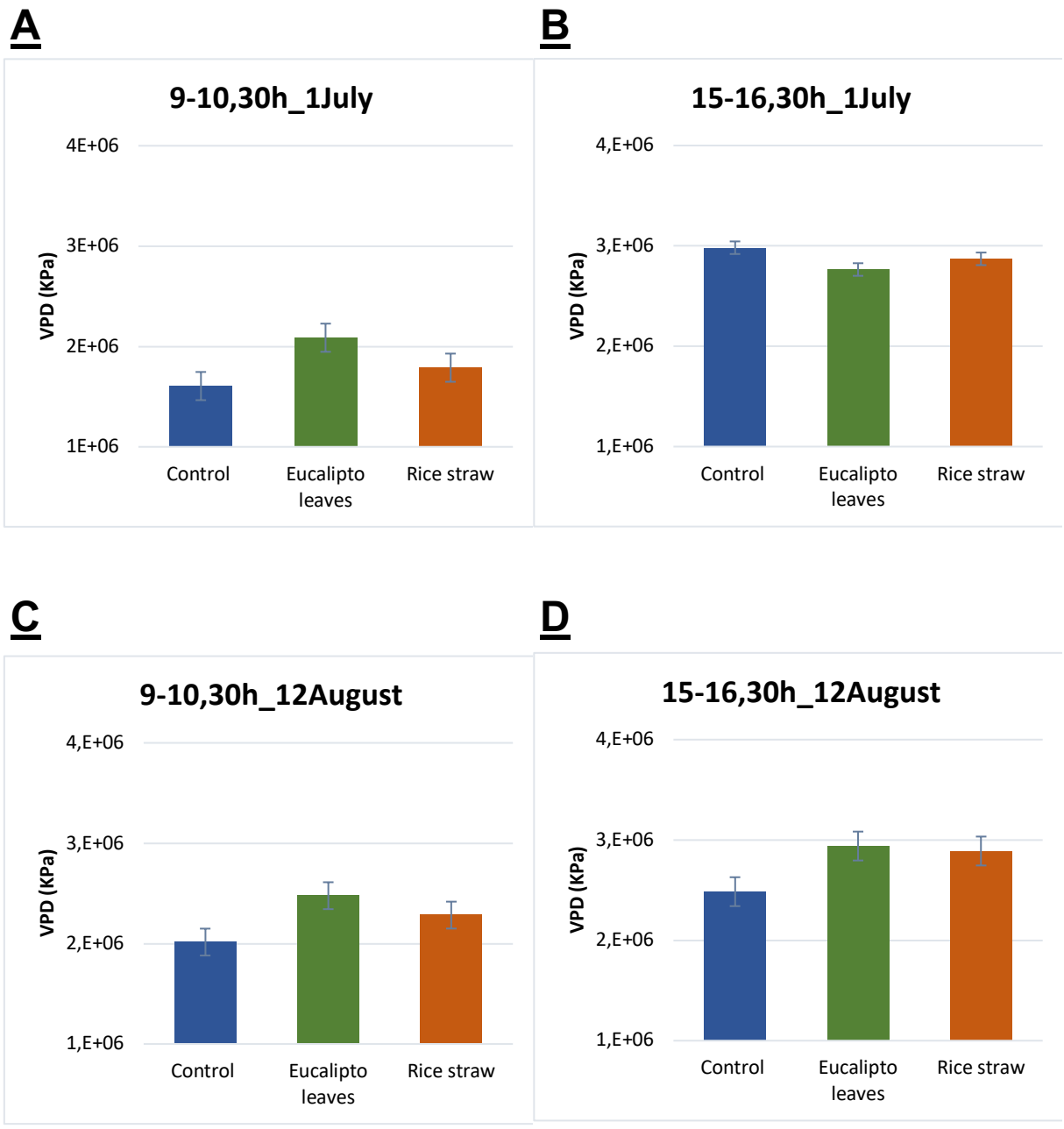

Figure A7 *Value of E_apparent (leaf transpiration) obtained by using LI-600 (Licor Biosystems)*

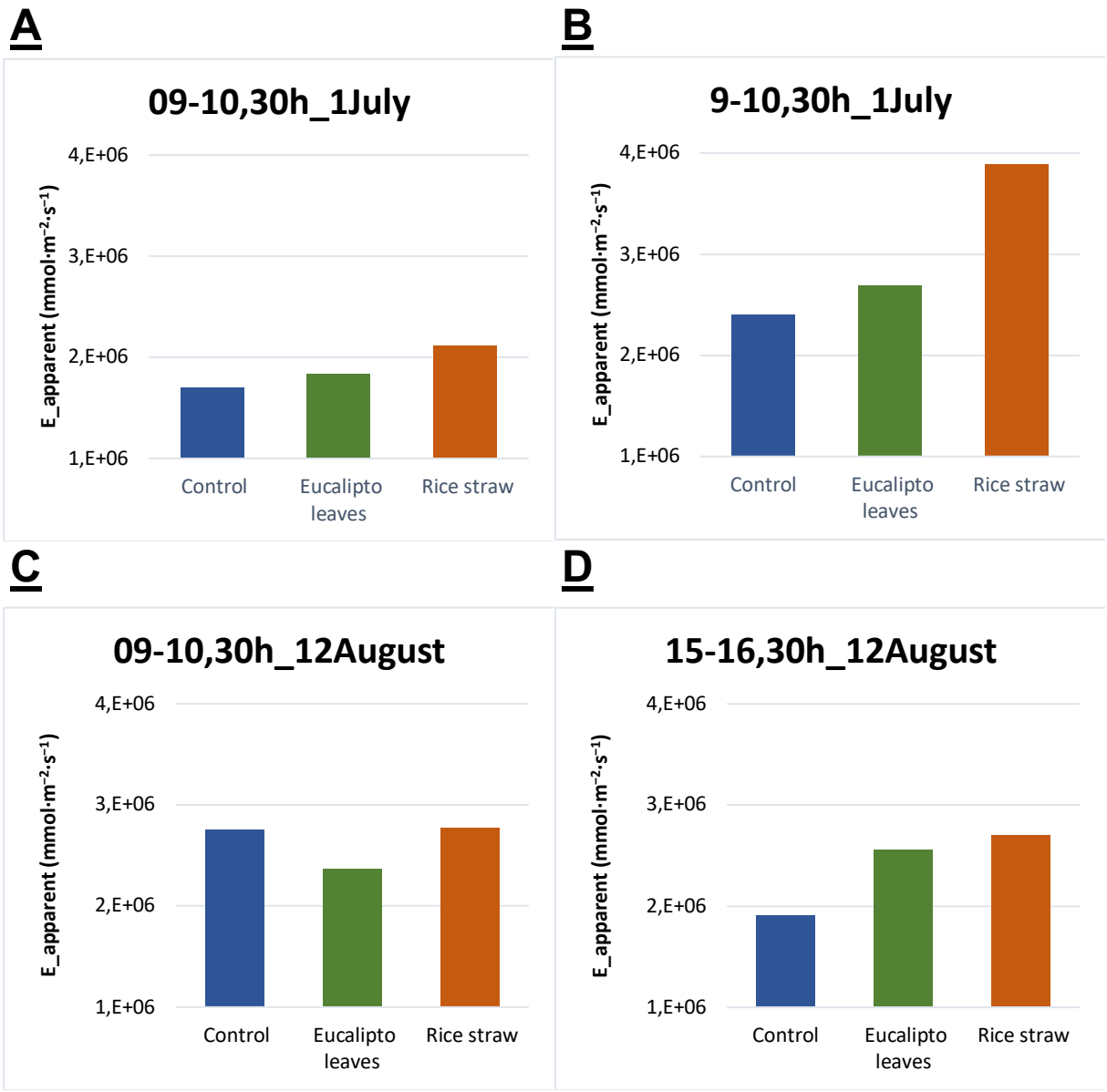

A

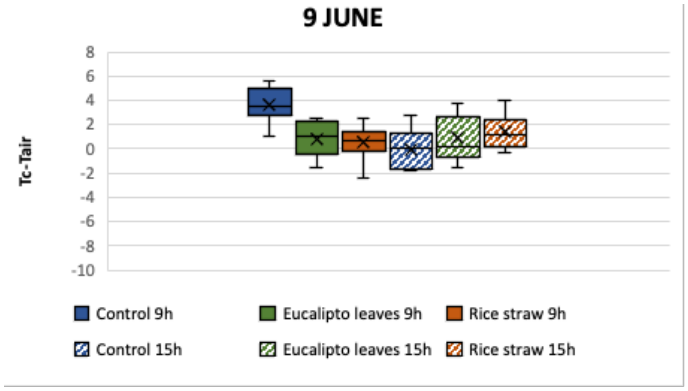

B

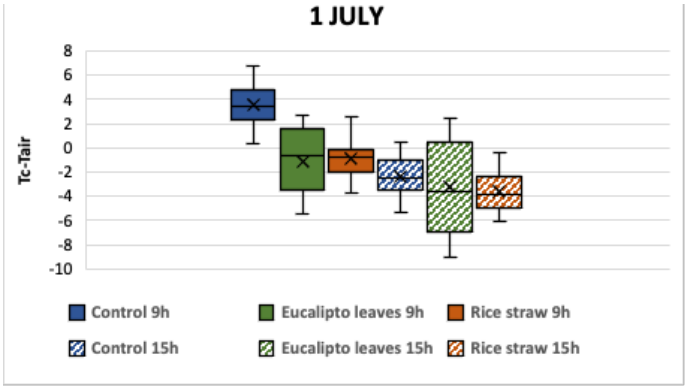

C

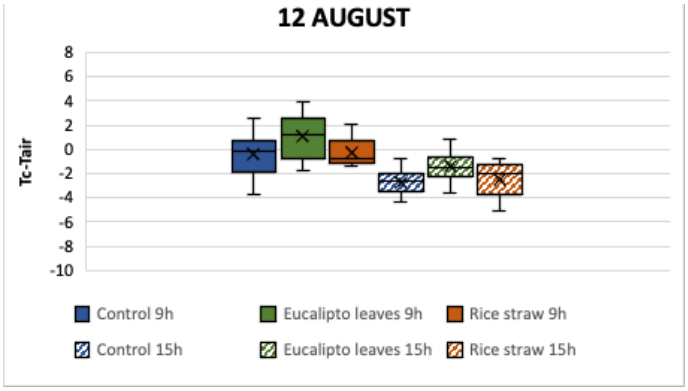

Figure A8 *Value of (Tc-Tair) for the treatments along the season*